INVESTIGATION OF PROMISING CONTROL ALTERNATIVES FOR SOLAR WATER HEATING SYSTEMS

by

MARK DAVID WUESTLING

A thesis submitted in partial fulfillment of the
requirements for the degree of

MASTER OF SCIENCE
(Mechanical Engineering)

at the

UNIVERSITY OF WISCONSIN-MADISON

1983

ACKNOWLEDGEMENTS

I would like to extend a special thank you to Professor Sanford A. Klein for his helpful ideas and guidance, a better advisor I could not have hoped for. I would also like to thank Professor John A. Duffie for his never ending supply of suggestions.

I also appreciate the willingness of my fellow co-workers to aid in difficult problems. I have made some wonderful friends here in the Solar Lab and I truly hate to leave. Best wishes to everyone and good luck on all your future endeavors.

This work has been supported by the Solar Heating and Cooling Research and Development Branch, Office of Conservation and Solar Applications, U.S. Department of Energy.

ABSTRACT

Although the performance of solar domestic hot water (SDHW) systems has been well studied, there are several promising control alternatives which have not been thoroughly investigated. Reduced constant collector flow rates, variable collector fluid flow rates, and variable volume storage are several alternative strategies. This thesis presents the results of an analytical study using the TRNSYS simulation program in which the thermal performance of SDHW systems utilizing these alternative control strategies while operating under realistic conditions in several different climates of the United States is examined. The effects on system performance of: time of year, collector area and quality, preheat storage tank volume and energy losses, controller temperature deadbands, auxiliary set temperature, total daily usage, and load distribution are also investigated.

Most SDHW systems use on-off control and circulate the fluid through the collector at relatively high constant flow rates (approximately 50 ℓ /hr m^2) in order to achieve a high value of collector heat removal factor, F_R. When systems with typically sized storage tanks (approximately 75 ℓ / m^2) are operated at high collector flow rates, a high degree of thermal stratification cannot be obtained. When the benefits of high thermal stratification are considered, improvements in annual system performance from 10 to 15 percentage points over fully-mixed systems operating at high collector flow rates can be obtained by reducing the constant collector flow rate

to approximately 20 percent that of conventional collector flow rates.

Several variable collector fluid flow rate control strategies are investigated in this thesis. Varying the flow rate to obtain a specified collector outlet temperature causes an improvement in performance over conventional fully-mixed systems. Further improvement can be realized by varying the collector flow to achieve a constant temperature rise across the collector. Both of these strategies, however , do not perform as well as the reduced constant collector flow rate, on-off control. By varying the collector flow rate proportionately to the utilizable radiation (level of incident radiation above the critical threshold level) system performance very nearly equal to the optimum reduced fixed flow performance can be achieved. However, this strategy requires advance knowledge of future radiation levels and ambient temperatures.

System performance can also be improved through the use of a variable volume storage tank. The collectors are fed directly from the mains water and the collector outlet empties into a storage tank where the level of fluid is allowed to vary. Load flow is withdrawn from this tank as needed. Mixing of hot and cold water is thus avoided and the collectors operate with the lowest possible inlet temperatures (and thus high collector efficiency).

TABLE OF CONTENTS

LIST OF FIGURES

LIST OF TABLES

NOMENCLATURE

This list contains all the symbols used in the text. Each symbol is also defined the first time it occurs in the text.

A	surface area
BC	base case system
b_o	incidence angle modifier coefficient
C_1	total desired daily collector flow
C_2	daily proportionality constant
C_3	monthly proportionality constant
C_p	constant pressure specific heat
C_v	constant volume specific heat
F'	collector efficiency factor
F_R	collector heat removal factor
$F_R(\tau\alpha)_n$	intercept of the collector efficiency vs. $(T_i-T_a)/G_T$ curve
F_RU_L	negative of the slope of the collector efficiency vs. $(T_i-T_a)/G_T$ curve
G	instantaneous incident radiation on a horizontal surface per unit area
hr	hours
H_T	total incident radiation on the collector surface per unit area
HQ	higher quality collector
Kg	kilogram

$K_{\tau\alpha}$	incidence angle modifier
ℓ	liter
LQ	lower quality collector
m	meter
$\dot{m}$	mass flow rate
M	total daily, or instantaneous, mass
N	number of days in the month
Q_u	rate of useful energy gain
r	non-test flow rate correction ratio
t	time
U	tank loss coefficient
$(UA)_t$	total overall tank loss coefficient area product
U_L	collector loss coefficient
W	watt
β	collector slope
ϕ	utilizability
θ	incidence angle

Superscripts

–	monthly average daily

Subscripts

a	ambient
AT	auxiliary storage tank
AUX	auxiliary heater

BT	beam component incident on collector surface
c	collector
C	critical
eg	effective incidence for ground-reflected diffuse radiation
env	storage tank environment
ef	effective incidence for sky diffuse radiation
G	ground-reflected diffuse component incident on collector surface
i	inlet
L	load
MAX	maximum
main	mains supply water
MIN	minimum
o	outlet
PT	preheat storage tank
r	storage fluid recirculated through collector
S	sky diffuse component incident on collector surface
SET	auxiliary storage tank thermostat set point
T	incident on collector surface
$\vert_{test}$	test conditions
$\vert_{use}$	use or actual conditions

CHAPTER 1

INTRODUCTION

Although the performance of conventional solar domestic hot water (SDHW) systems has been well studied, there are several promising control alternatives which have not been thoroughly investigated. Reduced constant collector fluid flow rates, variable collector fluid flow rates, and variable volume storage are several alternative strategies. The objective of this investigation has been to determine the merit of these control alternatives. This chapter first describes the system configuration and operation of a conventional direct two-tank SDHW system. The configuration and operation of systems utilizing these alternative control strategies are then outlined. A summary of previous work is also included.

1.1 Conventional SDHW System Control Strategy

A conventional direct two-tank SDHW system is shown schematically in Figure 1.1. The preheat tank contains water which is circulated through the solar collectors when the incident solar radiation is sufficient to allow useful energy gains. When water from the auxiliary tank is removed to satisfy a load, it is replaced by solar heated water from the preheat tank. The water contained in the auxiliary tank is maintained at a specified set temperature by two internal heaters. The system also includes a tempering valve which limits the temperature of the delivered water to the set temperature by mixing with mains water as needed. The circulation of fluid through the collector is controlled in an on-off fashion by a differential temperature sensing

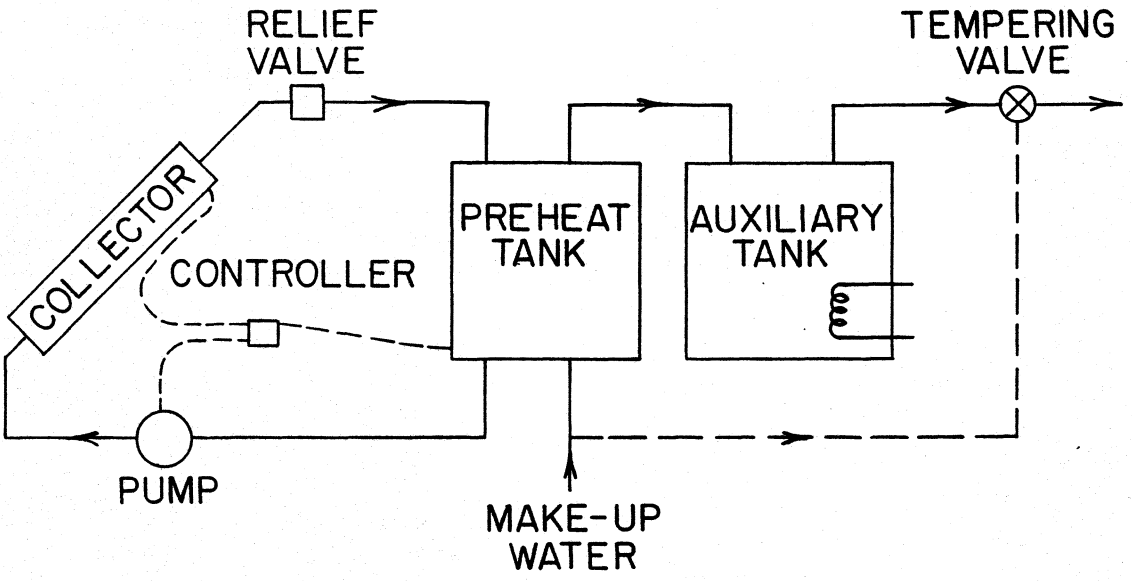

Figure 1.1 Constant Preheat Storage Volume System Schematic

controller. When the fluid temperature at the collector outlet reaches a specified amount above the water temperature in the bottom of the preheat tank (deadband upper limit) the circulation pump is activated. This temperature difference is then monitored and when it falls below a specified amount (deadband lower limit) circulation ceases.

When operated, the pump circulates the collector fluid at a relatively high constant flow rate (approximately 50 ℓ /hr m^2) which results in a high value of the collector heat removal factor, F_R, and consequently higher collector efficiency. This method of control was thought to be optimum because the preheat storage tank was considered fully mixed and any benefits due to thermal stratification were neglected. There is, however, a thermal disadvantage associated with

such high flow rates. With typically sized storage (approximately 75 ℓ/m^2), high collector fluid flow rates cause the storage fluid to recirculate through the collector loop on the order of three to four tank turnovers per day. Both simulations and experiments (1,2) have shown that a high degree of thermal stratification cannot be obtained with such recirculation rates.

1.2 Alternative Control Strategies-Constant Volume Storage

Thermal stratification can be enhanced by reducing the collector fluid flow rate. Stratification could also be enhanced through the use of properly designed diffusers or floating inlets and outlets. Reducing the flow rate has two opposing effects. Lower flow rates result in lower values of F_R which reduces collector efficiency; but lower flow rates also result in less recirculation and a higher degree of thermal stratification. This increased stratification results in lower collector inlet temperatures and thus increased collector efficiency. Both computer simulations and experiments (3-9) have shown that the increase in collector efficiency due to lower inlet temperatures often outweighs the decrease in efficiency due to the reduction in F_R, and that an optimum flow rate exists at about 20 percent of conventional collector flow rates. Increased stratification also causes higher temperature water to be sent to the auxiliary tank which results in a reduction of auxiliary energy. Any solar heated water remaining in the tank at the end of the day is at the lowest possible temperature and thus a minimum of energy is wasted. If the load is sufficiently large, all the useful energy collected can be

removed from the preheat tank in a perfectly stratified system, where as all the energy can never be totally removed from a fully-mixed system due to the continual mixing with mains water.

Jesch and Braun (4) support the benefits of stratification using TRNSYS (10) simulations to predict the annual performance of a SDHW system similar to that shown in Figure 1.1. The pump is activated when the useful energy collection exceeds the pumping power required. The collector is modeled using the Hottel-Whillier (11) equation corrected for non-test flow rates, and the preheat storage tank is modeled with the Type 4, multi-node model contained in TRNSYS. Annual results are presented for Madison, Wisconsin and Brussels, Belgium for two different collector types, and one,three, and ten node storage tank models.

The existence of a reduced flow rate optimum is also supported by van Koppen (5) who uses a very simple system model with harmonically varying radiation. He uses a two-node floating inlet storage tank model which neglects energy losses. Many other simplifying assumptions are made and some experimental results are presented.

Veltkamp (6) uses a more detailed system model than van Koppen, which uses a one-dimensional, multi-node tank model with floating inlets. A three day comparison of the multi-node model with experimental results shows that 64 nodes are required to accurately represent thermal stratification. Annual performance predictions using Dutch reference year weather data (12) as hourly inputs and a 16 node storage tank are presented which show that an optimum in system performance exists at a reduced constant collector flow rate of

approximately 1/3 of conventional flow rates. The effects of collector type and plumbing scheme on a combined space and water heating system are also examined.

Rademaker (7) suggests that optimum performance occurs when only a slight amount of recirculation is allowed but that very near optimum performance is obtained when collector flow rate is reduced just enough to avoid recirculation. To implement this near optimum strategy would involve adjusting the collector flow rate such that the total daily collector flow equals the initial volume of cold water in the preheat storage tank plus the load flow during collector on time. A different collector fluid flow rate would thus be required each day. Rademaker's conclusions are based on a simplistic model of SDHW system performance over one clear day with no load.

In references 8 and 9 Veltkamp and van Koppen summarize previous work and provide more details on combined solar systems for space and water heating. The strong coupling between optimum collector flow and optimum load flow is discussed and the existence of a reduced flow rate optimum is shown. The optimum collector to loadthroughput ratio is shown to be insensitive to collector area and quality, storage tank volume, load distribution, and climate. Reference (8) also compares the performance of a moderately stratified system to the previously studied perfectly stratified system.

1.2.1 Reduced Constant Collector Fluid Flow Rate

Perhaps the simplest alternative control strategy is reduced constant collector fluid flow rate using on-off control. The system

configuration is the same as the conventional direct two-tank system shown in Figure 1.1. The pump is controlled in the conventional manner using a differential temperature sensing controller with fixed upper and lower deadbands. The only difference from the conventional system is that the constant flow rate collector fluid circulation pump operates at a flow rate significantly lower than conventionally high flow rates. This constant collector fluid flow rate can be specified such that the preheat tank is full of solar heated water at the end of the collection period and a minimum of this heated water has been recirculated through the collector. This allows a higher degree of thermal stratification.

Due to the fluctuations in weather, and thus collector on time, a constant collector flow rate would result in a different total collector flow each day. In order to limit recirculation it would be necessary to specify a different fixed collector flow rate each day. This control strategy would require advance knowledge of future weather conditions and thus be difficult to apply in practice. However, near optimum performance might be achieved by properly selecting a monthly or annual fixed flow rate such that energy collection is not quite maximized on days with low radiation levels and a slight amount of recirculation is allowed on days with high radiation levels.

1.2.2 Variable Collector Fluid Flow Rate

Reducing the collector fluid flow rate enhances system performance by increasing the thermal stratification in the preheat storage tank. Perhaps energy collection and thus system performance can be further

improved by modulating, or varying, the collector fluid flow rate. Conventional temperature deadband control with a constant collector flow rate causes the collector outlet temperature, or rise in fluid temperature across the collector, to vary with the incident radiation and ambient temperature. A variable collector flow rate would enable a specified collector outlet temperature or rise in collector fluid temperature to be obtained. The collector flow rate could also be varied proportionately to utilizable radiation (i.e. difference between the radiation incident on the collector and the critical threshold level).

These variable collector fluid flow rate strategies could be implemented on the conventional system shown in Figure 1.1 with the addition of a new controller and either a variable speed pump or a thermostatically controlled flow valve.

1.2.2.a Specified Collector Outlet Temperature

Optimal control with this strategy might involve choosing a fixed collector outlet temperature such that the total daily collector flow, or monthly average total daily collector flow, is the largest possible while still avoiding recirculation. Or perhaps the collector outlet temperature should be a few degrees above the auxiliary set point as suggested by Cole (1). In this way, the water would never be heated to a temperature higher than necessary except for the few degrees above auxiliary set point which are to compensate for thermal energy losses from the preheat storage tank.

There are some physical limitations to the maximum or minimum collector outlet temperatures that can be obtained. In order to achieve higher collector outlet temperatures, the pump flow rate must be reduced. However, as collector flow rate decreases so does the collector heat removal factor, F_R. Thus, there is an upper limit on the outlet temperature that can be achieved with any given incident radiation and collector inlet temperature. The minimum outlet temperature obtainable would be limited by the maximum pump flow rate. When the bottom of the preheat tank reaches the specified collector outlet temperature the pump turns off. Choosing a collector outlet temperature too low could cause shut off to occur too early in the day and thus waste available energy that might otherwise be collected.

1.2.2.b Specified Collector Fluid Temperature Rise

This control strategy is very similar to the constant collector outlet temperature control. The only difference being that the specified collector outlet temperature is continually altered so that it remains a fixed temperature rise above the temperature at the bottom of the preheat storage. Correct specification of the constant fluid temperature rise across the collector could improve performance over constant temperature outlet control on days with low radiation and in late afternoon.

1.2.2.c Proportional to Utilizable Radiation

Perhaps the most promising variable flow rate control strategy is that of varying the collector fluid flow rate proportionately to the

utilizable solar radiation. The utilizable radiation is that level of incident radiation above the critical threshold level. The critical threshold level is simply the minimum amount of incident radiation necessary to overcome collector losses, or produce useful energy gain. A variable speed pump could be controlled proportionately to the incident radiation by either measuring the radiation at the collectors, or by powering the pump with a small photovoltaics panel located near the collectors whose output would be proportional to the incident radiation. The flow rate could be controlled proportionately to the utilizable radiation by also measuring the collector inlet and ambient temperatures. In order to avoid recirculation, the total daily collector flow would have to be limited. This would require advance knowledge of future weather conditions which would make practical application difficult.

1.3 Alternative Control Strategies-Variable Volume Storage

Another possible means of improving SDHW system performance is through the use of a variable volume preheat storage tank (3,4). A variable volume system is shown schematically in Figure 1.2. The collectors are fed directly from the mains water and the collector outlet empties into a storage tank where the level of fluid is allowed to vary. Load flow is withdrawn from this tank as needed. If collector flow occurs when the preheat tank is full, it is allowed to recirculate through the collectors. If load flow occurs when it is empty, make-up water is added from the mains. Internal heating elements keep the water in the auxiliary tank at the set temperature

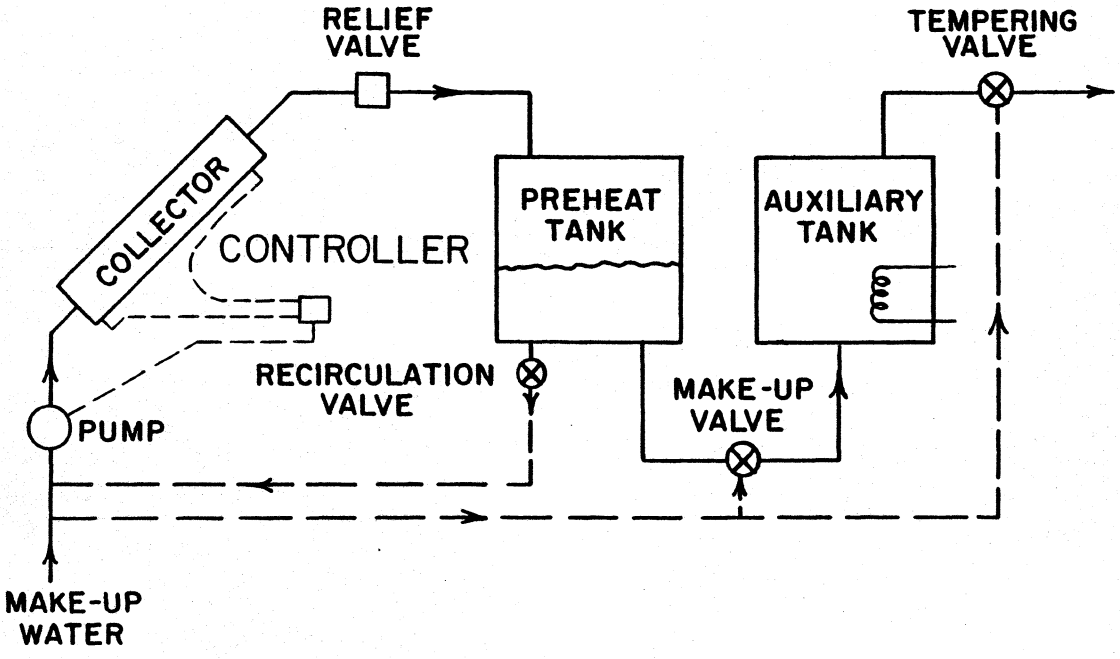

Figure 1.2 Variable Preheat Storage Volume System Schematic

and a tempering valve limits the temperature of the water delivered to the load to the set temperature. Mixing of solar heated and mains supply water in the preheat tank is eliminated which enables more of the collected energy to be removed from the preheat tank. The collectors operate with the lowest possible inlet temperature, and thus at high collector efficiency. The performance of this system might also be improved through the use of floating inlets and outlets in the preheat tank, thus allowing some of the benefits of thermal stratification. It might also be desirable to limit the collector flow to avoid filling the preheat storage and causing recirculation.

1.3.1 Reduced Constant Collector Fluid Flow Rate

This variable volume system could be controlled with a fixed collector flow rate, on-off differential control similar to that described in Section 1.2.1. The only difference being that the differential controller would sense the collector outlet and inlet temperatures instead of the fluid temperatures at the collector outlet and bottom of the preheat tank.

1.3.2 Variable Collector Fluid Flow Rate

Further improvement in the performance of SDHW systems using variable volume storage might be realized through the use of any of the variable collector fluid flow rate schemes previously described in Section 1.2.2.

1.4 Objective

The objective of this thesis is to study the thermal performance of SDHW systems utilizing the aforementioned alternative control strategies. Previous work (3-9) is validated and expanded upon through the use of detailed TRNSYS (13) simulations.

Chapter 2 gives a description of how TRNSYS was used to model the SDHW systems. A detailed description of all the nonstandard TRNSYS components (ie. not included in the current TRNSYS library) is given. The assumptions made in these models and their accuracy is discussed.

Chapter 3 presents the results of an analytical study using the TRNSYS simulation program to predict the performance of these alternative SDHW systems while operating under realistic conditions.

The effects on system performance of: collector fluid flow rate, time of year, location, collector area and quality, preheat storage tank volume and energy losses, controller temperature deadbands, auxiliary set temperature, total daily load, load distribution, and degree of thermal stratification are investigated. The performance of constant volume systems using variable collector flow rates to achieve a fixed collector outlet temperature or fixed collector temperature rise, and variable flow rates based on the utilizable radiation are examined. Finally the performance results of systems using variable volume storage while operating with either constant or variable collector flow rates are presented.

Chapter 4 draws conclusions from these results and discusses their accuracy and implications. A general discussion concerning alternative control strategies is included with suggestions for future work in this area.

CHAPTER 2

COMPONENT MODEL DESCRIPTION

All components used in modeling the conventional and alternative control strategy systems are standard TRNSYS (13) subroutines except the: collector model, plug-flow storage tank model, variable volume storage tank model, plug-flow recirculation monitor, and critical radiation calculator. This chapter presents a description of the formulation and operation of these models. A brief description of the Type 4, multi-node, storage tank is also included. The documentation and subroutine listings of these models is in Appendix A. Sample TRNSYS simulation decks for the: base case, plug-flow, on-off control, constant reduced collector fluid flow rate system; daily proportionality constant calculation; and variable volume, variable flow rate system are listed in Appendix B.

2.1 Collector Model

The collector model has both a fixed and variable flow rate mode of operation. In the fixed or constant flow rate mode, the collector outlet temperature is calculated based on ambient conditions, collector inlet temperature, and a specified constant collector fluid flow rate. Both the conventional on-off control and the reduced constant collector flow rate, on-off control, systems use this mode. The proportional to utilizable radiation control also uses this mode. A different flow rate is supplied to the collector model from the TRNSYS deck (the calculation of which is outlined in Section 3.3.3) each simulation time step.

In the variable flow rate mode, a collector fluid flow rate is calculated based on ambient conditions, collector inlet temperature, and a user specified outlet temperature. This outlet temperature is a constant in the specified collector outlet temperature system control; and is updated each simulation time step to be a constant amount above the temperature in the bottom of the preheat tank in the fixed collector temperature rise system control.

2.1.1 Constant Collector Fluid Flow Rate

The collector performance is modeled with the Hottel-Whillier (11) Equation:

$$Q_u = A_c[F_R(\tau\alpha)_n K_{\tau\alpha} G_T - F_R U_L(T_i - T_a)]^+ \qquad [2\text{-}1]$$

where:

Q_u = rate of useful energy gain

A_c = collector area

$F_R(\tau\alpha)_n$ = intercept of the collector efficiency vs. $(T_i-T_a)/G_T$ curve at $\dot{m}_c|_{test}$, at normal solar incidence

$K_{\tau\alpha}$ = incidence angle modifier

G_T = instantaneous incident radiation on the collector surface per unit area

$F_R U_L$ = negative of the slope of the collector efficiency vs. $(T_i-T_a)/G_T$ curve at $\dot{m}_c|_{test}$

T_i = collector inlet temperature

T_a = ambient temperature

The parameters $F_R U_L$ and $F_R(\tau\alpha)_n$ are obtained from a least squares curve fit to performance test data taken at some $\dot{m}_c|_{test}$, where the collector efficiency, η, is expressed as:

$$\eta = Q_u/G_t = F_R(\tau\alpha)_n K_{\tau\alpha} - F_R U_L (T_i - T_a)/G_t \qquad [2\text{-}2]$$

The incidence angle modifier (14) is a function of solar incidence angle and can be represented as:

$$K_{\tau\alpha} = 1 - b_o[(1/\cos\theta)^{-1} - 1] \qquad [2\text{-}3]$$

where:

b_o = incidence angle modifier coefficient from ASHRAE 93-77 test (b_o is positive)

θ = incidence angle, angle between beam radiation on a surface and the normal to that surface

The collector model treats beam, diffuse sky, and ground-reflected radiation independently and evaluates $K_{\tau\alpha}$ using:

$$K_{\tau\alpha} = (K_{\tau\alpha,B} G_{BT} + K_{\tau\alpha,S} G_S + K_{\tau\alpha,G} G_G)/G_T \qquad [2\text{-}4]$$

where:

$K_{\tau\alpha,B}$ = incidence angle modifier for beam radiation

G_{BT} = beam component of G_T

$K_{\tau\alpha,S}$ = incidence angle modifier for diffuse sky radiation

G_S = diffuse sky component of G_T

$K_{\tau\alpha,G}$ = incidence angle modifier for ground-reflected radiation

G_G = ground-reflected component of G_T

$K_{\tau\alpha,B}$ may be evaluated with Equation [2-3] using θ. $K_{\tau\alpha,S}$ and $K_{\tau\alpha,G}$ may also be evaluated with Equation [2-3] substituting θ_{es} and θ_{eg} respectively for θ. θ_{es} and θ_{eg} are effective angles for sky and ground-reflected diffuse radiation and are given by (15):

$$\theta_{es} = 59.98 - 0.1388\beta + 0.001497\beta^2 \qquad [2\text{-}5]$$

$$\theta_{eg} = 90.0 - 0.5788\beta + 0.002693\beta^2 \qquad [2\text{-}6]$$

where:

β = collector slope

The values of collector performance parameters $F_R U_L$ and $F_R(\tau\alpha)_n$ are affected by collector flow rate through the dependence of F_R on flow rate per unit area. This dependence is shown in Figure 2.1 and may be expressed as (14):

$$F_R = \frac{\dot{m}_c C_p}{A_c U_L}\left[1 - e^{-(A_c U_L F'/\dot{m}_c C_p)}\right] \qquad [2\text{-}7]$$

where:

F_R = collector heat removal factor

$\dot{m}_c$ = collector fluid flow rate

C_p = collector fluid constant pressure specific heat

F' = collector efficiency factor

U_L = collector loss coefficient

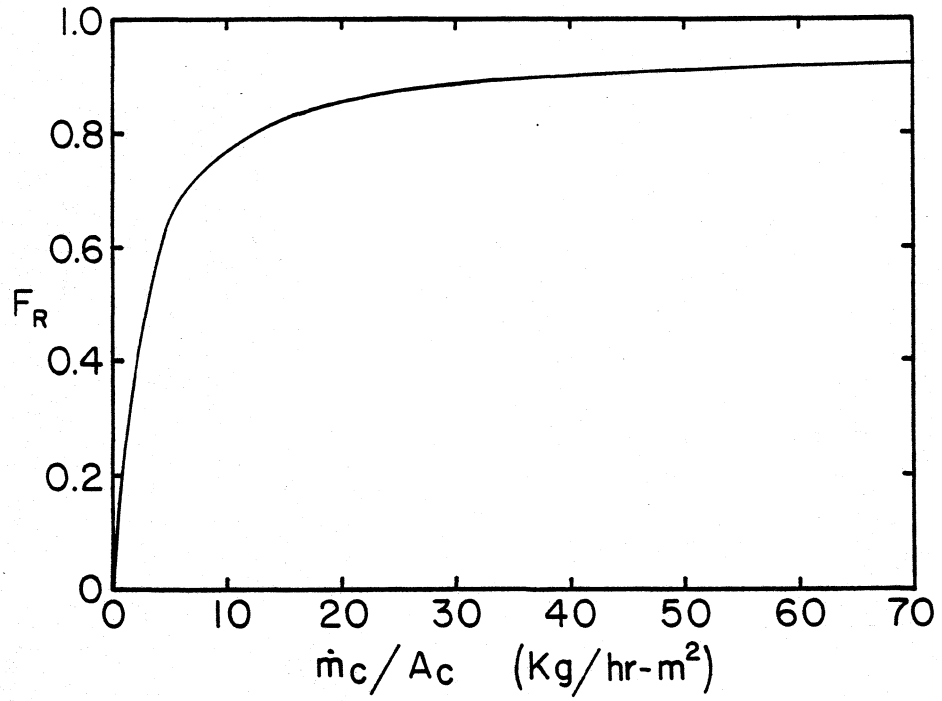

Figure 2.1 Dependence of Collector Heat Removal Factor on Collector Fluid Flow Rate per Unit Area

Assuming the collector efficiency factor, F', and the collector loss coefficient, U_L, are independent of flow rate, $F_R U_L$ and $F_R(\tau\alpha)_n$ can be modified for any flow rate using an analytical correction ratio, r, which is derived in reference (14).

$$r = \frac{\dfrac{\dot{m}_c C_p}{A_c F' U_L}\left[1 - e^{(A_c F' U_L/\dot{m}_c C_p)}\right]\Big|_{use}}{\dfrac{\dot{m}_c C_p}{A_c F' U_L}\left[1 - e^{(A_c F' U_L/\dot{m}_c C_p)}\right]\Big|_{test}} \qquad [2\text{-}8]$$

For liquid collectors $F'U_L$ in both the numerator and denominator of Equation [2-8] may be evaluated at the test flow rate using (14):

$$F'U_L = \frac{\dot{m}_c C_p}{A_c} \ln\left[1 - \frac{A_c F_R U_L}{\dot{m}_c C_p}\right] \qquad [2\text{-}9]$$

At conventional flow rates (50 ℓ /hr m^2) the flow through the absorber plate tubes is generally laminar, but the temperature profile may not be fully developed. Heat transfer relations for the developing region (16) give the heat transfer coefficient as a function of flow rate. For the base case collector considered in this study, the heat transfer coefficient at slow flow rates (approximately 10 ℓ /hr m^2) was on the order of thirty percent less than for conventional collector flow rates. However, the magnitude of the fluid heat transfer coefficient, relative to the other factors such as bond conductance, etc., is such that F' is reduced by only one percent at slow flow rates.

Axial conduction in the absorber plate and variations in collector loss coefficient due to axial temperature gradients were neglected in the collector model. The effect of these assumptions at reduced flow rates has been examined by Phillips (15). Although these factors can have a significant effect on collector performance, they can be minimized with proper collector design.

For constant collector flow rate operation, there exists a minimum amount of radiation necessary for collector energy gains to outweigh collector losses and produce useful energy gains. This critical threshold level, $G_{T,C}$, may be determined by setting the useful energy

gain in Equation [2-1] to zero and solving for G_T:

$$G_{T,C} = \frac{F_R U_L (T_i - T_a)}{F_R (\tau\alpha)_n K_{\tau\alpha}} \qquad [2\text{-}10]$$

2.1.2 Variable Collector Fluid Flow Rate

When variable collector flow rate operation is used to obtain a specified collector outlet temperature, or temperature rise across the collector, a new collector flow rate is calculated within the collector model each simulation time step. This flow rate is determined as follows. Using $F' U_L$ from Equation [2-9] evaluated at the test collector flow rate in both the numerator and denominator of Equation [2-8] enables Equation [2-8] to be expressed as:

$$r = \frac{\frac{\dot{m}_c C_p}{A_c}\left[1 - e^{(A_c F' U_L / \dot{m}_c C_p)}\right]\Big|_{use}}{\frac{\dot{m}_c C_p}{A_c}\left[1 - e^{(A_c F' U_L / \dot{m}_c C_p)}\right]\Big|_{test}} \qquad [2\text{-}11]$$

The denominator of Equation [2-11] is simply Equation [2-7] evaluated at the test flow rate divided by U_L, thus:

$$r = \frac{\frac{\dot{m}_c C_p}{A_c}\left[1 - e^{(A_c F' U_L / \dot{m}_c C_p)}\right]\Big|_{use}}{F_R U_L} \qquad [2\text{-}12]$$

Inserting Equation [2-12] into Equation [2-1] to correct for non-test flow rate yields:

$$Q_u = \frac{\dot{m}_c C_p\left[1 - e^{(A_c F' U_L/\dot{m}_c C_p)}\right]\left[F_R(\tau\alpha)_n K_{\tau\alpha} G_T - F_R U_L(T_i - T_a)\right]}{F_R U_L} \quad [2\text{-}13]$$

The rate of useful energy collection may also be expressed as:

$$Q_u = \dot{m}_c C_p (T_o - T_i) \quad [2\text{-}14]$$

where:

T_o = collector outlet temperature

Equating Equations [2-13] and [2-14], canceling $\dot{m}_c C_p$ from both sides and rearranging:

$$e^{-(A_c F' U_L/\dot{m}_c C_p)}\Big|_{use} = 1 - \frac{F_R U_L(T_o - T_i)}{F_R(\tau\alpha)_n K_{\tau\alpha} G_T - F_R U_L(T_i - T_a)} \quad [2\text{-}15]$$

Taking the natural logarithm of both sides and solving for $\dot{m}_c$ yields:

$$\dot{m}_c = \frac{-A_c F' U_L}{C_p \ell n\left[1 - \frac{F_R U_L(T_o - T_i)}{F_R(\tau\alpha)_n K_{\tau\alpha} G_T - F_R U_L(T_i - T_a)}\right]} \quad [2\text{-}16]$$

or:

$$\dot{m}_c = \frac{-A_c F' U_L}{C_p \ell n\left[1 - \frac{(T_o - T_i)}{F_R(\tau\alpha)_n K_{\tau\alpha} G_T / F_R U_L - (T_i - T_a)}\right]} \qquad [2\text{-}17]$$

The necessary flow rate to obtain any collector outlet temperature can be calculated based on ambient conditions and collector inlet temperature using Equation [2-17]. In order to avoid the occurrence of unrealistically high collector flow rates, the model has a maximum flow rate which is input as a user specified parameter. When this occurs, Equation [2-13] is used to calculate the rate of useful energy gain at the maximum collector flow rate. Collector outlet temperature is then calculated using Equation [2-14]. For all variable collector flow rate simulations run, the maximum collector flow rate was set to 150 ℓ /hr m^2.

For variable collector flow rate operation there also exists some minimum amount of radiation required for collector energy gains to outweigh collector losses and achieve the desired outlet temperature. This minimum required radiation may be determined by taking the limit of Equation [2-14] as useful energy gain tends towards zero. Because both the collector inlet and outlet temperatures are fixed the collector flow rate will go to zero. Taking the limit of Equation

[2-17] as collector flow rate goes to zero yields:

$$e^{1/\ell n\left[1 - \frac{(T_o - T_i)}{F_R(\tau\alpha)_n K_{\tau\alpha}\, G_T/F_R U_L - (T_i - T_a)}\right]} = 1 \qquad [2\text{-}18]$$

thus:

$$1 - \frac{(T_o - T_i)}{F_R(\tau\alpha)_n K_{\tau\alpha}\, G_T/F_R U_L - (T_i - T_a)} = 0 \qquad [2\text{-}19]$$

and solving for G_T:

$$G_{T,MIN} = \frac{F_R U_L (T_o - T_i)}{F_R(\tau\alpha)_n K_{\tau\alpha}} \qquad [2\text{-}20]$$

The collector inlet temperature in Equation [2-10] has been replaced by collector outlet temperature in Equation [2-20]; thus the minimum radiation for variable collector flow rate operation is generally higher than for constant flow rate operation because the incident radiation must not only outweigh collector losses but must also be sufficient to achieve the desired outlet temperature as well.

2.2 Multi-Node Storage Tank Model

The thermal performance of the auxiliary tank was modeled with the TRNSYS (13) ,Type 4, multi-node storage tank using one node (i.e. fully-mixed). The preheat tank was also modeled with Type 4, using one node for the fully-mixed case, and 3, 5, 7, and 10 nodes for varying degrees of stratified storage. The multi-node tank model represents

thermal stratification by dividing the tank into a user specified number of fully-mixed, equal volume, segments or nodes. Mass and energy balances are performed individually on each node. The resulting set of differential equations are then solved simultaneously. Veltkamp (5) has shown that in order to accurately model the performance of a stratified storage tank at low flow rates as many as 60 nodes may be required. With this many nodes, very small simulation time steps are required, so simulations of SDHW performance for extended periods of time are expensive.

2.3 Plug-Flow Storage Tank Model

Rather than using the TRNSYS, Type 4, multi-node tank model, to represent stratification in the preheat storage tank, an algebraic, plug-flow model (13) was used. One important advantage of the plug-flow model is that it does not solve systems of simultaneous equations as does the multi-node model, and is therefore much less costly to use. This model uses a variable number of variable size segments of fluid to model stratification. A description of its operation is shown in Figure 2.2, which is a series of tank temperature profiles where fluid temperature is plotted vs. height inside the tank. The top profile represents some initial temperature profile at time t_1. When collector flow occurs a uniform temperature segment of fluid, whose size depends on collector flow and simulation time step, is inserted into the tank profile at the appropriate location thus shifting the position of all existing segments below the inlet. If a load flow occurs the profile is again shifted by insertion of a segment

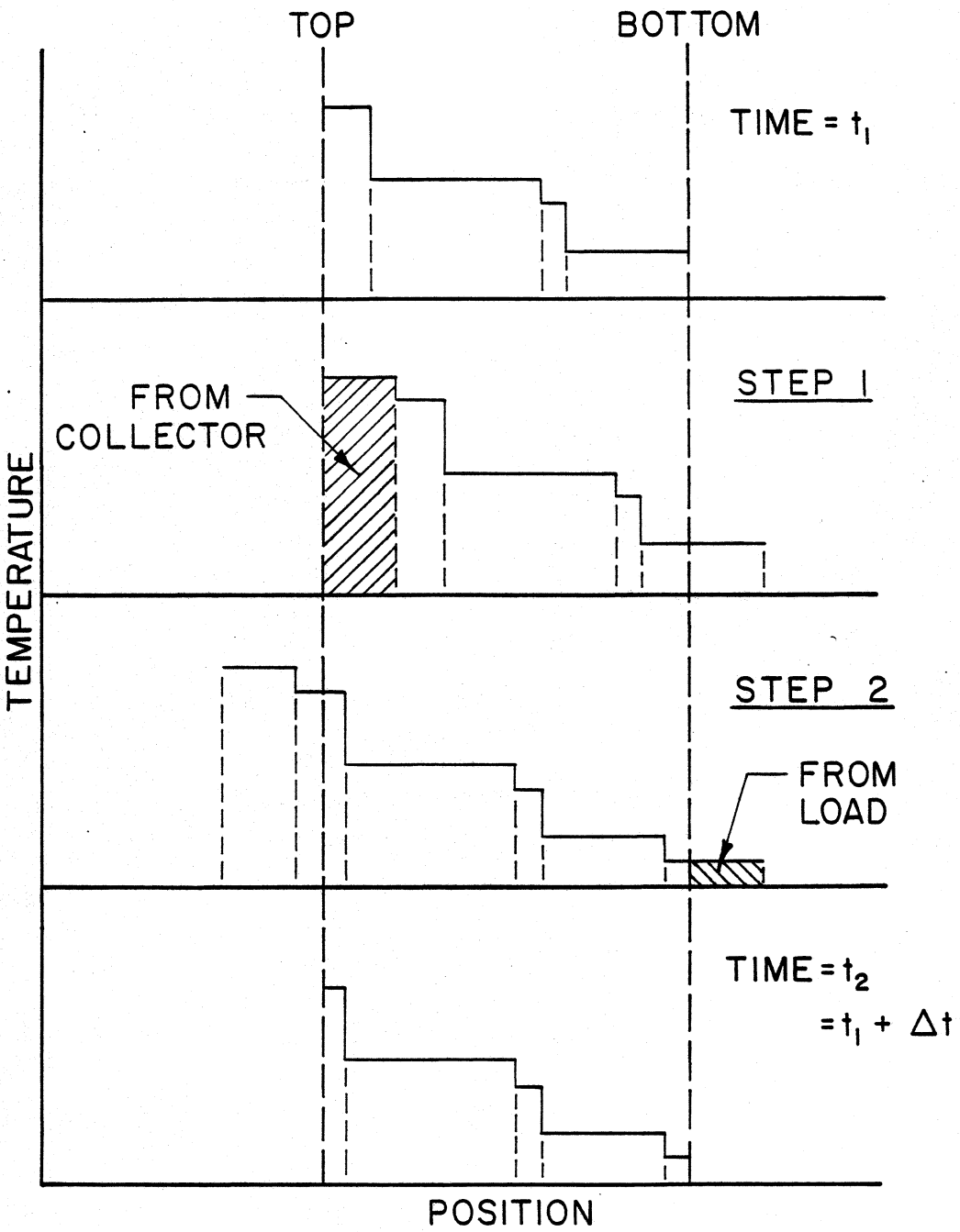

Figure 2.2 Operation of Plug-Flow Storage Tank Model

of fluid at the mains temperature and equal in size to the load flow. The segments and/or fraction of segments whose position falls outside the bounds of the tank are returned to the collector and/or load. The return temperatures are calculated based on a volume-weighted average. Storage losses are then calculated individually for each segment. Each segment is assumed to be a uniform temperature slug of fluid and there is no interaction between segments, such as conduction or convective mixing. There are two modes of operation. In mode 1, the tank has fixed inlet positions and any temperature inversions are eliminated by mixing with appropriate adjacent nodes. In mode 2, the tank has variable inlet positions and new segments are inserted at levels nearest to their own temperature which produce no temperature inversions (i.e. perfect stratification). If the inlet temperatures are within 0.5 ° C of an existing segment, the collector or load flow will combine with that segment instead of creating a new one.

The variable inlet mode should provide an upper limit on system performance because it allows the maximum possible thermal stratification. All results presented in this study, unless otherwise indicated were generated using the plug-flow tank in the variable inlet mode, thus they represent an upper limit on performance of SDHW systems at reduced flow rates. A fully-mixed preheat tank (1 node) more accurately predicts the performance of SDHW systems at high flow rates and thus provides the lower limit on performance. A performance comparison between the variable and fixed inlet plug-flow tank models, and the multi-node model appears in Section 3.2.1.

2.4 Variable Volume Storage Tank Model

The basic operation of the variable volume storage tank is described in Section 1.3. It contains a variable mass of fully-mixed fluid. An energy balance at time t can be written on the tank as:

$$\dot{m}_c C_p T_o - \dot{m}_L C_p T - \dot{m}_r C_p T - (UA)_t (T - T_{env}) = \frac{C_v d(MT)}{dt} \qquad [2\text{-}21]$$

where:

$\dot{m}_L$ = load flow rate

T = instantaneous temperature of fluid in tank

$\dot{m}_r$ = tank fluid recirculation to collector flow rate

$(UA)_t$ = total overall tank loss coefficient area product

T_{env} = environmental temperature surrounding tank

C_v = tank fluid constant volume specific heat

M = instantaneous mass of fluid in tank

t = time

A mass balance on the tank may also be written as:

$$\dot{m}_c - \dot{m}_L - \dot{m}_r = \frac{dM}{dt} \qquad [2\text{-}22]$$

The variable volume tank model uses an analytical solution to these two simultaneous differential Equations ([2-21] and [2-22]) to calculate the mass and temperature of the fluid in the tank each simulation time step. Tank energy losses and energy flow rates out of the tank are then calculated.

2.5 Other Nonstandard TRNSYS Components

Two other nonstandard TRNSYS components called "RECIR" and "IF-CALC" were used in the simulations. The RECIR subroutine is used in all plug-flow simulations. It keeps track of an imaginary boundary in the preheat tank between the solar heated water and the cooler mains temperature water. It also outputs the flow rate of solar heated water recirculating to the collector, when recirculation occurs; and the minimum amount of cold fluid in the bottom of the tank over a user specified period of time (i.e. one day), if recirculation does not occur. The "IF-CALC" subroutine simply performs logical if statements to aid in the calculation of the instantaneous critical level.

CHAPTER 3

SIMULATION RESULTS AND DISCUSSION

This chapter presents the results of an analytical study using the TRNSYS simulation program to predict the performance of SDHW systems utilizing the aforementioned control strategies while operating under realistic conditions. The effects on system performance of: collector fluid flow rate, location, time of year, collector quality and area, preheat storage tank volume and energy losses, controller temperature deadbands, auxiliary set temperature, total daily load, load distribution, and degree of thermal stratification are investigated. Then the performance of constant volume systems using variable collector flow rates to achieve a fixed collector outlet temperature or fixed temperature rise, and variable flow based on the utilizable radiation is examined. Next the performance results of systems using variable volume storage while operating with either constant or variable collector flow rates are presented. Finally a direct comparison between all the alternative control strategies examined is given.

All results presented in this chapter are based on the previously described systems. The basic system specifications for all systems used are as listed in Table 3.1 unless otherwise indicated. The mains water temperature varies as shown in Table 3.2 and the base case load distribution is the Rand profile (18). The differential temperature controller has an 8.9 ° C upper deadband and a 1.7 ° C lower deadband. Typical meteorological year (TMY) weather data (19) were used in all simulations. All performance comparisons made in this chapter are

Table 3.1 System Specifications

Description	Value
Base Case Collector:	
A_c	4.2 m^2
$F_R(\tau\alpha)_{n\ test}$	0.805
$F_R U_{L\ test}$	4.73 $W/m^2\ ^\circ C$
$\dot{m}_c\|_{test}$	72 $\ell/hr\ m^2$
b_o	0.0989
Preheat Tank:	
V_{PT}	303 ℓ
U_{PT}	1.081 $W/m^2\ ^\circ C$
T_{env} (PT & AT)	21 $^\circ C$
Auxiliary Tank:	
V_{AT}	151 ℓ
U_{AT}	1.047 $W/M^2\ ^\circ C$
T_{SET}	60 $^\circ C$
$\dot{Q}_{AUX,MAX}$ (2 heaters)	4500 W each
Load:	
Volume (Distributed over Rand profile)	300 ℓ/day
Higher Quality Collector: (Corrected to $\dot{m}_c$ = 72 ℓ/hr m^2)	
$F_R(\tau\alpha)_n$	0.754
$F_R U_L$	3.62 $W/m^2\ ^\circ C$
Lower Quality Collector: (Corrected to $\dot{m}_c$ = 72 ℓ/hr m^2)	
$F_R(\tau\alpha)_n$	0.697
$F_R U_L$	8.57 $W/m^2\ ^\circ C$

Table 3.2 Yearly Variation of Mains Temperature

Month	T_m(°C)	Month	T_m(°C)	Month	T_m(°C)
January	8.2	May	17.7	September	26.1
February	9.6	June	19.1	October	20.8
March	10.4	July	19.5	November	13.1
April	12.5	August	24.9	December	10.4

presented as absolute improvements given in solar fraction.

3.1 Conventional SDHW System Control

The performance of a conventional, direct, two-tank SDHW system operating during March in Madison, Wisconsin is shown in Figure 3.1. Solar fraction is plotted vs. collector fluid flow rate per unit collector area. The solar fraction is defined as the ratio of energy delivered by the solar system to the energy required to meet the load, including auxiliary tank energy losses. The system used is that shown in Figure 1.1 and described in Section 1.1. The preheat storage is modeled as a fully-mixed tank using the TRNSYS, Type 4, multi-node model with one node.

3.1.1 Effect of Collector Fluid Flow Rate

Figure 3.1 shows a decrease in fully-mixed system performance with decreasing collector flow rate. This is a direct result of poorer collector performance at reduced flow rate. Reducing the collector

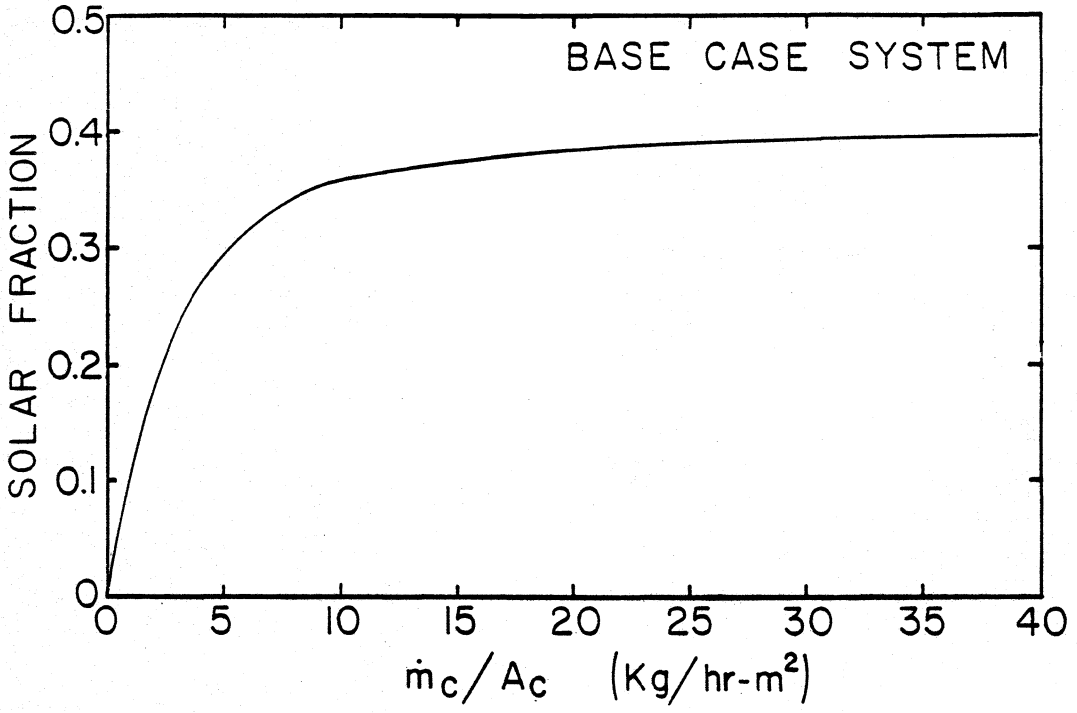

Figure 3.1 Fully-Mixed System Performance, Solar Fraction vs. Collector Flow Rate per Unit Area; for March in Madison, WI, A_c = 4.2 m², V_{PT} = 303 ℓ, LOAD = 300 ℓ/day

fluid flow rate has two opposing effects on collector performance. As shown in Figure 2.1 the collector heat removal factor, F_R, decreases with flow rate per unit area thus reducing collector performance. However, a reduction in collector flow rate indirectly causes a decrease in collector inlet temperature, and thus an increase in collector efficiency. This reduction in inlet temperature is shown in Figure 3.2 which is a tank temperature profile vs. time plot comparing the high and low flow rate operation of a fully-mixed system. The increase in efficiency due to this slight reduction in collector inlet temperature is not sufficient to outweigh the decrease in performance due to the reduction in F_R. The overall system performance therefore

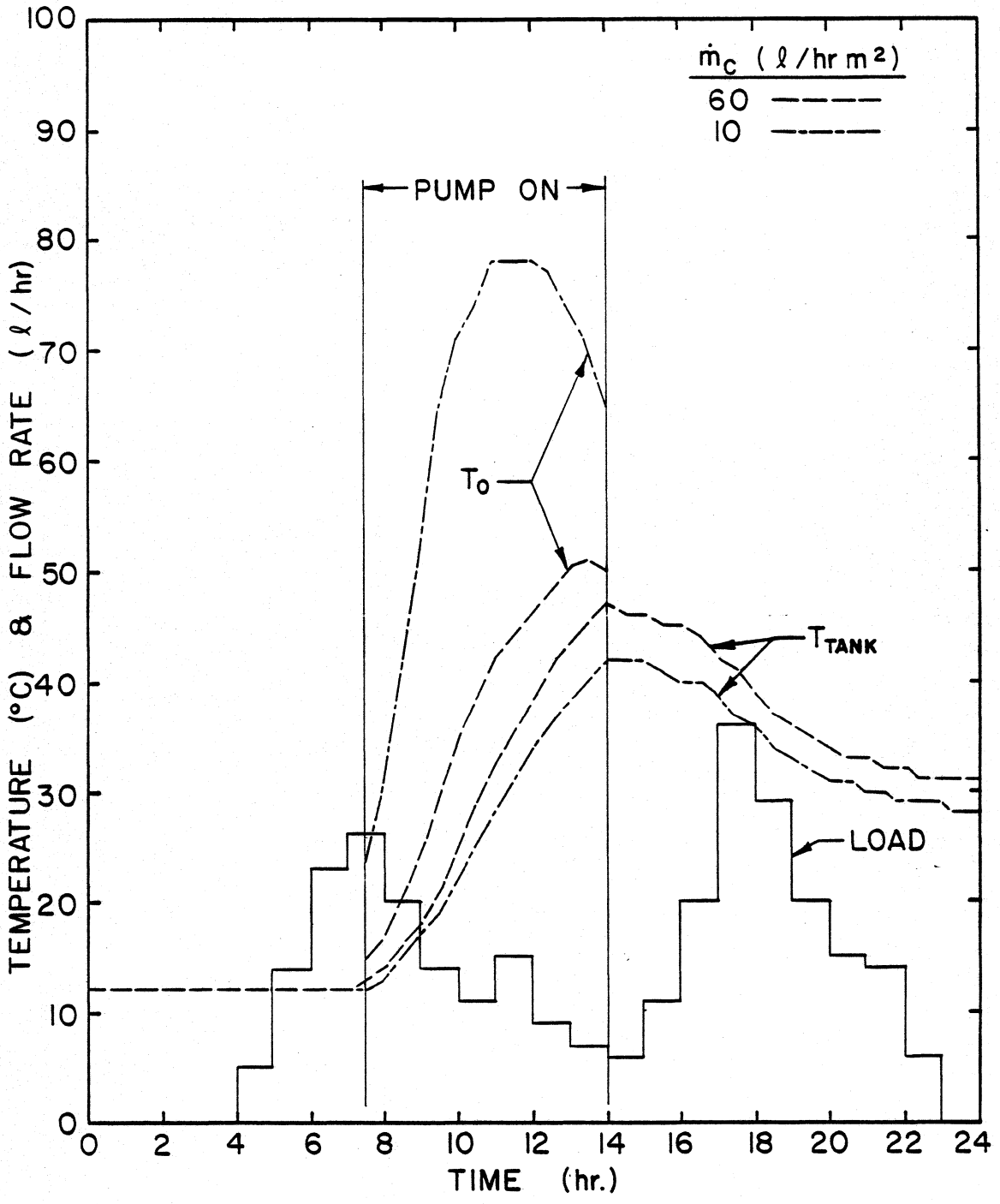

Figure 3.2 Fully-Mixed System Preheat Storage Tank Temperature Profiles; for March 2nd in Madison, WI, A_c = 4.2 m^2, V_{PT} = 303 ℓ, LOAD = 300 ℓ/day

decreases with collector flow rate. Considering the preheat storage tank as fully-mixed and thus neglecting any benefits associated with thermal stratification leads one to choose the high collector fluid flow rate control strategy as optimum.

3.2 Constant Volume Storage-Reduced Constant Collector Fluid Flow Rate

All results presented in Section 3.2 are for the direct, two-tank SDHW system shown in Figure 1.1 and described in Section 1.2.1, which will be further referred to as the base case system. The system operates at reduced constant collector flow rates with on-off differential control. The plug-flow storage tank model operating in the variable inlet mode is used in all simulations except where indicated otherwise.

3.2.1 Effect of Collector Fluid Flow Rate

When the benefits of increased thermal stratification at reduced collector fluid flow rates are considered, the increase in collector efficiency due to a decrease in collector inlet temperature often outweighs the reduction in collector performance due to a decrease in F_R. Figure 3.3 shows this to be the case as a reduced collector flow rate optimum does exists. Lower collector inlet temperatures also cause lower critical threshold levels, and thus longer collector on-times and greater useful energy collection. Figure 3.3 also compares the performance predictions of the multi-node and plug-flow tank models. The system using a multi-node model with three nodes

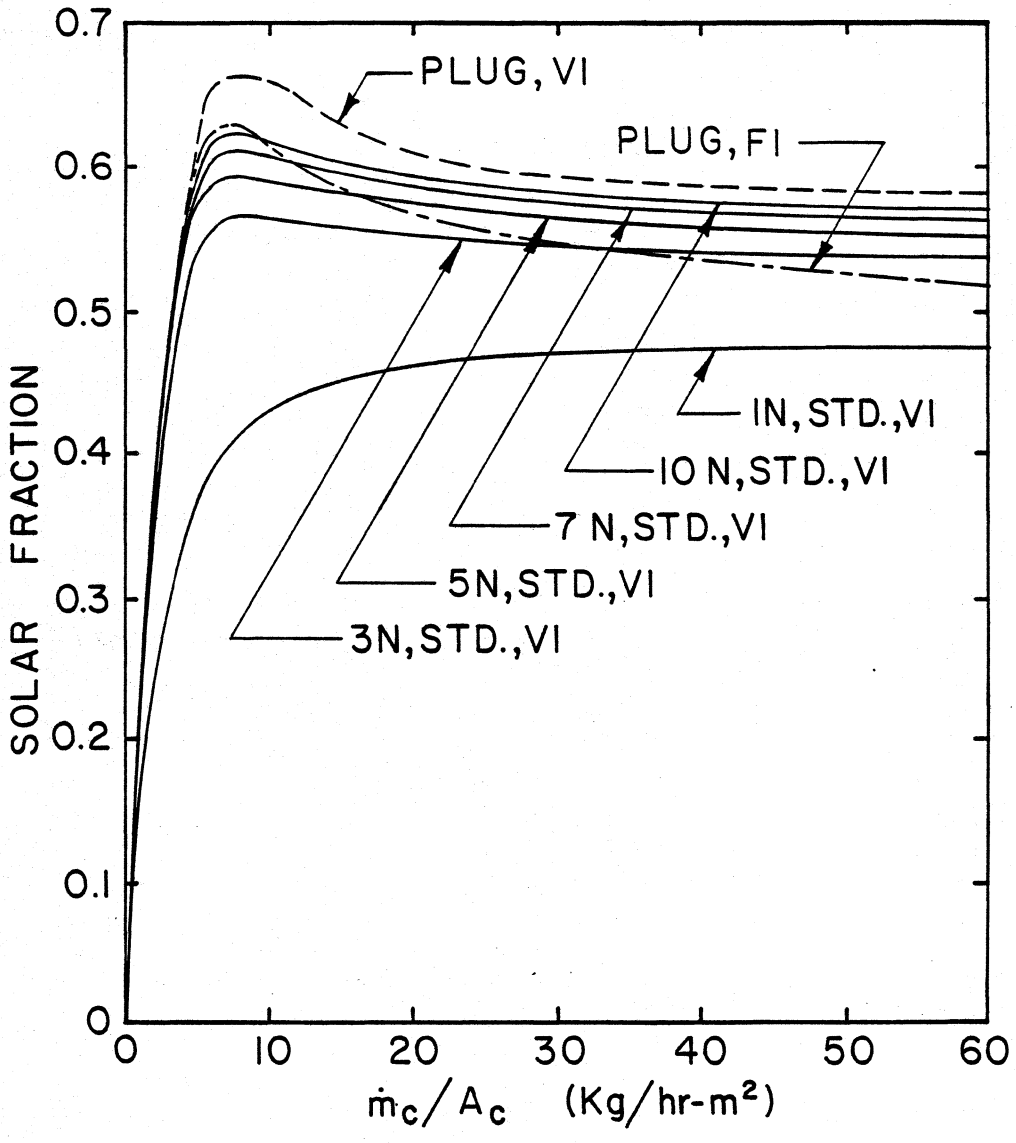

Figure 3.3 Plug-Flow vs. Multi-Node Storage Tank Model Comparison; for May in Madison, WI, A_c = 4.2 m^2, V_{PT} = 303 ℓ ,LOAD = 300 ℓ/day

operating in the variable inlet mode shows a distinct improvement over the one node, or fully-mixed system. The five, seven, and ten node variable inlet models show progressively smaller improvements in performance. The system with a plug-flow tank model in the variable inlet mode compares very well with the predictions of a multi-node model as the number of nodes specified grows large. The variable inlet plug-flow tank model represents perfect thermal stratification and thus gives an upper limit on the performance of SDHW systems. The performance of systems utilizing the fixed inlet mode of the plug-flow tank model decreases more rapidly with increasing collector flow rate and begins to approach the performance of the fully-mixed, multi-node tank model. The fixed inlet mode thus represents systems with a moderate degree of thermal stratification in storage. The fixed and variable inlet modes of the multi-node model perform similarly in that both modes show an optimum solar fraction at a collector flow rate of about 10 ℓ/hr m^2. The performance of the fixed inlet mode decreases slightly faster than the variable inlet mode as collector flow rate increases. The fully-mixed, multi-node tank model should more accurately represent conventional systems operating at high collector flow rates while the plug-flow tank model should more accurately represent the performance of stratified systems operating at reduced flow rates. Because the variable inlet mode of the plug-flow tank model represents perfect stratification and thus gives a maximum, or upper limit on the performance which could be achieved, it was used in all the remaining constant storage volume simulations.

Figures 3.4a through 3.4f are tank temperature profile vs. time plots for the variable inlet, plug-flow tank model operating at collector flow rates of 60, 20, 10, 9, 8, and 6 ℓ/hr m^2 respectively. The decrease in collector inlet temperature with decreasing collector flow rate per unit area can be easily seen by comparing Figures 3.4a through 3.4f. The collector outlet temperature, and thus the temperature of the load flow to the auxiliary, increases as collector flow rate decreases. The optimum collector flow rate for this day was nine ℓ/hr m^2. It yielded the highest average delivery temperature to the load while keeping the collector inlet temperature at a minimum.

3.2.2 Effect of Time of Year

Figure 3.5 shows the annual performance of the base case system in Madison, Wisconsin. The yearly optimum of 53.4 percent occurs at a collector fluid flow rate of nine ℓ/hr m^2, which is about twenty percent of the conventional 50 ℓ/hr m^2. The stratified storage at this reduced flow rate results in an annual solar fraction which is 14.7 percentage points greater than that which would be achieved with a fully mixed preheat tank operating at conventional collector flow rates. Time of year has some effect on optimum flow rate. As day length, and thus pump operation time decrease, optimum flow rate increases. The monthly optimums are near the yearly optimum and the curves are fairly flat in the vicinity of the optimum. Thus, only a slight improvement could be realized by adjusting the flow rate on a monthly basis.

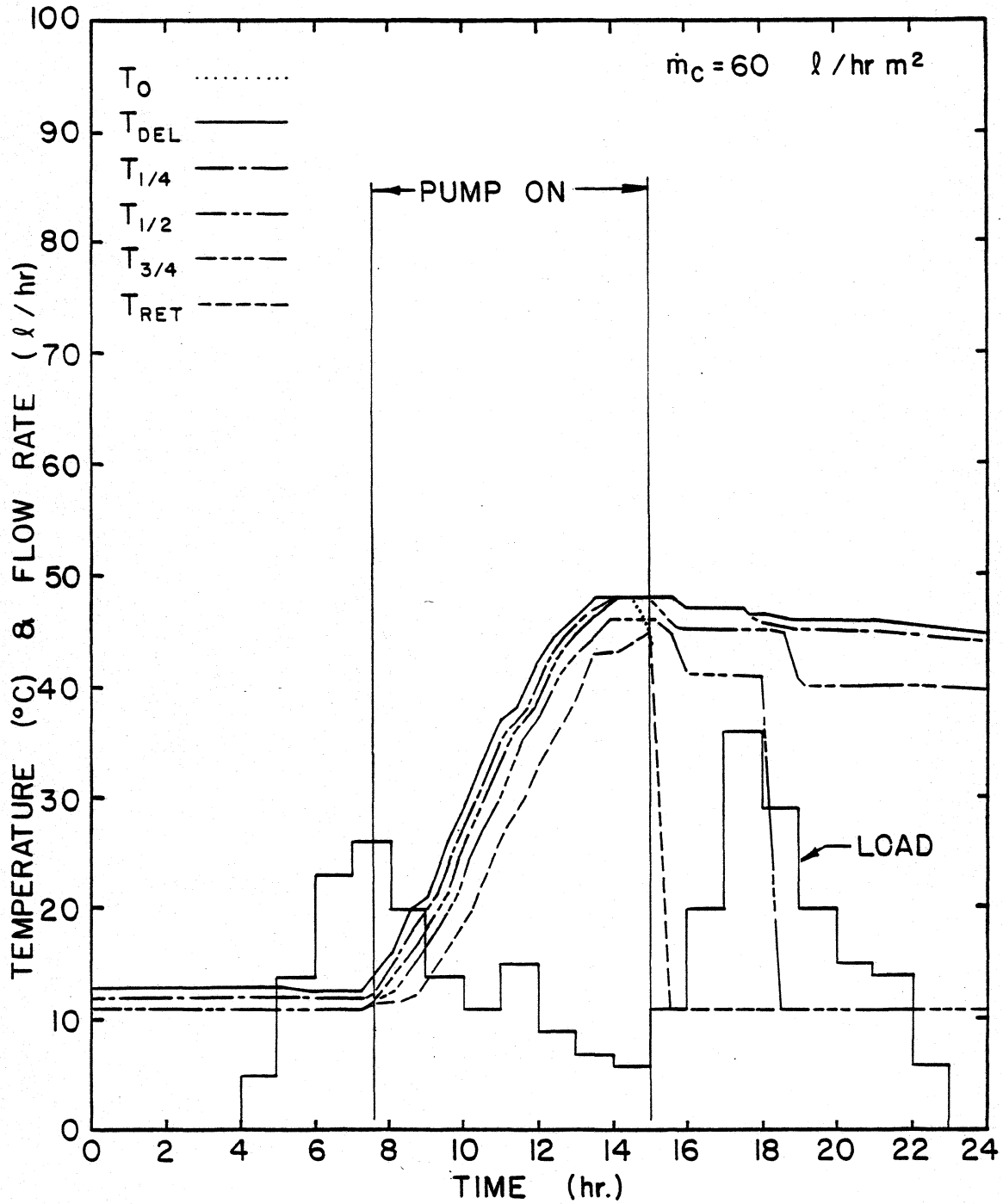

Figure 3.4a Base Case System Preheat Storage Tank Temperature Profile; for March 2nd in Madison, WI, $\dot{m}_c$ = 60 ℓ/hr m², A_c = 4.2 m², V_{PT} = 303 ℓ, LOAD = 300 ℓ/day

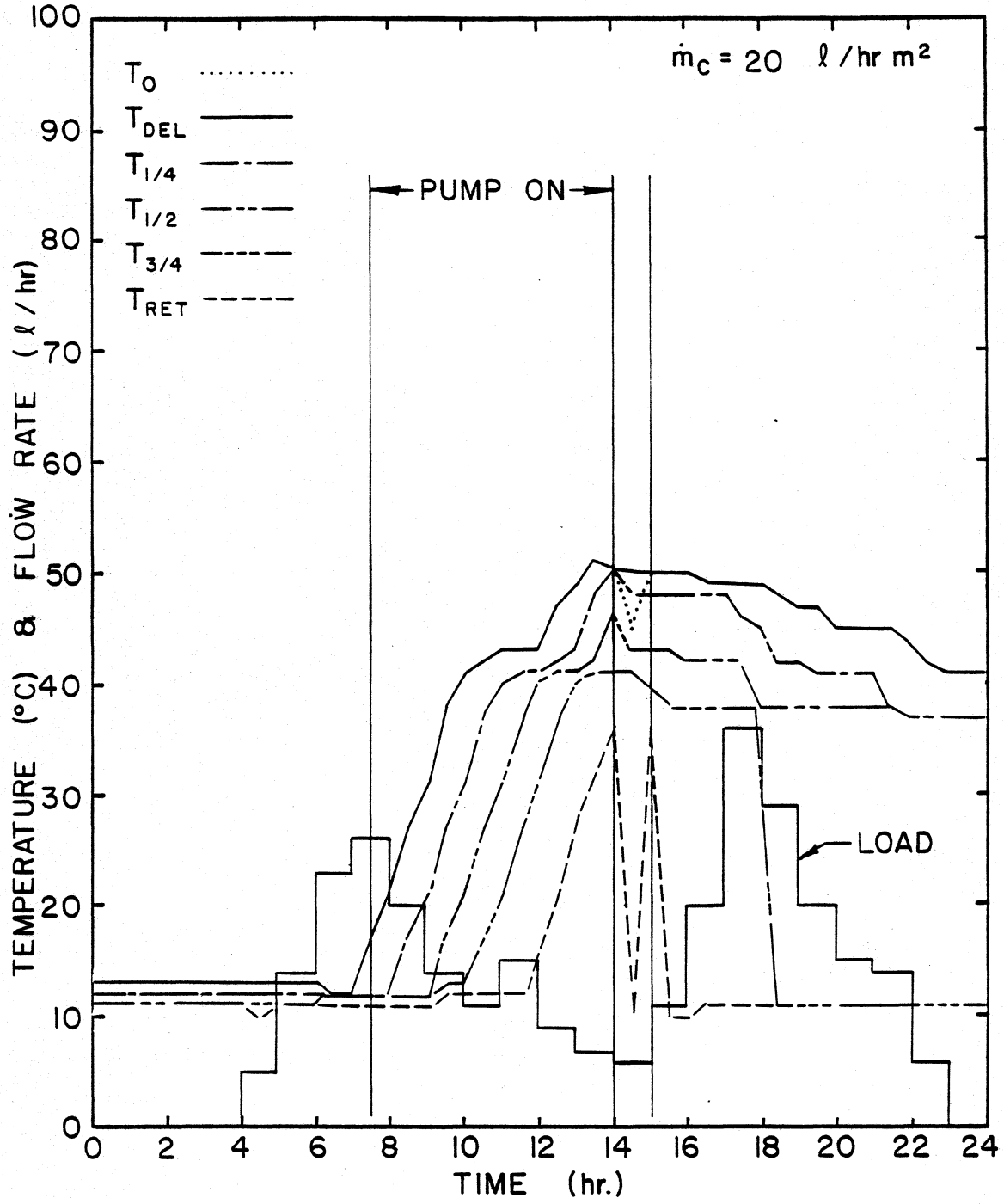

Figure 3.4b Base Case System Preheat Storage Tank Temperature Profile; for March 2nd in Madison, WI, $\dot{m}_c$ = 20 ℓ/hr m², A_c = 4.2 m², V_{PT} = 303 ℓ, LOAD = 300 ℓ/day

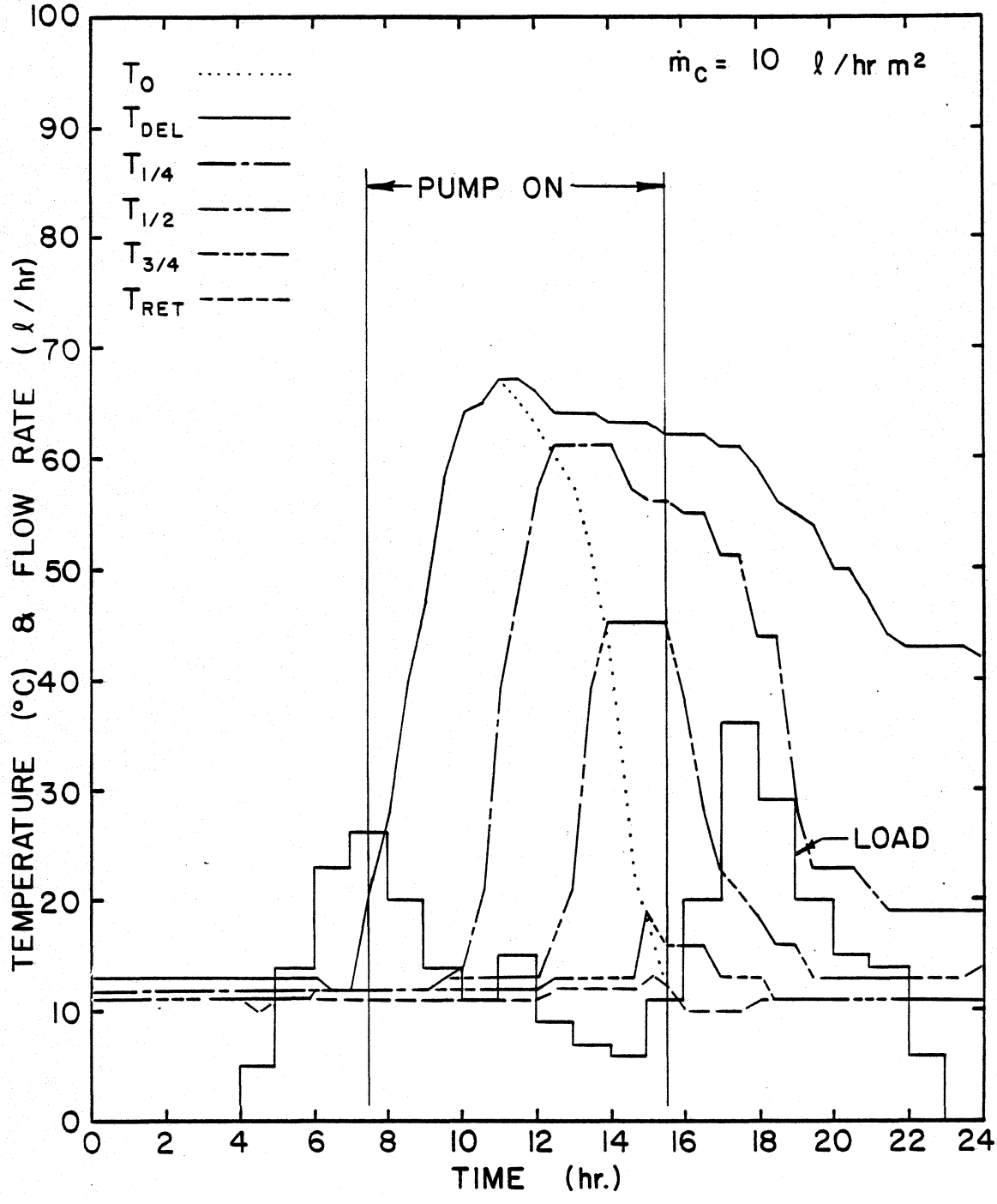

Figure 3.4c Base Case System Preheat Storage Tank Temperature Profile; for March 2nd in Madison, WI, $\dot{m}_c$ = 10 ℓ/hr m², A_c = 4.2 m², V_{PT} = 303 ℓ, LOAD = 300 ℓ/day

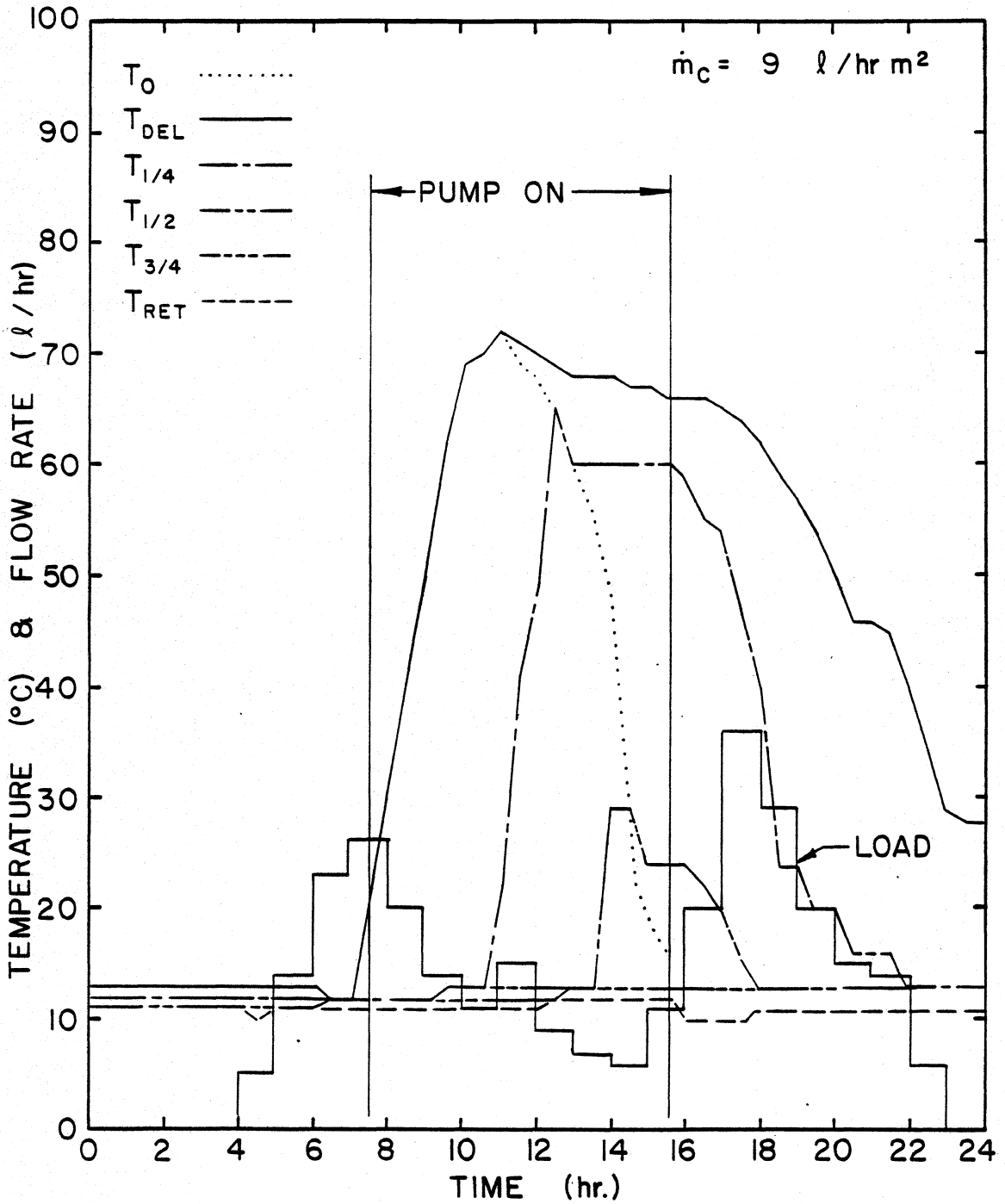

Figure 3.4d Base Case System Preheat Storage Tank Temperature Profile; for March 2nd in Madison, WI, $\dot{m}_c$ = 9 ℓ/hr m², A_c = 4.2 m², V_{PT} = 303 ℓ, LOAD = 300 ℓ/day

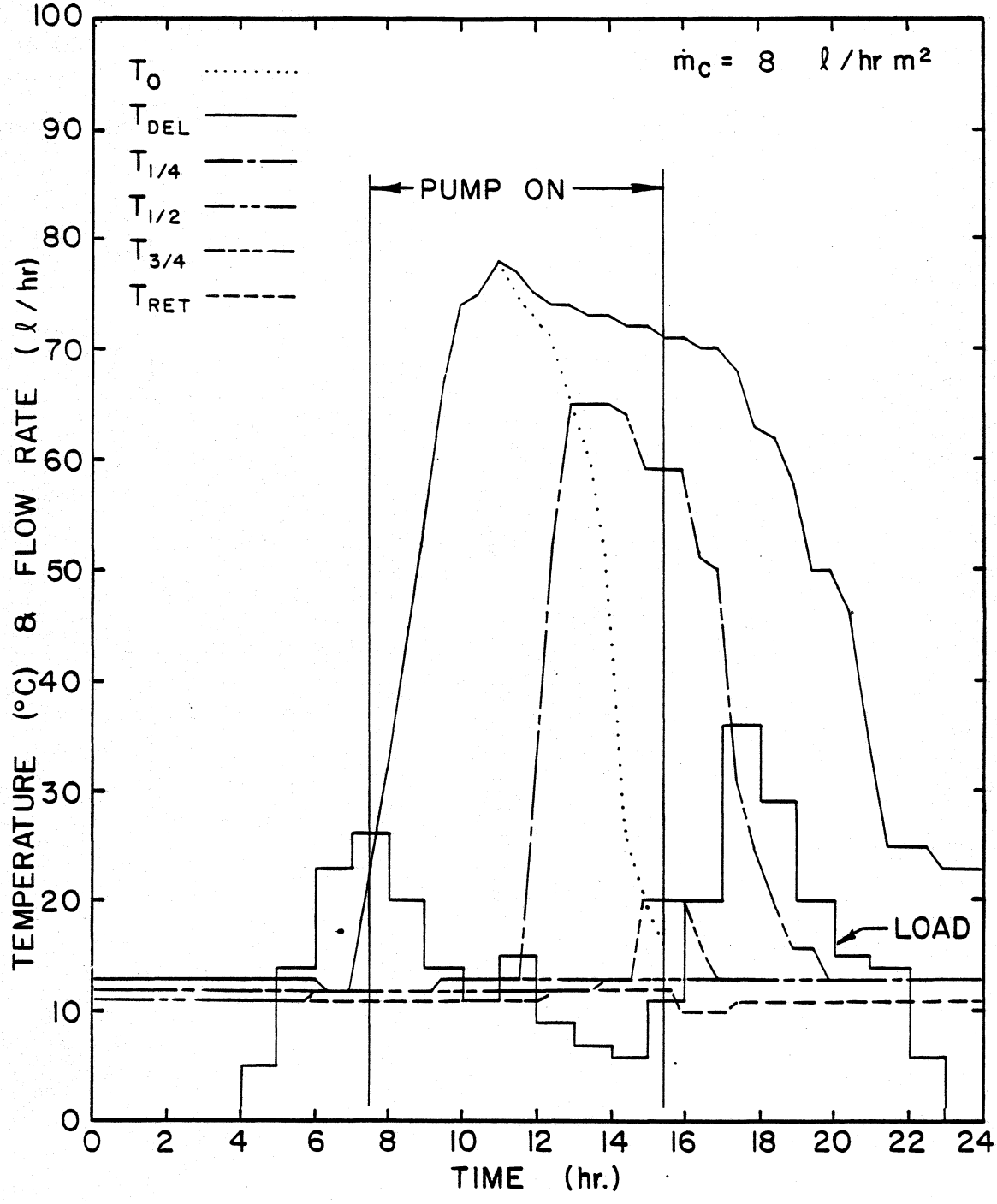

Figure 3.4e Base Case System Preheat Storage Tank Temperature Profile; for March 2nd in Madison, WI, $\dot{m}_c$ = 8 ℓ/hr m², A_c = 4.2 m², V_{PT} = 303 ℓ, LOAD = 300 ℓ/day

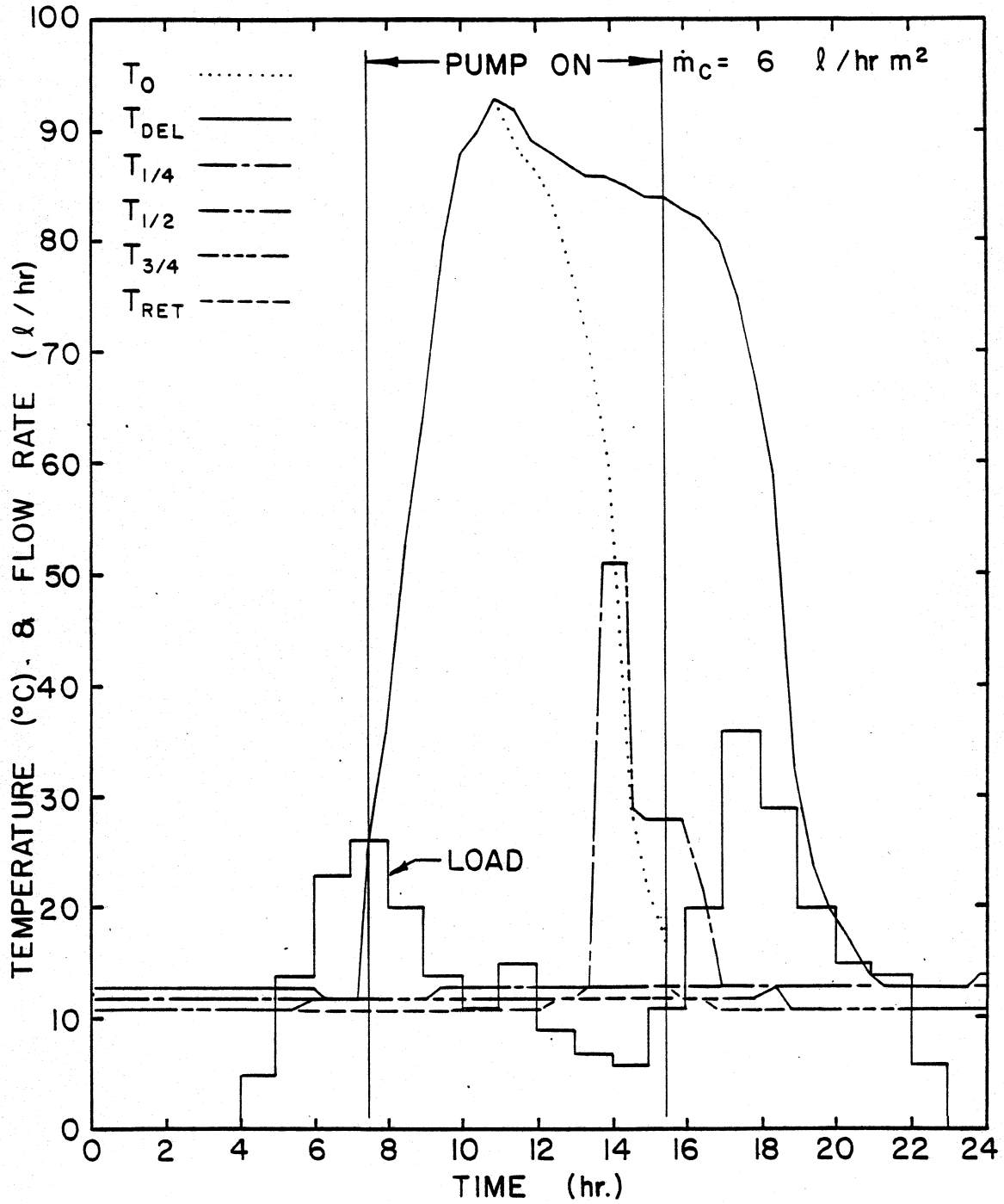

Figure 3.4f Base Case System Preheat Storage Tank Temperature Profile; for March 2nd in Madison, WI, $\dot{m}_c$ = 6 ℓ/hr m², A_c = 4.2 m², V_{PT} = 303 ℓ, LOAD = 300 ℓ/day

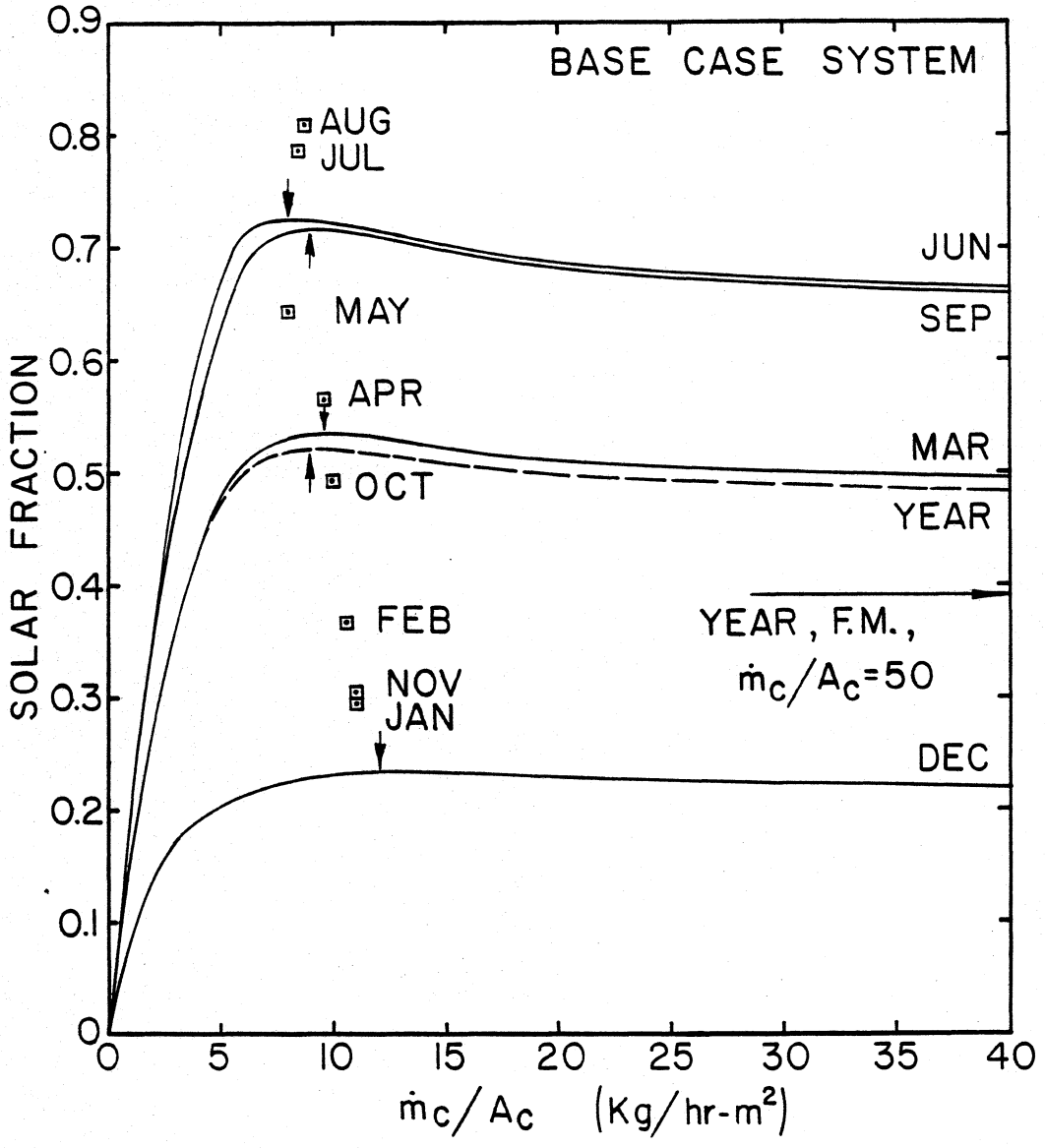

Figure 3.5 Base Case System Performance, Solar Fraction vs. Collector Flow Rate per Unit Area; for Year in Madison, WI, A_c = 4.2 m^2, V_{PT} = 303 ℓ, LOAD = 300 ℓ/day

Figure 3.6 shows the effect on daily recirculation resulting from choosing one specific collector flow rate for the base case system operating in March in Madison. The minimum daily volume of mains temperature water in the preheat storage, or the daily volume of solar heated water recirculated through the collectors is plotted vs. day of the month. The performance on the second day of the month corresponds to the results shown in Figures 3.4a through 3.4f. The optimum collector flow rate occurs at nine ℓ/hr m^2 because it yields the best combination of maximizing energy collection on poorer days (days with lower radiation levels) and avoiding too much recirculation on good days (days with higher radiation levels).

3.2.3 Effect of Location

The same system was used to run annual simulations in both Seattle, WA and Albuquerque, NM. The results are shown in Figures 3.7 and 3.8 respectively. In Seattle, the solar system provided approximately 43 percent of the annual load at an optimum collector flow rate of nine ℓ/hr m^2, which is 11.5 percentage points above the fully-mixed storage tank operating at conventional flow rates. In Albuquerque, an annual solar fraction of 84 percent was obtained at a flow rate of nine ℓ/hr m^2, which is 18.5 percentage points above fully-mixed storage. An annual simulation was also run in Albuquerque using the same system but with 1/2 the collector area (2.1 m^2). These results are shown in Figure 3.9. This case resulted in an annual solar fraction of 52.5 percent at an optimum flow rate of 14 ℓ/hr m^2, which is a 12.6 percent improvement over fully-mixed. The existence of a

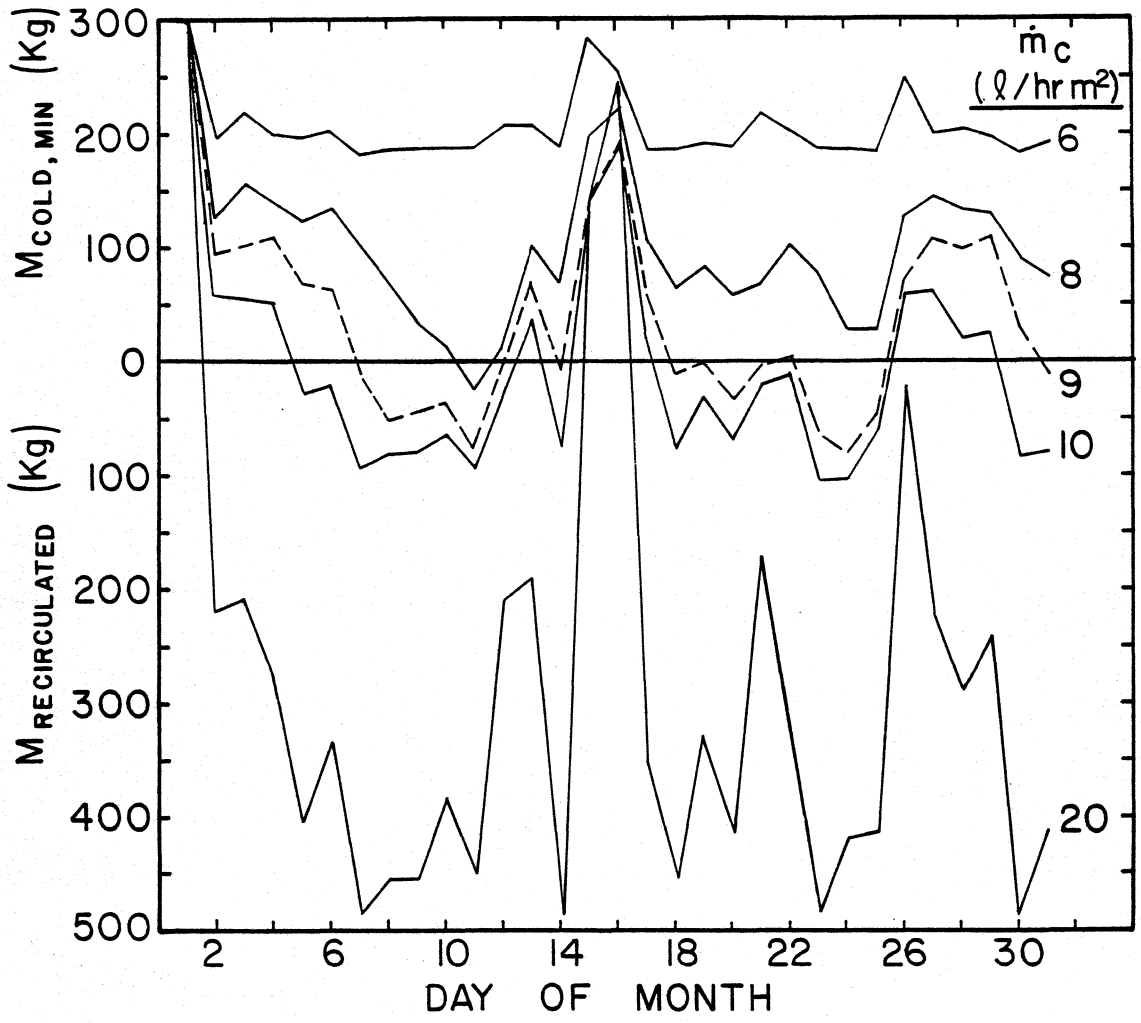

Figure 3.6 Fluctuation of Base Case System Preheat Storage Recirculation Through Collectors with Day of Month, Operating with Different Fixed Collector Flow Rates; for March in Madison, A_c = 4.2 m^2, V_{PT} = 303 ℓ, LOAD = 300 ℓ/day

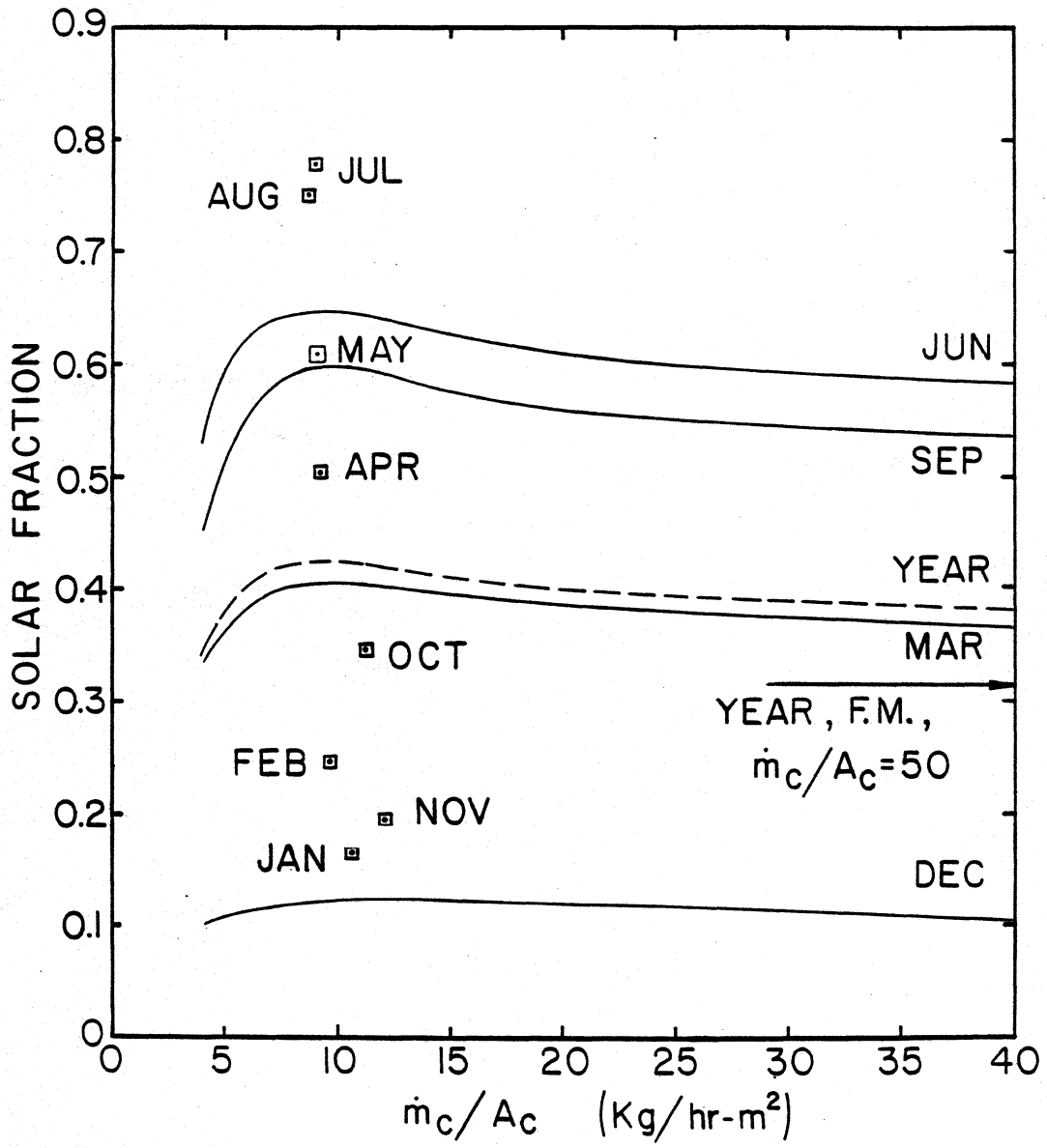

Figure 3.7 Base Case System Performance, Solar Fraction vs. Collector Flow Rate per Unit Area; for Year in Seattle, WA, A_c = 4.2 m^2, V_{PT} = 303 ℓ, LOAD = 300 ℓ/day

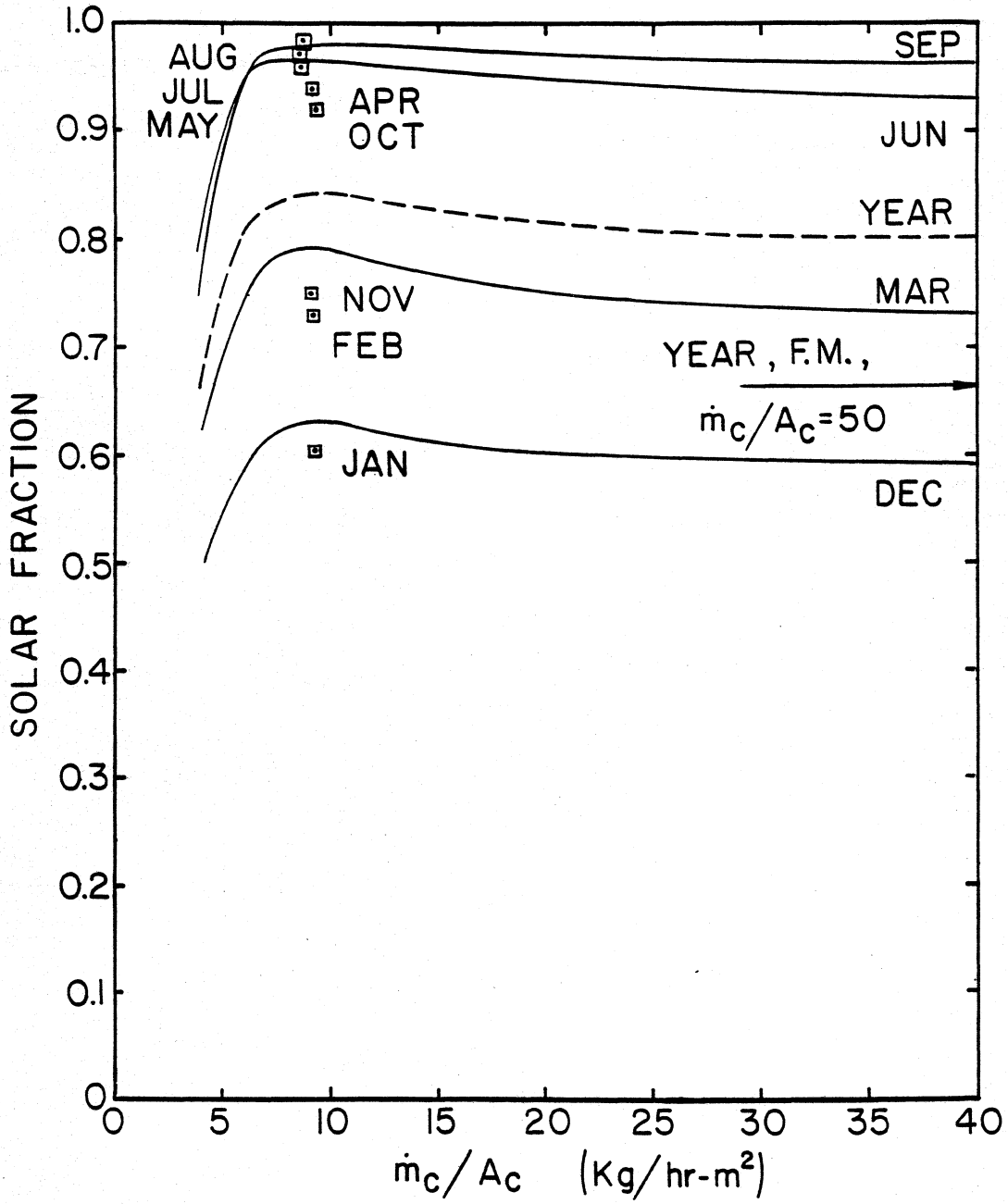

Figure 3.8 Base Case System Performance, Solar Fraction vs. Collector Flow Rate per Unit Area; for Year in Albuquerque, NM, A_c = 4.2 m^2, V_{PT} = 303 ℓ, LOAD = 300 ℓ/day

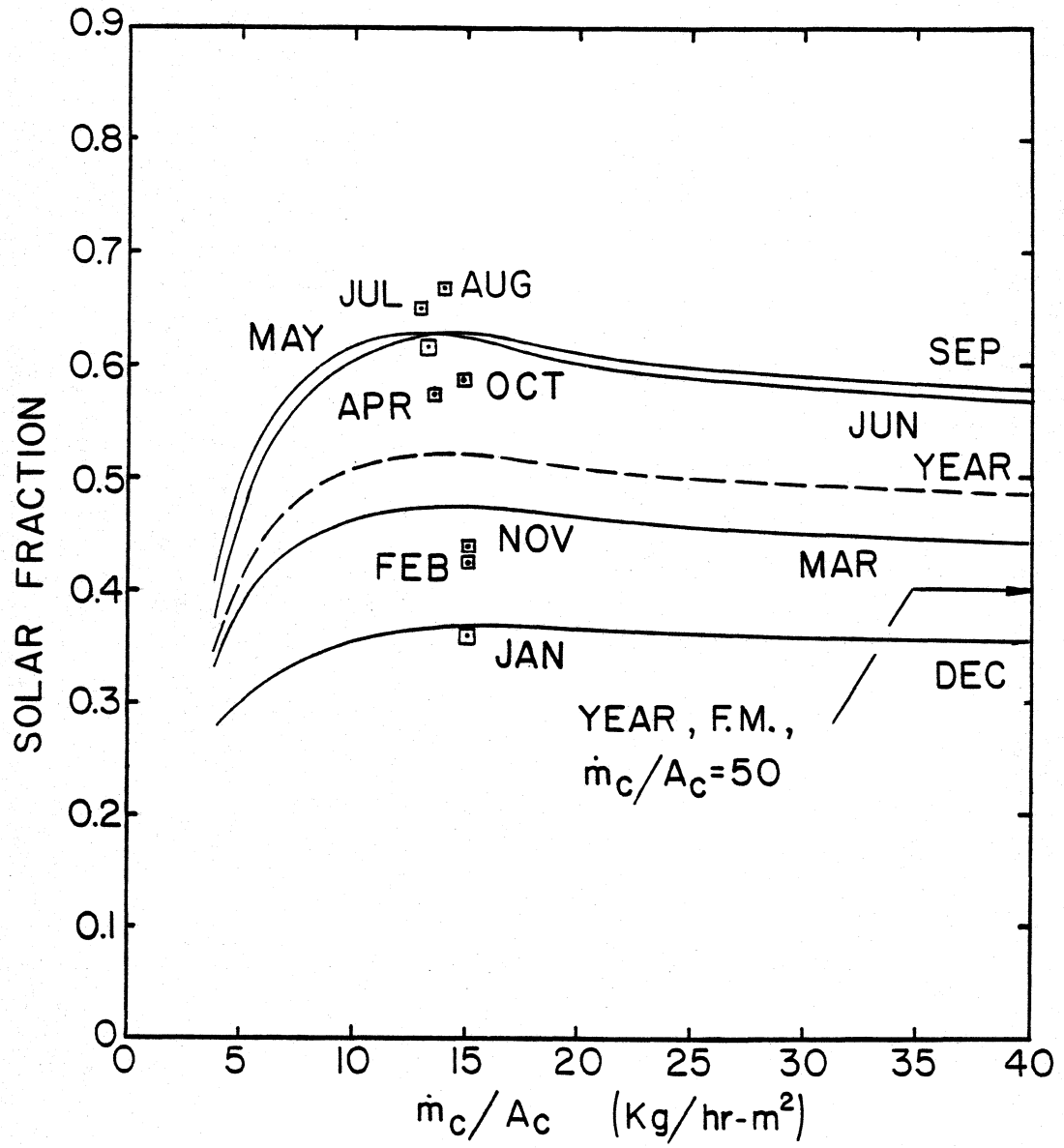

Figure 3.9 Base Case System Performance, Solar Fraction vs. Collector Flow Rate per Unit Area; for Year in Albuquerque, NM, A_c = 2.1 m^2, V_{PT} = 303 ℓ, LOAD = 300 ℓ/day

reduced flow rate optimum for all locations tested supports the benefits of thermal stratification in SDHW systems for the range of climates examined. Both the Seattle and Albuquerque results showed time of year dependence similar to that found in Madison.

3.2.4 Correlation of Optimum Performance to $\overline{M}_c/M_L$

The results shown in Figure 3.5 are replotted vs. the ratio of monthly average daily total collector flow to daily total load flow ($\overline{M}_c/M_L$) in Figure 3.10. The yearly optimum flow rate occurs very near to a $\overline{M}_c/M_L$ ratio of one. The optimum $\overline{M}_c/M_L$ ratios in the warmer months are slightly greater than one. This suggests that as radiation levels and ambient temperatures increase, and thus useful energy collection increases, system performance can be improved slightly by allowing a small amount of recirculation.

The optimum $\overline{M}_c/M_L$ ratio for November, December, and January is below one. A one day analysis would indicate that the optimum ratio should never be below one (as shown by Rademaker(7)). However, on a monthly basis, the optimum ratio can be below one due in part to day-to-day weather fluctuations. Recall that $\overline{M}_c$ is defined as the monthly "average" total daily collector flow; thus as the $\overline{M}_c/M_L$ ratio increases towards one, too much recirculation may occur on the good days. The optimum $\overline{M}_c/M_L$ ratio is slightly affected by solar fraction, as shown in Figure 3.10. System performance in March nearly resembles the annual performance. The remainder of the results presented in Chapter 3 unless otherwise indicated will be for March in Madison, WI, but the same behavior exists when examined on an annual basis.

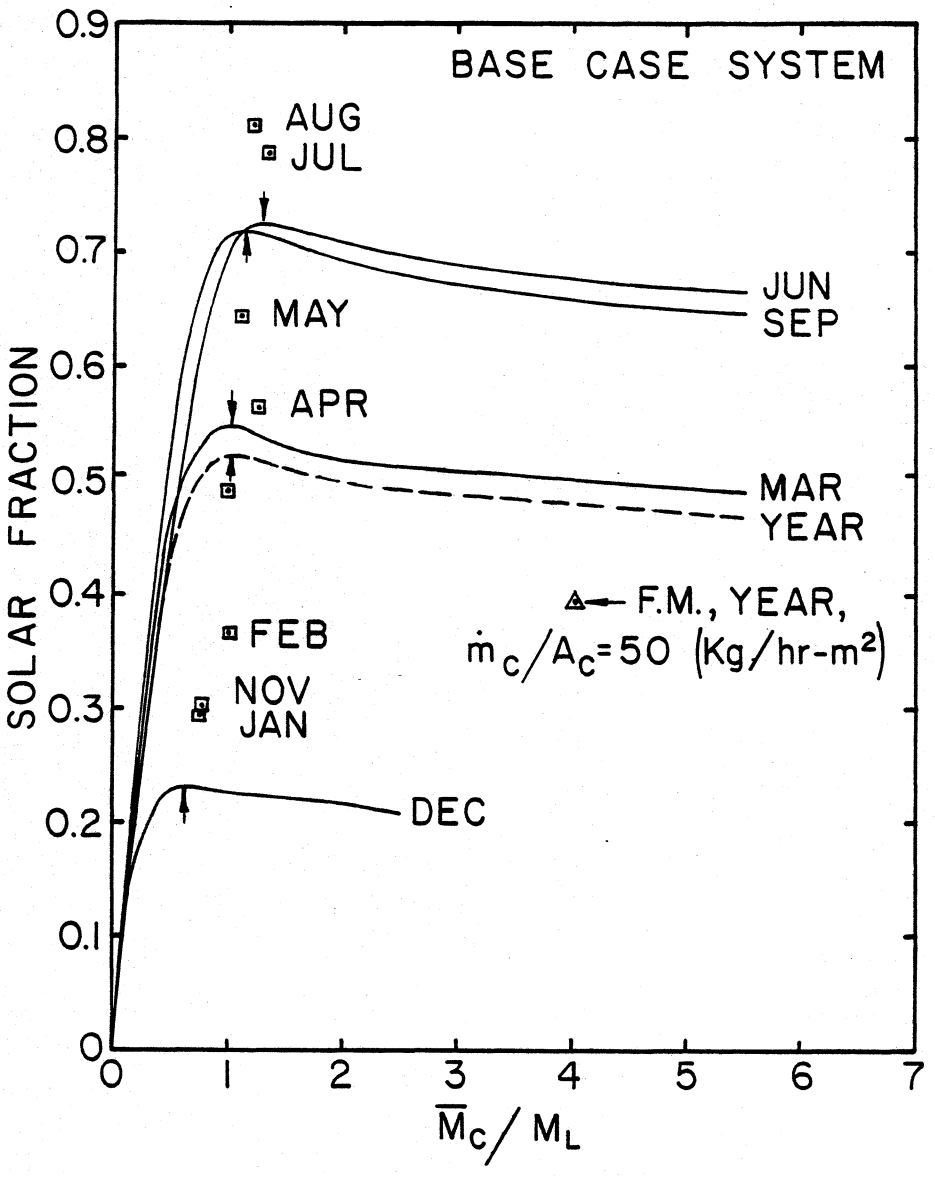

Figure 3.10 Base Case System Performance, Solar Fraction vs. the ratio of Monthly Average Daily Total Collector Flow to Daily Total Load Flow; for March in Madison, WI, A_c = 4.2 m², V_{PT} = 303 ℓ, LOAD = 300 ℓ/day

3.2.5 Effect of Collector Quality

The effect of collector quality on system performance is shown in Figure 3.11. The base case collector, BC, is single-glazed with a selective surface absorber. The higher quality collector, HQ, is double-glazed with a selective surface absorber and the lower quality collector, LQ, has one cover with a flat black absorber plate. The characteristics of these collectors are listed in Table 3.1. The base case collector and the higher quality collector yielded nearly identical performance and are represented as one curve in Figure 3.11. The collector quality does effect the solar fraction but has very little effect on the optimum $\overline{M}_c/M_L$ ratio. The optimum flow rate per unit area does increase slightly with increased collector quality however because the collector operating time increases.

3.2.6 Effect of Preheat Storage Tank Energy Losses

The effect of removing the preheat storage tank thermal energy losses from the base case system is also shown in Figure 3.11. System performance, represented by the BC, U_{PT}=0 curve, improves slightly and the optimum $\overline{M}_c/M_L$ ratio increases from near one to 1.15. With a zero tank loss coefficient, the colder fluid at the bottom of the tank cannot receive any gains form the environment. Thus, the average temperature at the bottom of the tank during collector on-time is lower and the collector operates longer, causing the $\overline{M}_c/M_L$ ratio to increase slightly at low collector flow rates. The absence of thermal losses from the warmer water located in the upper section of the tank accounts for the increase in performance.

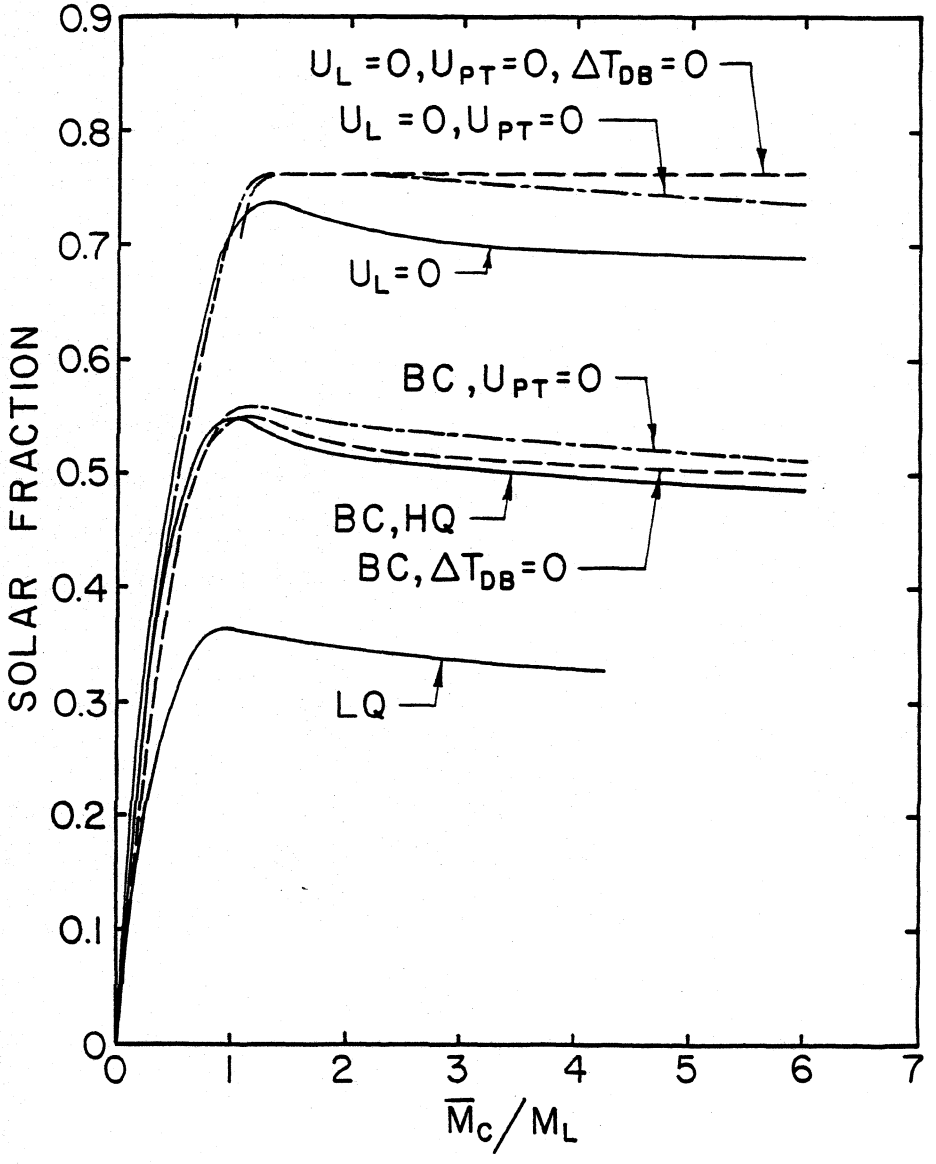

Figure 3.11 Effect of Collector Quality, Preheat Storage Energy Losses, and Collector Temperature Deadband on Base Case System Performance, Solar Fraction vs. the ratio of Monthly Average Daily Total Collector Flow to Daily Total Load Flow; for March in Madison, WI, A_c = 4.2 m^2, V_{PT} = 303 ℓ, LOAD = 300 ℓ/day

3.2.7 Effect of Controller Temperature Deadbands

Setting the differential controller temperature deadbands to zero has the effect of shifting the base case curve to slightly higher $\overline{M}_c/M_L$ ratios, as indicated by the BC, $\Delta T_{DB}=0$ curve in Figure 3.11. The zero degree deadbands cause the circulation pump to operate whenever the ambient temperature is greater than or equal to the temperature at the bottom of the preheat tank. Zero degree deadbands help the performance of ideal systems (i.e. systems with no parasitic energy requirements) slightly more at higher collector flow rates because of the larger energy quantities involved.

3.2.8 The Perfect SDHW System

Figure 3.11 also shows the performance that could be obtained with systems having no collector or tank thermal losses. If a collector had a loss coefficient of zero, a reduced flow rate optimum should not exist because the collector efficiency would be independent of inlet temperature. However, as indicated by the $U_L=0$ curve in Figure 3.11 for the particular system investigated an optimum does exists at a reduced flow rate. This optimum occurs because the net preheat storage tank energy losses increased with collector flow rate, thus reducing the net energy delivered by the solar system at higher flow rates. Increased collector flow rates cause a greater propagation of solar heated water down into the preheat tank which allows this heated water to incur energy loses for a longer period of time before it is removed to satisfy the load. When both the preheat tank and collector loss coefficients are set to zero a reduced collector flow rate optimum

still exists, as indicated by the U_L=0, U_{PT}=0 curve. The differential controller used in the base case simulation had a 8.9 ° C upper deadband and a 1.7 ° C lower deadband, which reduced the energy collection more at higher flow rates than at lower flow rates. As shown by the U_L=0, U_{PT}=0, ΔT_{DB}=0 curve in Figure 3.11, when the temperature deadbands are set to zero, the performance curve is flat and a reduced flow rate optimum does not exists.

3.2.9 Effect of Collector Area

Figure 3.12 shows the effects on performance of varying the collector area while the rest of the system remains unchanged. The optimum $\overline{M}_c/M_L$ ratio increases slightly with both collector area and solar fraction. The optimum total collector flow rate also increases with collector area, but the optimum collector flow rate per unit area decreases with increasing collector area.

An optimum collector flow rate exists at reduced flow rates primarily because the reduction in collector efficiency due to a reduction in F_R is more then compensated for by the increase in collector efficiency resulting from reduced collector fluid inlet temperatures. Collector fluid inlet temperature is a function of the total collector flow rate, while F_R is dependent on flow rate per unit area, as shown in Figure 2.1. This dependence of F_R on flow rate per unit area explains the location of the optimums in Figure 3.12. At a collector area of 1.4 m^2, the optimum $\overline{M}_c/M_L$ ratio is approximately 0.75 with a flow rate of 20.5 ℓ/hr m^2. Any increase in collector flow rate above this value will not produce an accompanying increase in

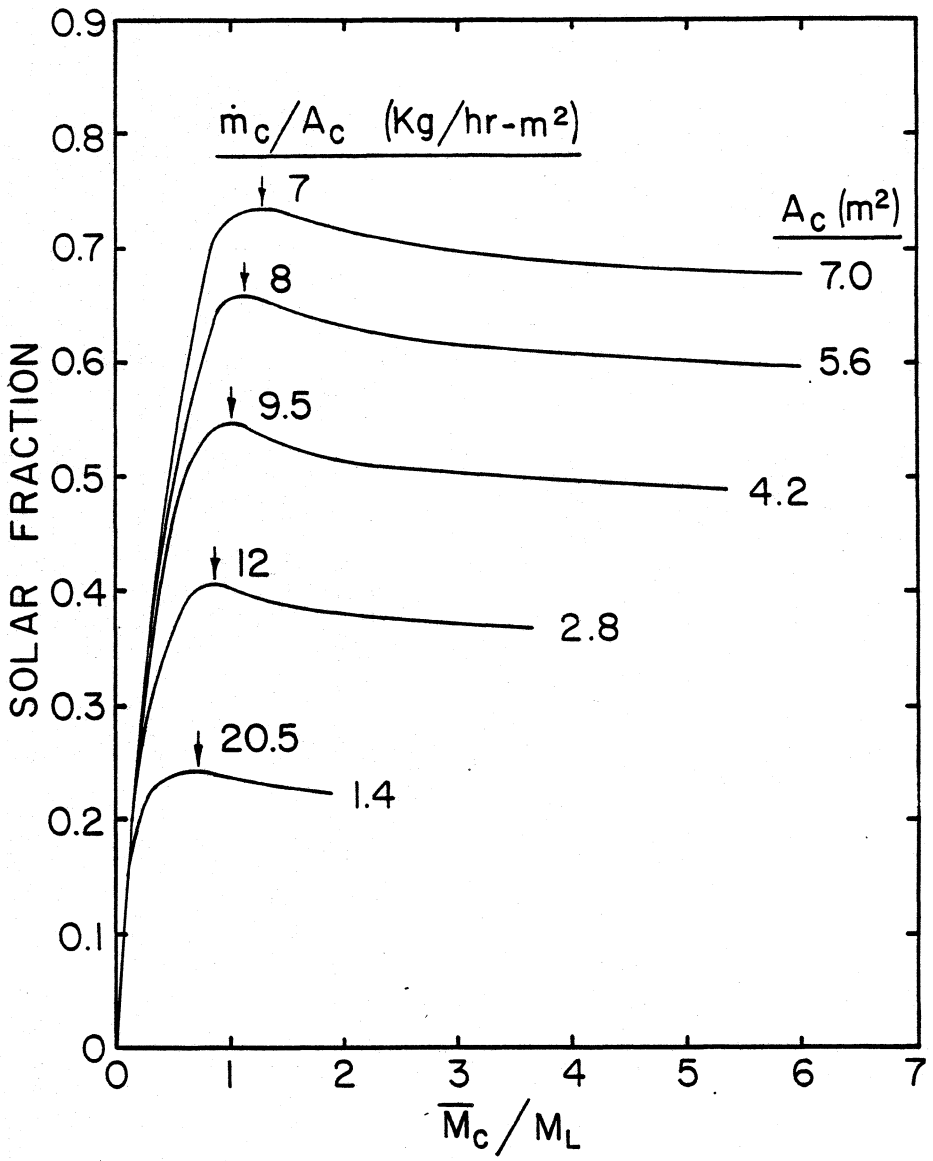

Figure 3.12 Effect of Collector Area on Base Case System Performance, Solar Fraction vs. the ratio of Monthly Average Daily Total Collector Flow to Daily Total Load Flow; for March in Madison, WI, A_c = 4.2 m^2, V_{PT} = 303 ℓ, LOAD = 300 ℓ/day

F_R great enough to overcome the reduction in collector efficiency resulting from an increased collector inlet temperature. The optimum $\overline{M}_c/M_L$ ratio of the larger collector areas is slightly greater than one because they operate at lower flow rates per unit area. Thus, an increase in collector flow rate will cause a large enough increase in F_R to outweigh its accompanying increase in collector inlet temperature.

3.2.10 Effect of Auxiliary Set Temperature

The effect of auxiliary set temperature on system performance was also examined by performing simulations at set temperatures of 50 ° C and 40 ° C. These results are shown in Figure 3.13. The optimum $\overline{M}_c/M_L$ ratio increases slightly with solar fraction and with decreasing set temperature. The optimum flow rate per unit area also increases slightly as the optimum $\overline{M}_c/M_L$ ratio increases.

An increase in collector flow rate causes lower collector outlet temperatures and thus lower temperatures in the upper section of the preheat storage tank. A larger flow also causes a greater propagation of energy down the tank, or higher temperatures in the middle and lower sections of the tank. This flattening of the preheat storage tank temperature profile helps to avoid sending over heated water to the auxiliary tank. It also causes higher temperature water to be sent to the load during latter use. Consequentially, a decrease in auxiliary set temperature causes a slight increase in the optimum collector flow rate, but the effect is small in the range between 40 ° C and 60 ° C.

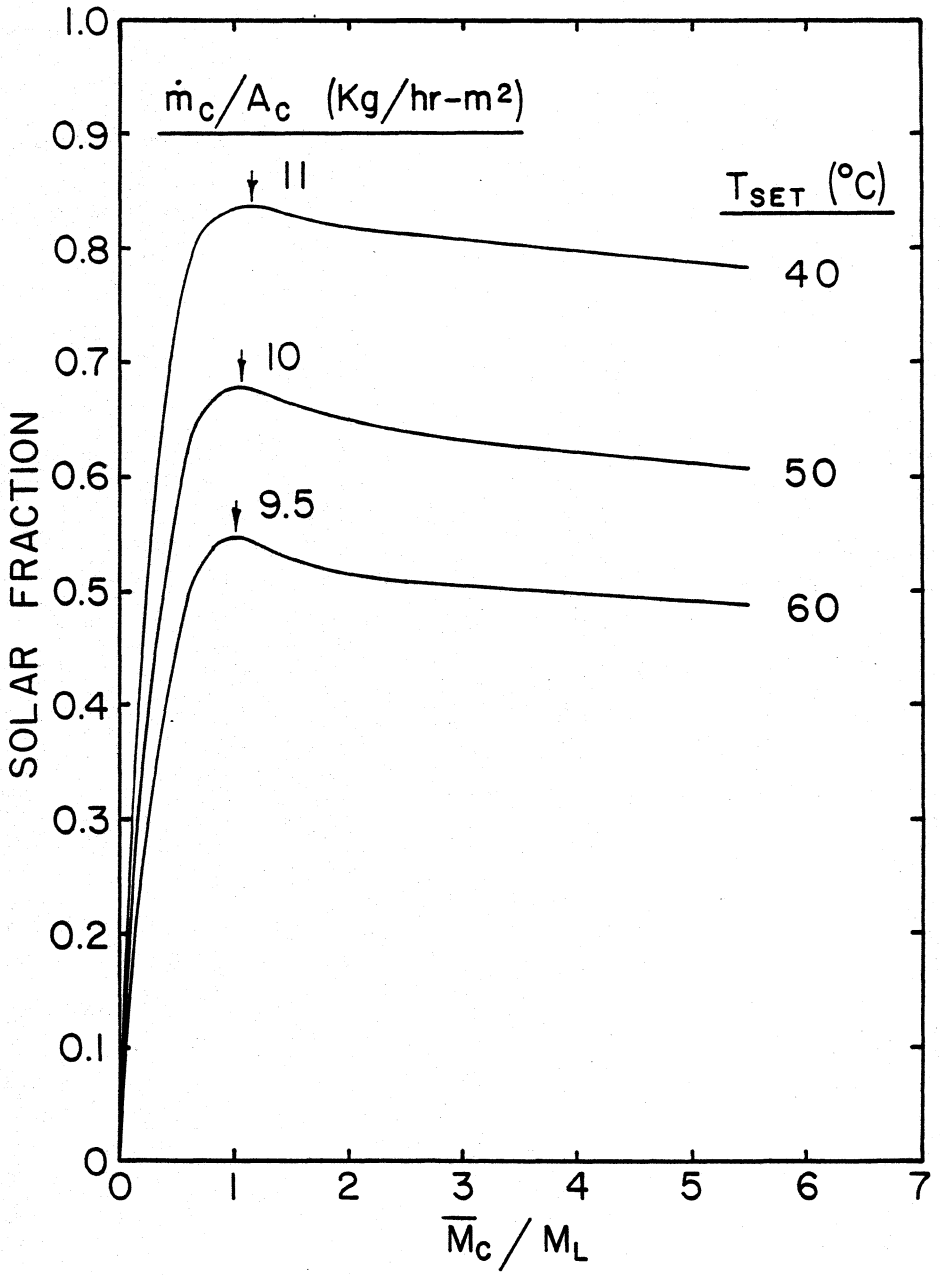

Figure 3.13 Effect of Auxiliary Set Temperature on Base Case System Performance, Solar Fraction vs. the ratio of Monthly Average Daily Total Collector Flow to Daily Total Load Flow; for March in Madison, WI, A_c = 4.2 m^2, V_{PT} = 303 ℓ, LOAD = 300 ℓ/day

3.2.11 Effect of Total Daily Load Draw

Figure 3.14 shows the effect of varying the total daily load on system performance for three different preheat storage tank volumes. The optimum $\overline{M}_c/M_L$ ratio for all tank sizes decreases slightly as the total daily draw increases. The optimum $\overline{M}_c$ actually increases with M_L, but to a lesser degree, and thus, due to the appearance of M_L in the denominator the optimum $\overline{M}_c/M_L$ ratio decreases.

As the total daily load flow increases, the load flow during collector on-time increases proportionately. However, with a fixed tank volume, the total collector flow can only increase by an amount equal to the increase in load flow during collector on time, while still avoiding recirculation. When the recirculation limitation is encountered, the optimum collector flow becomes independent of any load flow during collector off-time. The optimum $\overline{M}_c/M_L$ ratios are less than one for the 450 and 600 ℓ/day loads because of this recirculation limitation.

3.2.12 Effect of Preheat Storage Tank Volume

Figure 3.14 also shows the effect on performance of varying the preheat storage tank volume. For all load sizes the $\overline{M}_c/M_L$ ratio decreases slightly as the storage volume decreases.

The $\overline{M}_c/M_L$ ratio may not be the only important variable for storage tank sizes which are smaller than the average daily load. The optimum total daily collector flow is on the order of the load flow, unless the tank volume and load flow during collector on time are not large enough to avoid recirculation. A comparison of the 450 and 600 ℓ/day curves

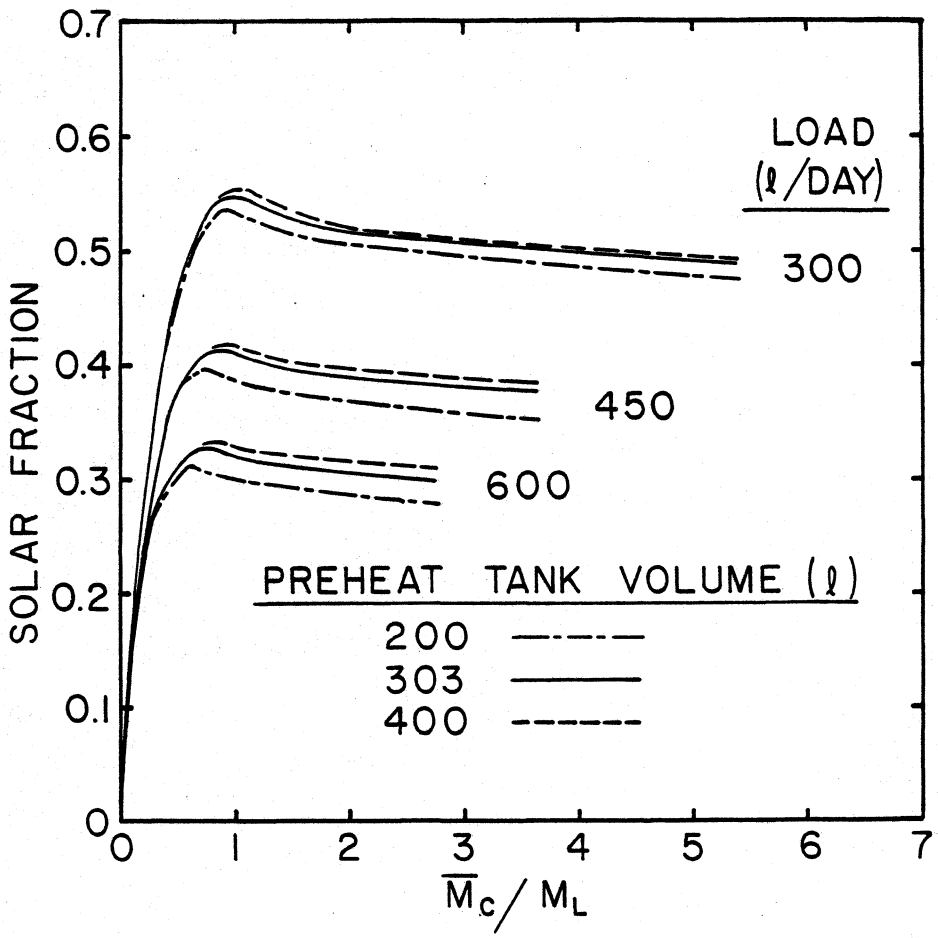

Figure 3.14 Effect of Total Daily Load Draw and Preheat Storage Volume on Base Case System Performance, Solar Fraction vs. the ratio of Monthly Average Daily Total Collector Flow to Daily Total Load Flow; for March in Madison, WI, A_c = 4.2 m^2, V_{PT} = 303 ℓ, LOAD = 300 ℓ/day

for preheat tank volumes of 200, 303, and 400 liters shows that smaller tank volumes cause the recirculation limitation to be encountered at lower $\overline{M}_c/M_L$ ratios.

3.2.13 Effect of Load Distribution

Figure 3.15 shows the effect of varying the load distribution. Seven hourly load profiles and one day-to-day profile were investigated. The base case distribution was the Rand (14) profile which is shown in Figure 3.16a. Curve II represents the performance of profile II shown in Figure 3.16b. The load is proportional to the monthly radiation distribution and occurs only during collector on-time. Curves III through VII represent constant load draws between the hours indicated in Figures 3.16b and 3.16c. The Rand profile and profiles II through VII are repeated each day. The day-to-day distribution represents a weekly cycle using the Rand profile each day with the total daily draw varying each day (as shown in Table 3.3), such that the load equals 2100 ℓ/week. The variation in performance with load distribution is caused by better matching of some profiles to incident radiation and the amount of nighttime preheat storage losses encountered by other profiles.

Profile II yields the best performance at $\overline{M}_c/M_L$ ratios less than 1.1 because the load distribution most closely matches the daily radiation distribution. The steeper preheat storage tank temperature profiles which occur at low $\overline{M}_c/M_L$ ratios (as indicated in Section 3.2.10) lend themselves very well to day time load distributions. Raising the $\overline{M}_c/M_L$ ratio causes flatter temperature profiles which

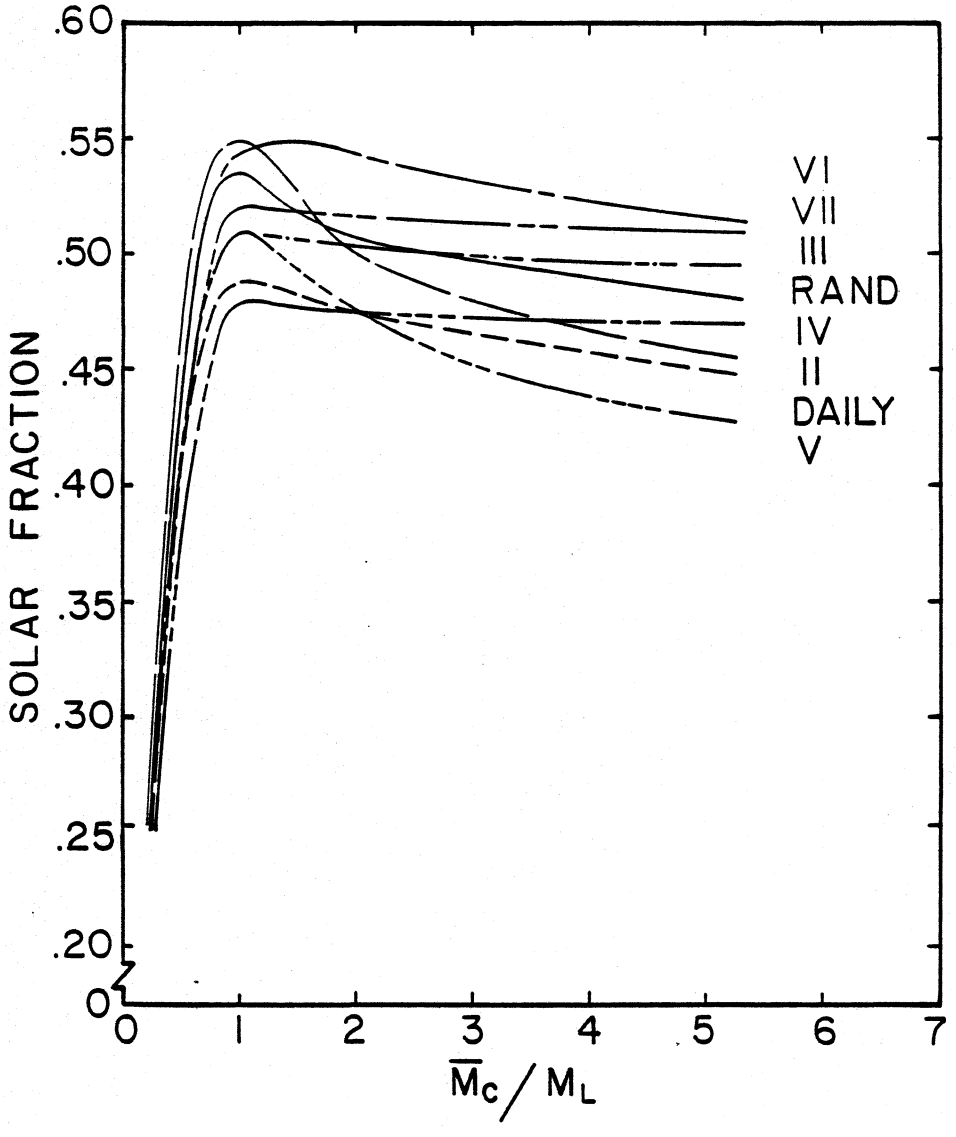

Figure 3.15 Effect of Load Distribution on Base Case System Performance, Solar Fraction vs. the ratio of Monthly Average Daily Total Collector Flow to Daily Total Load Flow; for March in Madison, WI, A_c = 4.2 m^2, V_{PT} = 303 ℓ, LOAD = 300 ℓ/day

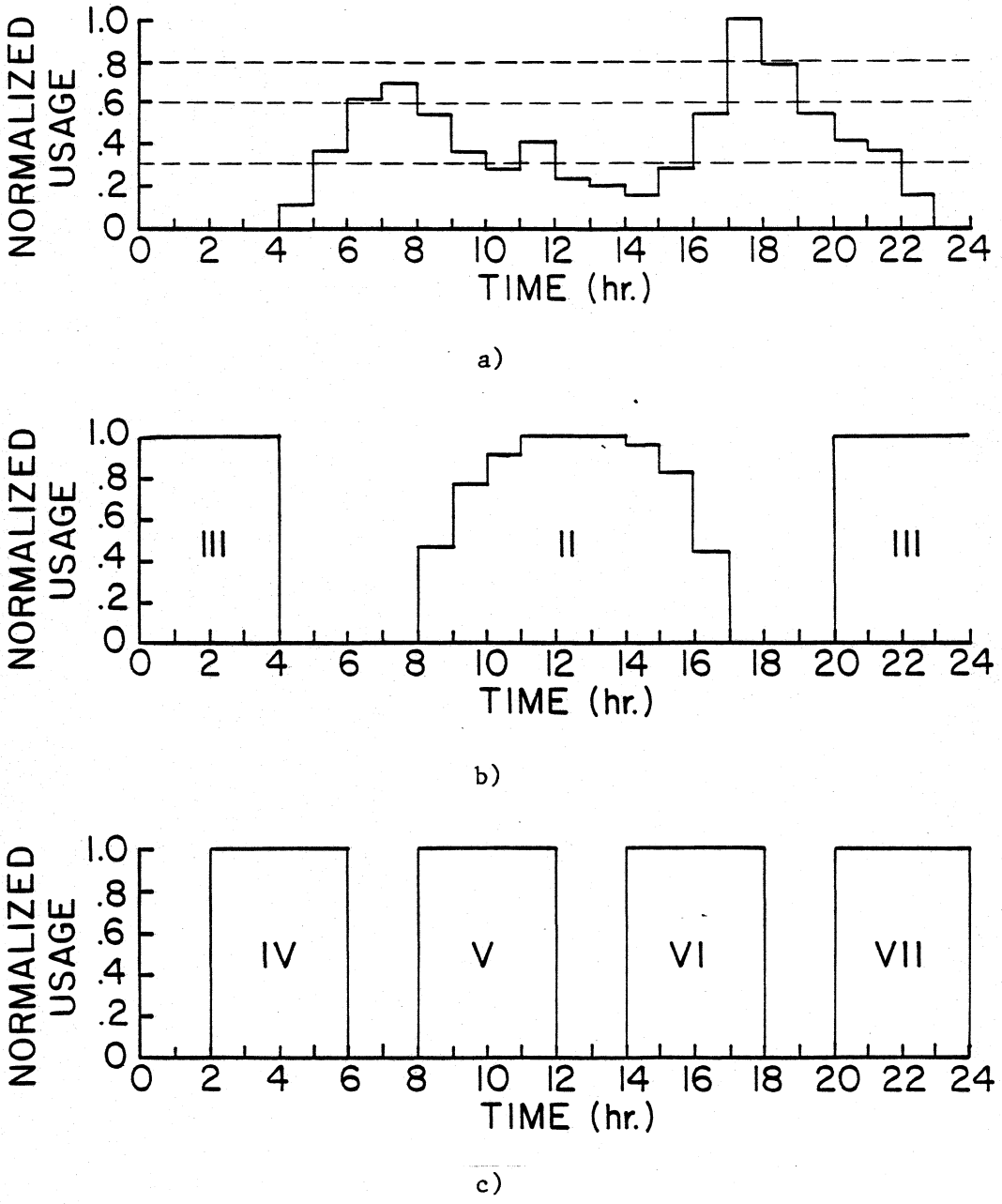

Figure 3.16 Load Distributions
a) Rand
b) 8 PM - 4 AM Constant, and Proportional to Monthly Radiation Distribution
c) 2-6 AM, 8-12 AM, 2-6 PM, AND 8-12 PM Constant

Table 3.3 Variation in Daily Load Draw for Day-to-Day Load Profile

Percent of Weekly Total						
Sunday	Monday	Tuesday	Wednesday	Thursday	Friday	Saturday
5.7	42.9	2.8	2.8	14.4	2.8	28.6

reduces the performance of systems with day time only load distributions.

Profile VI has the second best performance at low $\overline{M}_c/M_L$ ratios because a substantial portion of its load occurs during collector on-time. Any load flow removed from the top of the preheat tank during the collector operating period causes a slug of mains temperature water equal in volume to the load flow to be injected into the bottom of the tank. This allows a higher total daily collector flow, and thus a higher constant collector fluid flow rate to be specified, before any recirculation occurs. Thus this large afternoon load draw results in better system performance at higher $\overline{M}_c/M_L$ ratios.

The base case Rand distribution yields the next highest performance at low $\overline{M}_c/M_L$ ratios. Its performance also decreases as the $\overline{M}_c/M_L$ ratio increases, but to a lesser degree than profile II. Because the Rand profile is distributed throughout the day it performs better at higher $\overline{M}_c/M_L$ ratios than profile II.

In all simulations the Rand load profile was obtained by varying the load flow rate each hour and keeping that flow rate constant over the entire hour. It could also have been achieved by keeping the load flow rate constant at a specified value and varying the duration of time of each step in the profile. Comparison of these two methods showed a very small difference in system performance on the order of 0.1 percent. If the storage tank model accounted for the effects of internal mixing due to load flow, the differences between these two methods should show a greater effect on system performance.

The system operating at low $\overline{M}_c/M_L$ ratios with profiles VII, III, and IV gives the fourth, fifth, and eight highest performance respectively. Profiles III and IV have successively worse performance than profile VII because they cause the preheat storage tank to incur successively larger night time energy losses. Profiles VII, III, and IV have much flatter curves than the other profiles because they occur during collector off-time and thus do not effect when recirculation occurs.

Profile V gives the sixth best performance (nearly equal to profile III) at low $\overline{M}_c/M_L$ ratios and the eighth best, or worst, performance at high $\overline{M}_c/M_L$ ratios. It performs worse at high $\overline{M}_c/M_L$ ratios for two basic reasons. The solar heated water stays in the preheat tank all night before any load is removed, thus allowing the maximum amount of energy to be wasted as thermal losses. Profile V also attempts to remove energy form the preheat tank in the early morning hours when it contains the lowest amount. This profile does not perform the worst at low $\overline{M}_c/M_L$ ratios because the increased

stratification and higher collector outlet temperatures cause a higher percentage of the early morning load to be met.

The daily load profile shows results that are nearly parallel to the base case Rand distribution and are reduced by approximately 7 percentage points. This reduction is due to the high day-to-day variation in load draw which does not correspond well with the weather for the month tested.

The largest portion of the variation in performance between profiles is due to the existence of stratification. The effect of load distribution in fully-mixed systems has been examined analytically by Buckles and Klein (20) and experimentally by Fischer and Fanny (21). Their results showed variation in hourly load profile to have little effect on fully-mixed system performance at high collector flow rates.

All load profiles have optimum $\overline{M}_c/M_L$ ratios near one except profile VI which has a slightly higher optimum $\overline{M}_c/M_L$ ratio of approximately 1.4. This is due to the insertion of 300 liters of mains water into the bottom of the preheat storage tank in the afternoon, which allows the total daily collector flow to be greater, while still avoiding recirculation.

3.2.14 Effect of Mixing in the Preheat Storage Tank

System performance at reduced collector fluid flow rates depends highly on the degree of thermal stratification in the preheat storage tank. Figure 3.17 shows the effect on system performance of various degrees of mixing in the preheat tank. All curves were generated using the variable inlet plug-flow tank model except the curve labeled

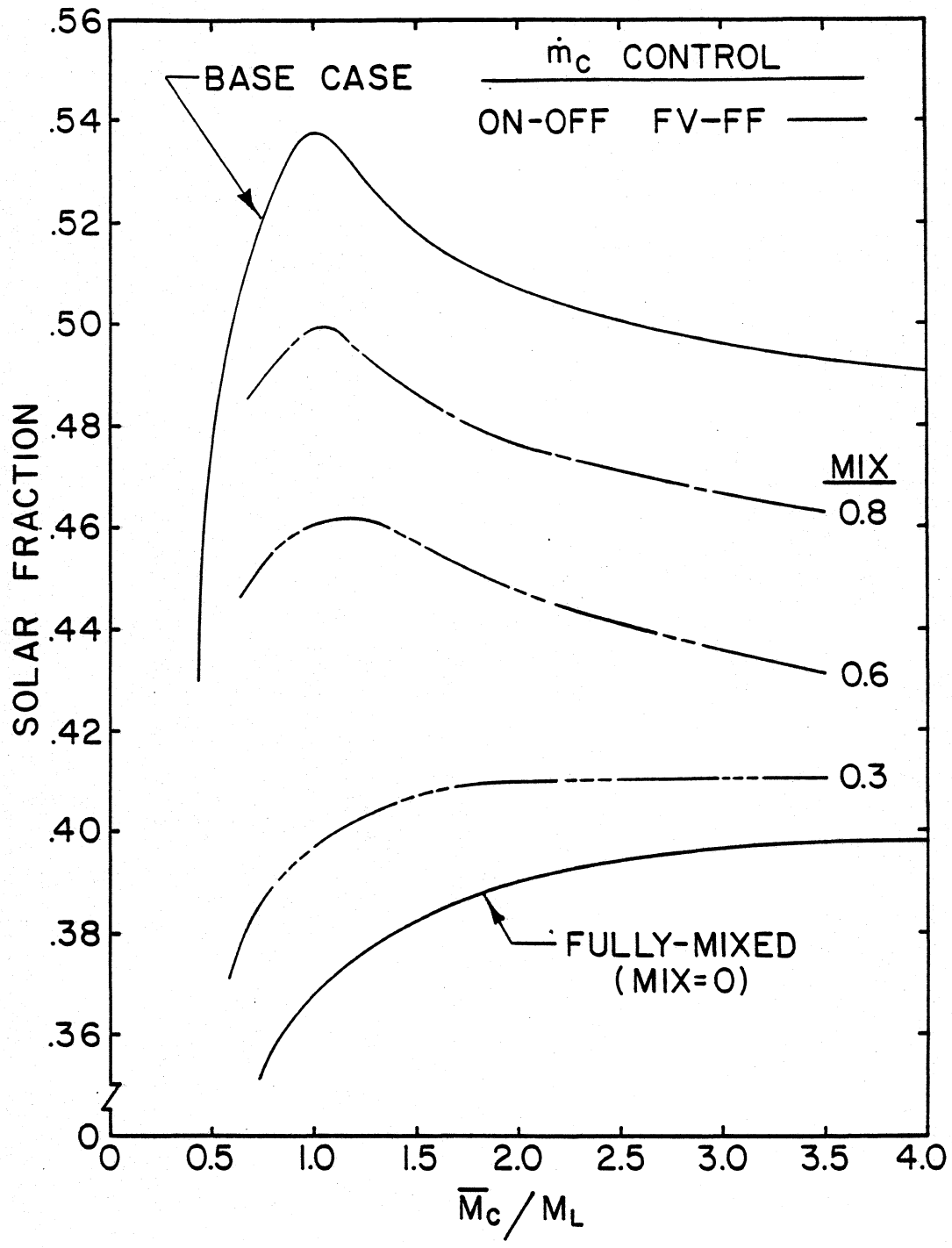

Figure 3.17 Effect of Mixing in Preheat Storage Tank on Base Case System Performance, Solar Fraction vs. the ratio of Monthly Average Daily Total Collector Flow to Daily Total Load Flow; for March in Madison, WI, A_c = 4.2 m^2, V_{PT} = 303 ℓ, LOAD = 300 ℓ/day

"FULLY-MIXED" which was obtained using the Type 4 multi-node tank model with one node. The curve labeled "BASE CASE" represents the perfectly stratified preheat tank. The mix equals 0.8 curve represents the performance of a system whose preheat tank was completely mixed each time the normalized load draw was greater than or equal to 0.8. This occurs once per day as shown in Figure 3.16a. Similarly the mix equals 0.6 and 0.3 curves correspond to systems whose preheat tank was completely mixed each time the normalized load was greater than or equal to 0.6 and 0.3 respectively. Thus the 0.6 and 0.3 curves represent successively greater frequencies of complete mixing, which is also shown in Figure 3.16a.

As the frequency of complete mixing increases, system performance drops. The 0.8 and 0.6 cures still show a reduced collector flow rate optimum near $\overline{M}_c/M_L = 1$, but the low $\overline{M}_c/M_L$ optimum disappears for the mix equals 0.3 curve. A plug-flow tank simulation was also run at mix equals zero which completely mixes the preheat storage every time step. The results, as expected, fall directly on top of the fully-mixed, multi-node results. These curves are not intended to represent what actually happens during load flow (i.e. complete mixing of preheat storage tank), but rather to give an approximation of system performance with less than perfect stratification. These results show the strong dependence of system performance on a high degree of thermal stratification.

3.3 Constant Volume Storage-Variable Collector Fluid Flow Rate

All results presented in Section 3.3 are for the direct, two-tank SDHW system shown in Figure 1.1 operating with the variable collector flow rate control modifications described in Section 1.2.2. Systems using variable collector flow rates to achieve a fixed collector fluid outlet temperature, or a fixed fluid temperature rise across the collector, and proportional to the utilizable radiation are examined. The plug-flow storage tank model operating in the variable inlet mode is used in all simulations except where indicated otherwise.

3.3.1 Specified Collector Fluid Outlet Temperature

Figure 3.18 compares the performance of three different variable collector flow rate control strategies to the performance of a fixed collector flow rate system with on-off temperature differential control. The fixed collector outlet temperature mode had a maximum solar fraction of 48.1 percent at an optimum $\overline{M}_c/M_L$ ratio of 0.62 which corresponds to a collector set temperature of 55 ° C. This is a 7.3 percent improvement over a fully-mixed system operating at 50 ℓ/hr m^2, but it is still 5.7 percent lower than the optimum performance of the reduced fixed flow rate system.

The main reason the variable collector flow rate - fixed outlet temperature control performs worse than the reduced constant collector flow rate - on-off control is because of its higher minimum radiation requirements. The minimum amount of incident radiation necessary for a variable flow rate collector to obtain a specific collector outlet temperature, $G_{T,MIN}$, (as given by Equation [2-20]), is generally higher

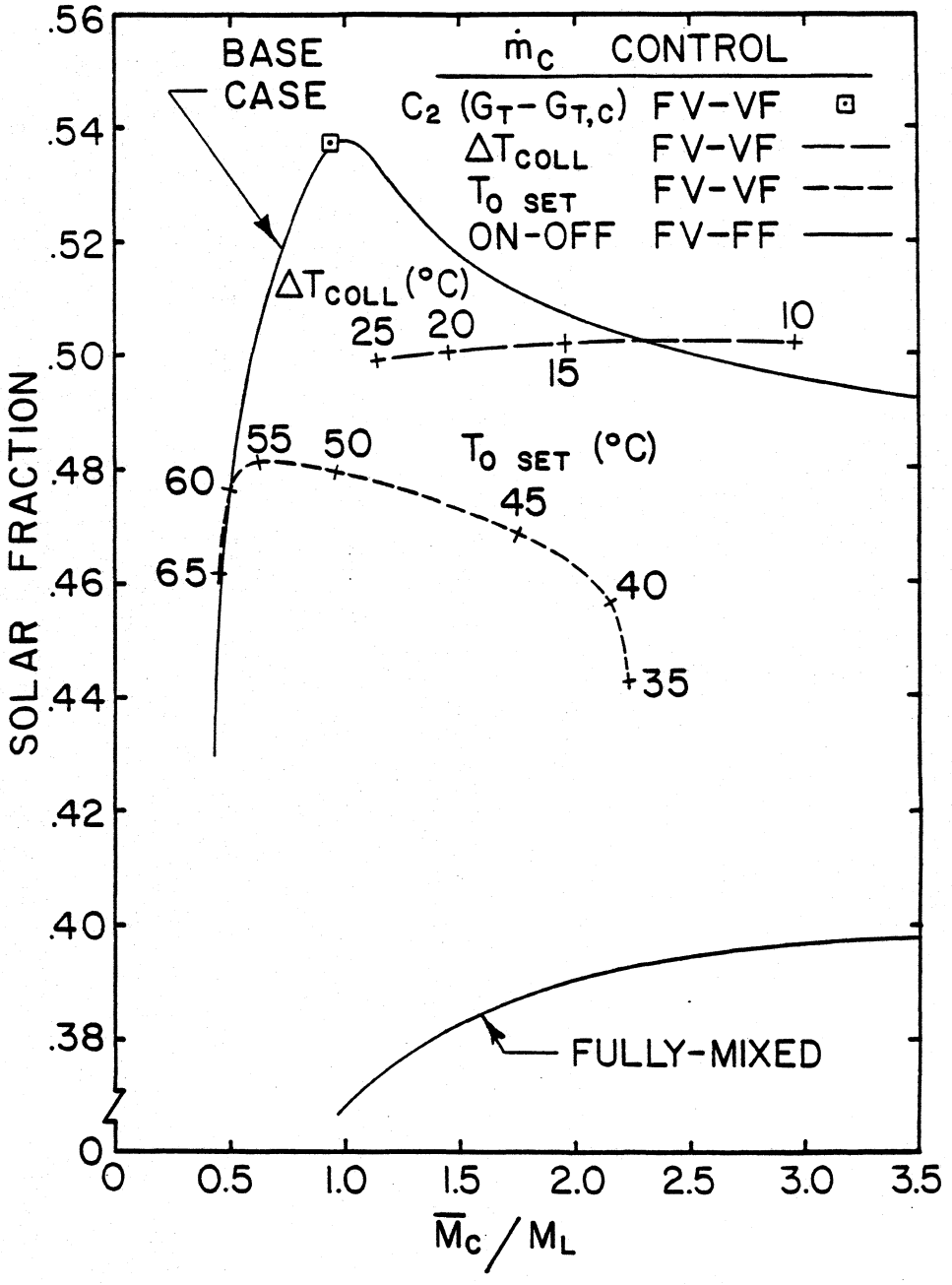

Figure 3.18 Constant Volume Storage with Variable Collector Flow Rate System Performance, Solar Fraction vs. the ratio of Monthly Average Daily Total Collector Flow to Daily Total Load Flow; for March in Madison, WI, A_c = 4.2 m^2, V_{PT} = 303 ℓ, LOAD = 300 ℓ/day

than the critical threshold level, $G_{T,C}$, (as is given in Equation [2-10]), which is the minimum amount of incident radiation required to produce a useful energy gain in a constant flow rate collector. As a result, collector on-time is reduced (thus reducing useful energy collection), and system performance is less than that which could be achieved with a reduced fixed flow rate system. As the specified collector outlet temperature is reduced, which lowers the $G_{T,MIN}$ levels, recirculation and a flattening of the preheat tank temperature profile begins to inhibit system performance. Early pump shut off (as discussed in Section 1.2.2a) can also waste collectable energy.

3.3.2 Specified Collector Fluid Temperature Rise

The results of the fixed collector fluid temperature rise control strategy are also shown in Figure 3.18. This mode of control has a maximum solar fraction of 50.3 percent at $\overline{M}_c/M_L = 2.5$ which is still 3.5 percent lower than the reduced fixed flow rate system. Recall that the fixed temperature rise control is similar to the fixed outlet temperature control, the difference being that the specified outlet temperature is continually updated to be a fixed amount above the inlet temperature. The fixed temperature rise control therefore, suffers the same disadvantage of $G_{T,MIN}$ levels higher than the constant flow rate $G_{T,C}$ levels (as described in Section 3.2.1). However, the $G_{T,MIN}$ levels for the fixed collector fluid temperature rise control are lower than the $G_{T,MIN}$ levels for the fixed collector outlet temperature control at the same $\overline{M}_c/M_L$ ratio. At a given $\overline{M}_c/M_L$ ratio, the specified collector temperature rise (which produced that $\overline{M}_c$) when added to the

collector inlet temperature, is less than the collector outlet temperature of the specified collector outlet temperature control mode operating at the corresponding $\bar{M}_c/M_L$ ratio. No collectable energy is wasted due to early pump shut off in the fixed temperature rise mode because the specified collector outlet temperature is always a fixed amount above the inlet temperature.

3.3.3 Proportional to Utilizable Radiation

In order to avoid recirculation while controlling the collector flow rate proportionately to the utilizable radiation (level of incident radiation above the critical threshold level) it is necessary to limit the total daily collector flow. This was done by calculating a daily proportionality constant, C_2, with a separate simulation in advance, such that the total daily collector flow would equal a specified amount, C_1.

$$C_2 = \frac{C_1}{\int_{day}(G_T - G_{T,C})^+ dt} \qquad [3\text{-}1]$$

where:

C_1 = total desired daily collector flow

C_2 = daily proportionality constant

G_T = instantaneous incident radiation

$G_{T,C}$ = instantaneous critical threshold radiation

The critical threshold level is derived in Section 2.1.2 and is:

$$G_{T,C} = \frac{F_R U_L (T_i - T_a)}{F_R (\tau\alpha)_n K_{\tau\alpha}} \qquad [3\text{-}2]$$

For calculation of the daily constant, C_2, the mains water temperature was used for the collector inlet temperature, T_i, in Equation [3-2]. This causes a slight error however, because the actual collector inlet temperature is affected by heat gains from the surroundings to the cooler fluid in the lower section of the preheat storage tank. Multiplying the daily constant by the actual instantaneous difference between the radiation incident on the collector and the critical threshold level yields the instantaneous collector flow rate:

$$\dot{m}_c = C_2 (G_T - G_{T,C})^+ \qquad [3\text{-}3]$$

Integrating Equation [3-3] over the day, very nearly gives the desired total daily collector flow C_1. Because optimum performance in previous simulations has been shown to occur near $\overline{M}_c/M_L = 1$, C_1 in Equation [3-1] was set equal to M_L, or 300 ℓ/day.

The results of varying the collector fluid flow rate proportionately to the utilizable radiation are shown in Figure 3.18. A maximum solar fraction of 53.7 percent is obtained at a $\overline{M}_c/M_L$ ratio of 0.951. This is approximately the same as the optimum reduced flow rate system performance. The $\overline{M}_c/M_L$ ratio is slightly less than one because of the calculation methods used, as previously discussed.

Optimal control (i.e. specifying a daily proportionality constant such that the total daily collector flow is as large as possible while still avoiding recirculation) requires advance knowledge of future weather conditions. This makes practical application difficult.

It is possible however, to calculate a monthly proportionality constant using Equation [3-4].

$$C_3 = \frac{C_1}{\overline{\phi H_T} N} \qquad [3\text{-}4]$$

where:

C_3 = monthly proportionality constant

$\overline{\phi}$ = monthly average daily utilizability

$\overline{H_T}$ = monthly average daily radiation on a tilted plane

N = number of days in the month

$\overline{H_T}$ may be determined as outlined by Klein (22) and several procedures are available for evaluating $\overline{\phi}$ (23-28). Equation 3.4 provides a means for practical application of controlling the collector flow rate proportionately to the utilizable radiation. Using a monthly proportionality constant would result in performance slightly lower than that which could be obtained with a daily proportionality constant.

3.4 Variable Volume Storage

The results presented in Section 3.4 are for the SDHW system with a fully-mixed, variable volume, preheat storage shown in Figure 1.2 and described in Section 1.3. The variable volume tank model (outlined in Section 2.4) is used to represent the preheat storage tank. The performance of variable volume systems operating at reduced constant collector fluid flow rates using on-off control and with variable collector flow rates proportional to the utilizable radiation will be presented.

3.4.1 Reduced Constant Collector Fluid Flow Rate

The performance of the variable volume system operating at reduced constant collector fluid flow rates using on-off differential control is shown in Figure 3.19. The performance of both perfectly stratified and fully-mixed constant volume systems is also shown for comparison purposes. A maximum solar fraction of 46.9 percent occurs at a $\overline{M}_c/M_L$ ratio of 0.918 which corresponds to a collector fluid flow rate of eight $\ell/hr\ m^2$. This is a 7.1 percent improvement over the fully-mixed system operating at high collector flow rates, but it is still 6.9 percent below the optimum reduced constant collector flow rate stratified system.

The variable volume system performs better than the fully-mixed constant volume system because it operates with lower collector inlet temperatures. It performs worse than the perfectly stratified constant volume system because the model considers fluid in the variable volume preheat tank to be fully-mixed. When no recirculation occurs, the

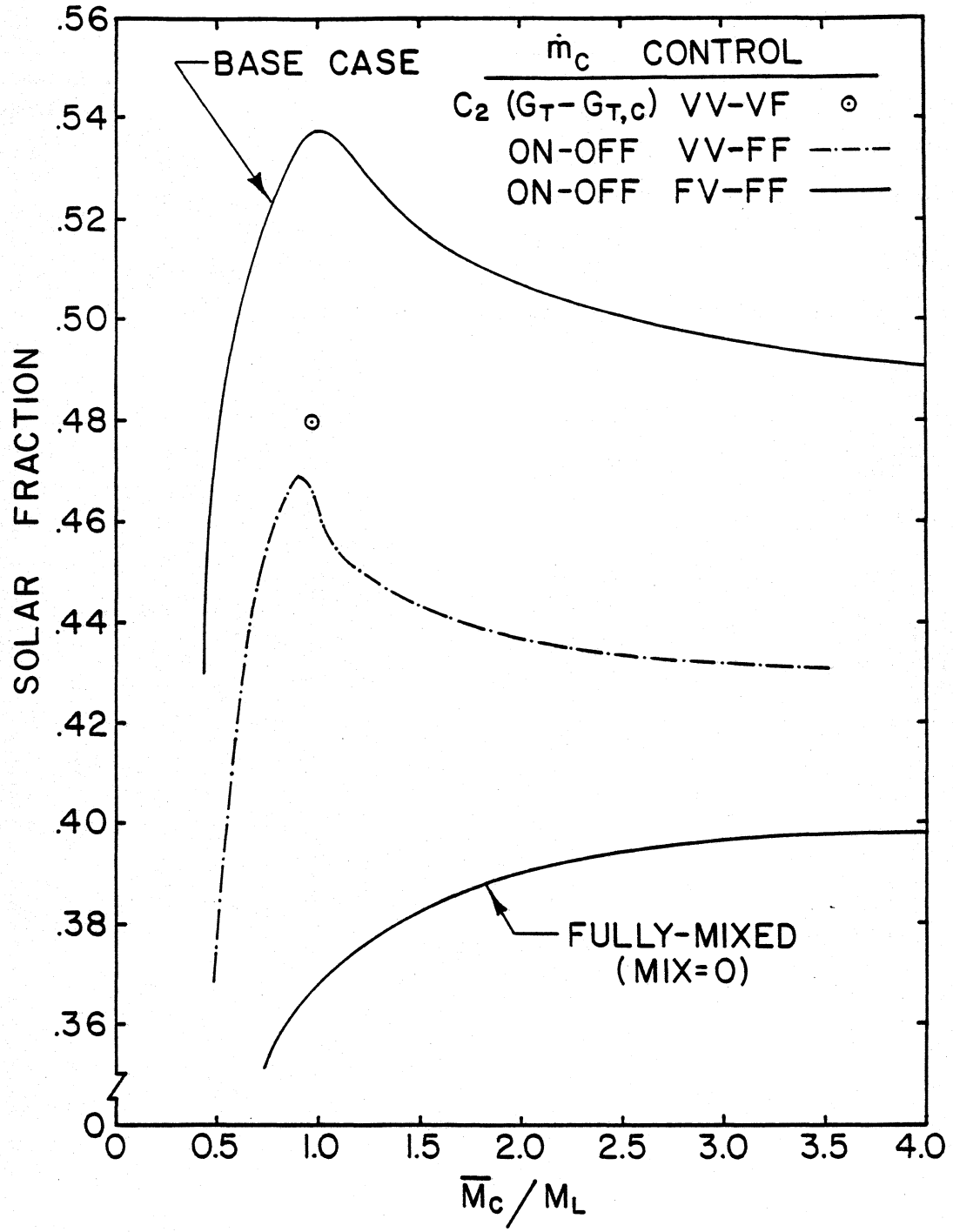

Figure 3.19 Variable Volume Storage with Constant and Variable Collector Flow Rate System Performance, Solar Fraction vs. the ratio of Monthly Average Daily Total Collector Flow to Daily Total Load Flow; for March in Madison, WI, A_c = 4.2 m^2, V_{PT} = 303 ℓ, LOAD = 300 ℓ/day

perfectly stratified constant volume system and the variable volume system have approximately equal collector inlet temperatures. However, when recirculation does occur, the variable volume system has higher collector inlet temperatures because its contents are fully-mixed. The variable volume system also has lower supply temperatures to the auxiliary than the stratified system. Stratification allows the soonest removal of the highest temperature fluid to satisfy load demand, which reduces auxiliary energy and preheat tank thermal losses, when compared to fully-mixed storage. The stratified storage also has energy gains to the colder water in the bottom of the tank which helps to offset the losses from the hot water in the upper portion of the tank. If the daily load is insufficient to remove all the solar heated water from the tank, less energy is left in stratified storage than in the fully-mixed storage.

At $\overline{M}_c/M_L = 2$ there is a 6.9 percentage point difference between the perfectly stratified and variable volume systems. Approximately 1/2 of this difference is caused by greater preheat storage tank energy losses in the variable volume system. The remaining difference is due to the combined effects in the variable volume system of: higher collector inlet temperatures when recirculation occurs, lower fluid temperatures into the auxiliary tank, and more energy left in the tank at the end of the evening. These differences can be easily seen by comparing Figure 3.20a with Figure 3.5b. At $\overline{M}_c/M_L = 0.9$ the daily load draw is sufficient to wipe out all the collected energy and no recirculation occurs . The difference in preheat storage losses then accounts entirely for the 6.5 percentage point difference. At this

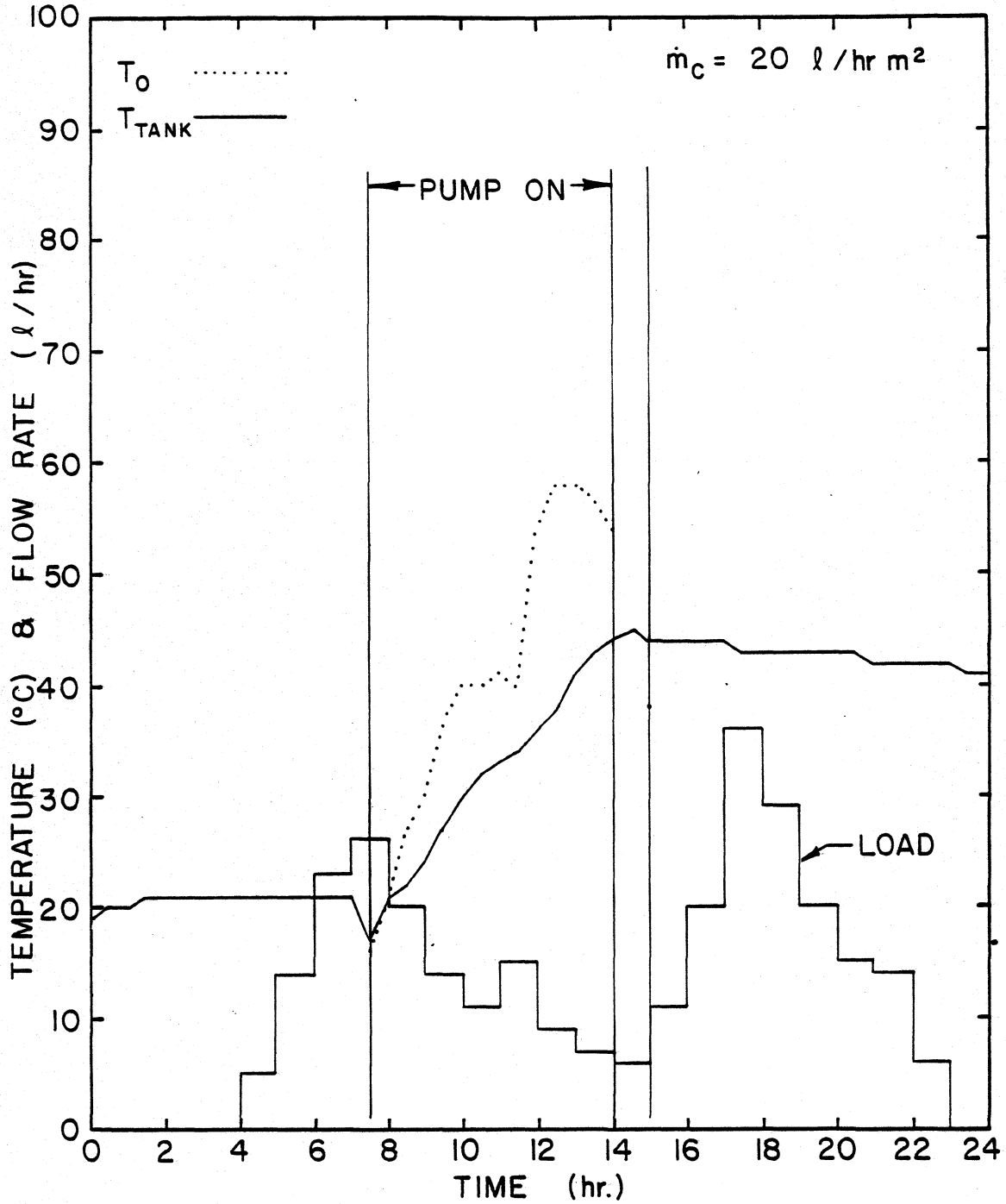

Figure 3.20a Variable Volume Storage with Constant Collector Flow Rate Preheat Storage Tank Temperature Profiles; for March 2nd in Madison, WI, $\dot{m}_c$ = 20 ℓ/hr m², A_c = 4.2 m², V_{PT} = 303 ℓ, LOAD = 300 ℓ/day

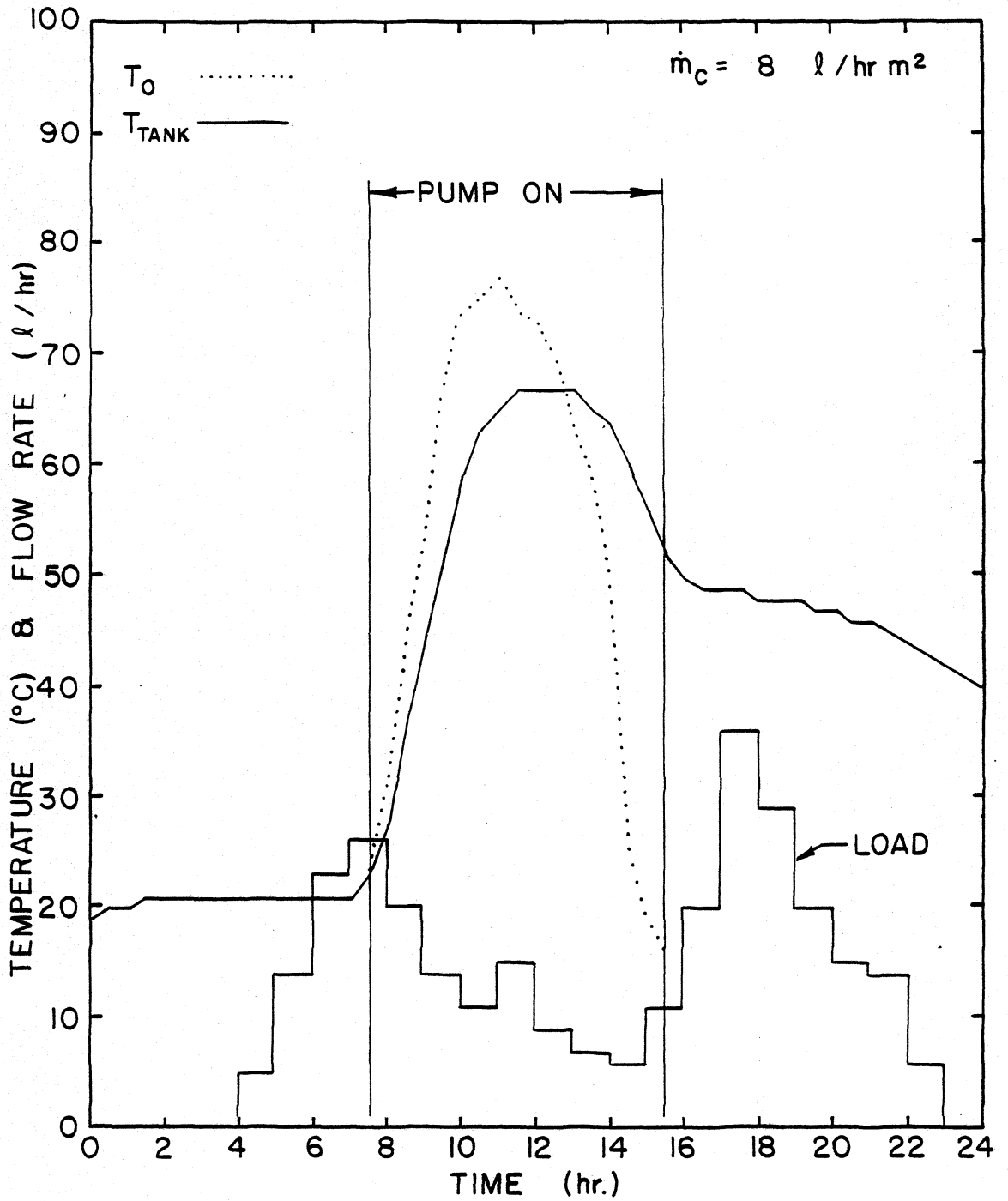

Figure 3.20b Variable Volume Storage with Constant Collector Flow Rate Preheat Storage Tank Temperature Profiles; for March 2nd in Madison, WI, $\dot{m}_c$ = 8 ℓ/hr m², A_c = 4.2 m², V_{PT} = 303 ℓ, LOAD = 300 ℓ/day

low $\overline{M}_c/M_L$ ratio, the thermal losses from the upper sections of the stratified system are low enough to be outweighed by gains from the surroundings in the lower sections and cause a net energy gain.

The gains from the surroundings to the lower sections of the preheat storage help system performance slightly by lowering net energy losses, but they also reduce collector performance by raising the collector inlet temperature slightly. These gains increase as collector fluid flow rate decreases (due to a higher degree of thermal stratification, or steeper temperature profiles), but the overall effect is small.

Figure 3.21 shows the performance of the base case and variable volume systems represented in Figure 3.19 operating with a preheat storage surroundings temperature equal to the mains temperature of 10.4 ° C. This prevents the occurrence of energy gains from the surroundings. The performance of both systems decreases approximately three percentage points due to increased energy losses from the preheat storage, but the relative difference between the fixed and variable volume systems remains nearly the same as in Figure 3.19. Comparison of Figures 3.19 and 3.21 shows that only at $\overline{M}_c/M_L$ ratios less than 0.9 do the effects of gains from the surroundings become noticeable. Comparison of Figures 3.19 and 3.21 also show the relative differences between the two systems at $\overline{M}_c/M_L = 0.9$ to be approximately equal, thus energy gains have a very minor effect. The fixed volume system performs 6.5 percentage points better than the variable volume system because its preheat storage energy losses are 3.7 times less than the

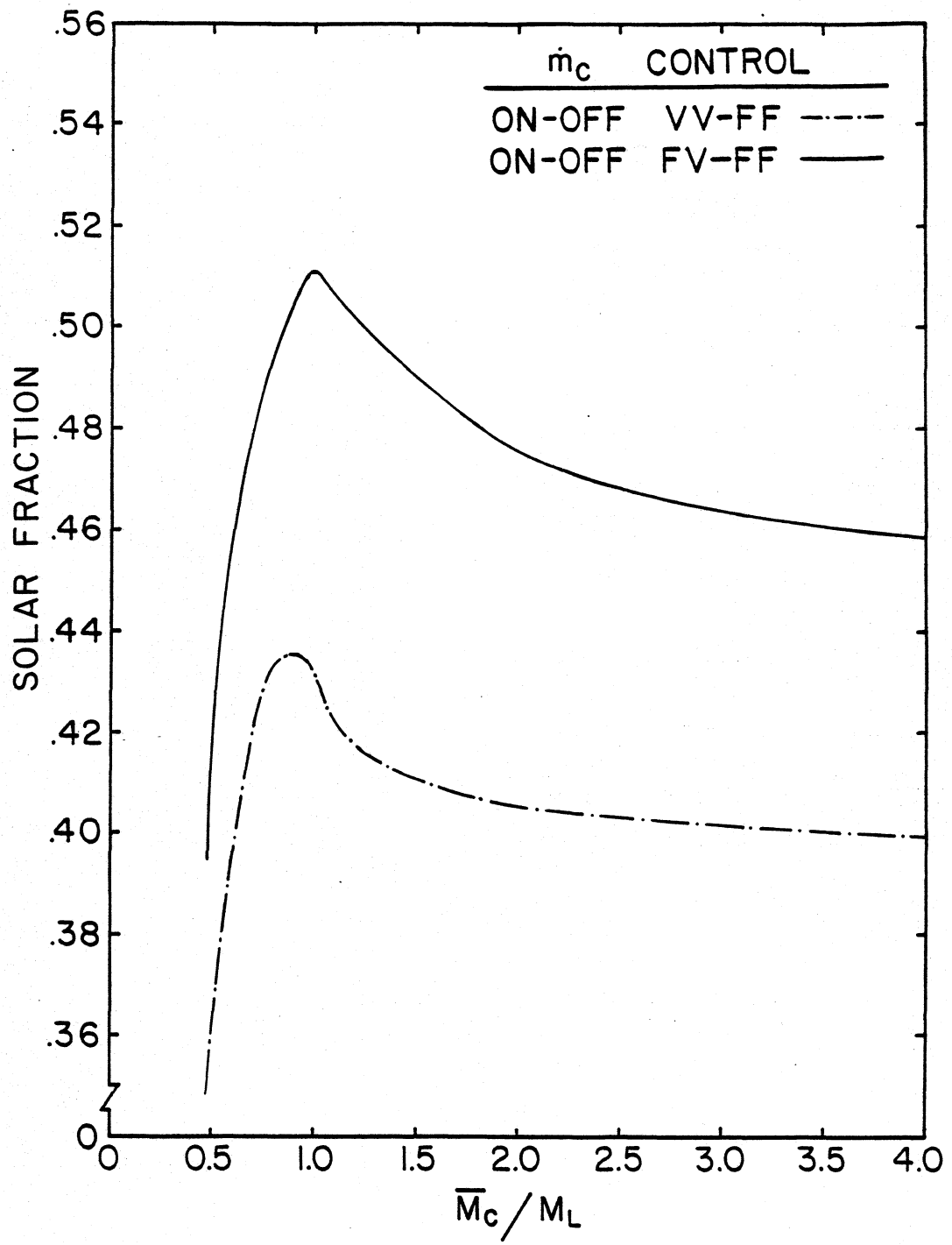

Figure 3.21 Constant vs. Variable Volume Storage System Performance Comparison for Constant Collector Flow Rate with $T_{env} = T_{main}$, Solar Fraction vs. the ratio of Monthly Average Daily Total Collector Flow to Daily Total Load Flow; for March in Madison, WI, A_c = 4.2 m^2, V_{PT} = 303 ℓ, LOAD = 300 ℓ/day

variable volume storage losses. Reduced losses are due to the high degree of thermal stratification which allows the highest temperature water to be removed as soon as possible, thus decreasing the opportunity for energy losses to occur. As $\overline{M}_c/M_L$ decreases, the effect of energy gains from the surroundings begins to appear. Reducing the surroundings temperature to the mains temperature causes the relative difference to decrease by one percentage point at $\overline{M}_c/M_L = 0.75$, and by 4 percentage points at $\overline{M}_c/M_L = 0.50$.

3.4.2 Variable Collector Fluid Flow Rate

The specified collector fluid outlet temperature and collector fluid temperature rise strategies were not examined in the variable volume system because they would still suffer from the disadvantage of higher minimum radiation levels, as for the constant volume storage. Varying the collector flow rate proportionately to the utilizable radiation was examined though, by using the same values of C_2 (daily proportionality constant) generated for the constant volume system in Section 3.3.3.

The result is a solar fraction of 47.9 percent at $\overline{M}_c/M_L = 0.968$. This is one percentage point higher than the optimum reduced constant collector flow rate strategy with on-off control. Proportional control allows more useful energy to be collected, the distribution of which when combined with the Rand load profile, results in higher delivery temperatures to auxiliary and lower preheat storage energy losses. This is shown by comparing Figures 3.20b and 3.22.

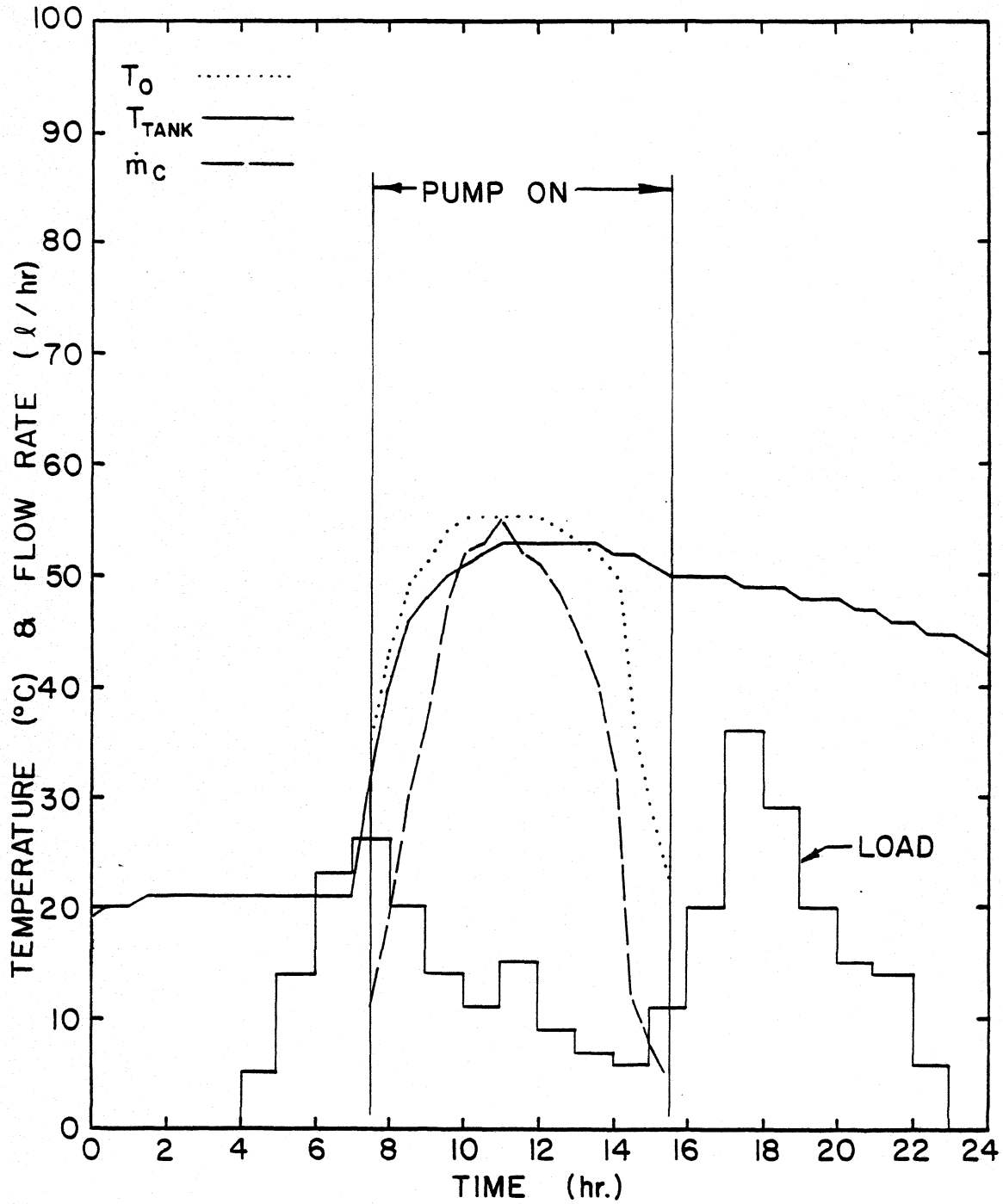

Figure 3.22 Variable Volume Storage with Variable Collector Flow Rate Preheat Storage Tank Temperature Profile; for March 2nd in Madison, WI, A_c = 4.2 m^2, V_{PT} = 303 ,LOAD = 300 /day

3.5 Comprehensive Summary

The performance of all the alternative control strategies examined is summarized in Figure 3.23 for March in Madison, Wisconsin. The constant volume - reduced constant collector fluid flow rate system is also shown with various degrees of mixing in the preheat storage. The perfectly stratified - reduced collector flow rate control strategy performs the best, which is fortunate as it is the easiest to practically apply. Its performance is highly dependent on stratification though, where as the variable volume system has a fully mixed preheat storage tank. The degree of thermal stratification that can be realistically achieved will determine whether or not the variable volume system is a better alternative.

The annual performance of all the strategies examined operating in Madison, Wisconsin is shown in Figure 3.24. The same trends in performance that occur on a monthly basis also occur on an annual basis.

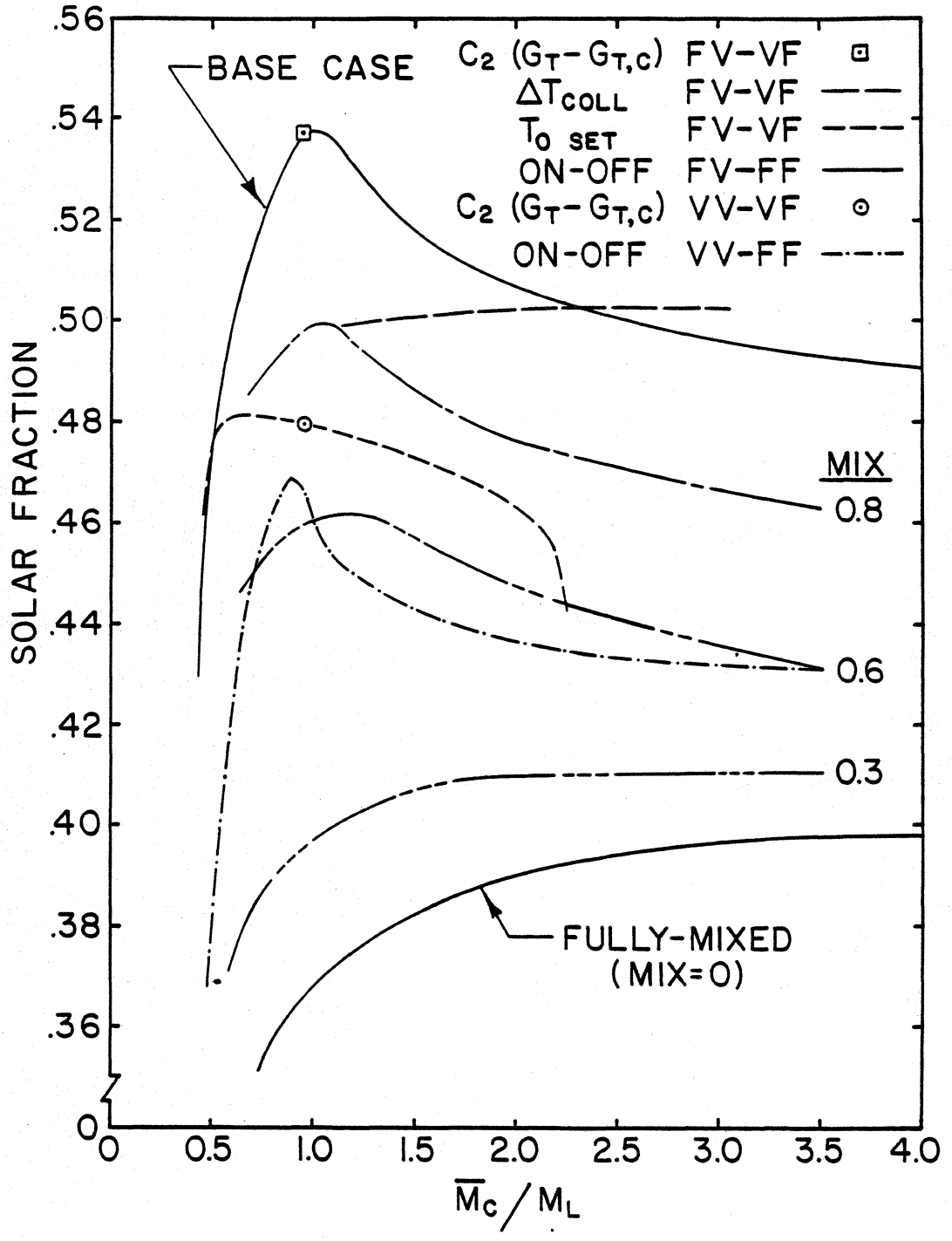

Figure 3.23 Comprehensive Comparison of all Alternative Control Strategies, Solar Fraction vs. the ratio of Monthly Average Daily Total Collector Flow to Daily Total Load Flow; for March in Madison, WI, A_c = 4.2 m^2, V_{PT} = 303 ℓ, LOAD = 300 ℓ/day

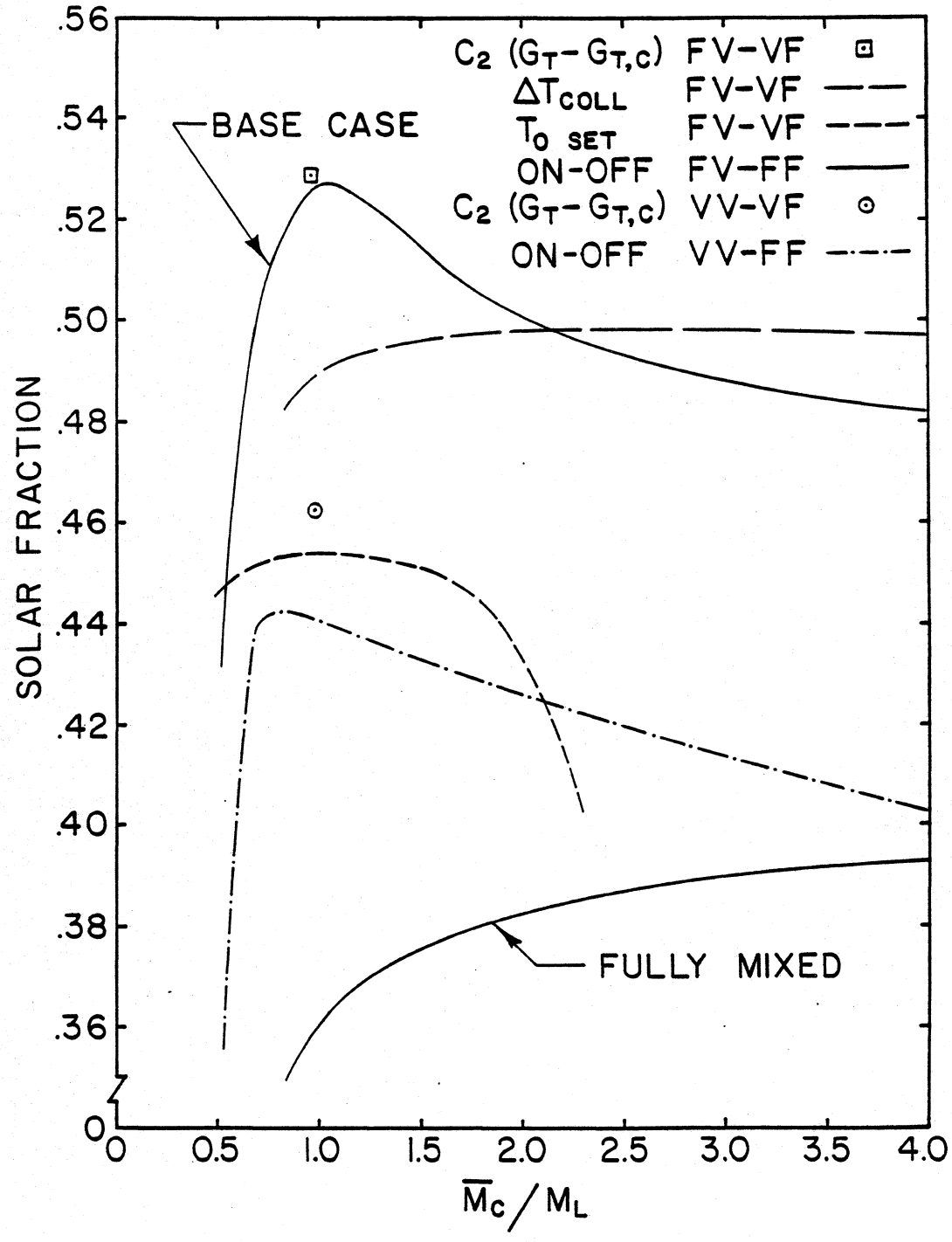

Figure 3.24 Comprehensive Comparison of all Alternative Control Strategies, Solar Fraction vs. the ratio of Monthly Average Daily Total Collector Flow to Daily Total Load Flow; for Year in Madison, WI, A_c = 4.2 m^2, V_{PT} = 303 ℓ, LOAD = 300 ℓ/day

CHAPTER 4

CONCLUSIONS AND RECOMMENDATIONS

This chapter discusses the conclusions that can be drawn from the results of this study concerning alternative SDHW control strategies. Recommendations for future work in this area are also included.

4.1 Conclusions

When conventional SDHW systems are operated at reduced fixed collector fluid flow rates (on the order of 20 percent that of conventional flow rates), simulation results indicate that a much higher degree of thermal stratification can be achieved in the preheat storage tank. The resulting increase in collector efficiency due to reduced collector inlet temperatures often outweighs the reduction in collector efficiency due to the lower values of F_R. System performance is also enhanced slightly by the reduction in preheat storage losses which occurs at reduced collector flow rates. For the particular constant storage volume, reduced constant flow rate systems investigated, the annual performance with stratified storage at reduced flow rates showed improvements from 11.5 to 14.7 percentage points greater than that which would be achieved with otherwise identical systems having fully-mixed storage tanks operating at conventional high flow rates.

The fixed collector outlet temperature and fixed collector temperature rise variable flow rate strategies using constant storage volume showed improvements of 7.3 and 9.5 percentage points respectively, when compared to fully-mixed systems operating at

conventional constant flow rates. Both strategies however performed worse than the simpler reduced constant flow rate, on-off differential temperature control. Proportional control based on the utilizable radiation (i.e. level of incident radiation above the critical level) performed very nearly as well as the optimum reduced constant flow rate strategy. This method requires knowledge of future weather conditions which makes practical application difficult.

The variable preheat storage volume system was examined operating in Madison with both a constant collector flow rate , on-off control strategy, and a variable collector flow rate proportional to the utilizable radiation. The constant collector flow rate showed a 4.9 percentage point improvement in annual performance over the fully-mixed system operating at high collector flow rates. Varying the collector flow rate proportionally to the utilizable radiation yielded a 6.9 percentage point improvement over the fully-mixed system. Neither strategy however, performs as well as the constant storage volume, reduced constant collector flow rate on-off control.

Parasitic power requirements were neglected in this investigation. However, if they were included, the reduced collector flow rate system would show an even greater relative improvement over conventional high flow rate systems.

The optimum system performance occurs very near to a monthly average daily total collector flow to daily total load flow ($\overline{M}_c/M_L$) ratio of one. The optimum $\overline{M}_c/M_L$ ratio shows some time of year dependence but this is due mainly to day length variations. The optimum collector flow rate per unit area is less dependent on time of

year and thus only a slight improvement in performance could be realized by adjusting the collector flow on a monthly basis.

Fixed controller temperature deadbands were found to reduce system performance slightly at higher flow rates, thus increasing the relative difference in performance between slow and high flow rate systems. An alternative control strategy might be to activate the circulation pump when the useful energy collection is greater than the pumping power required, although this would be difficult to implement.

Collector area and quality, preheat storage energy losses, and auxiliary set temperature all had some effect on solar fraction but showed very little effect on the optimum $\overline{M}_c/M_L$ ratio.

The storage tank volume, daily load, and load distribution have a direct effect on the optimum fixed flow rate, because of their impact on the occurrence and amount of recirculation. The optimum $\overline{M}_c/M_L$ ratio ranged from 0.6 to 1.4 for the range of parameters examined.

4.2 Recommendations

The optimum in system performance at reduced collector flow rates depends entirely on the degree of thermal stratification. The plug-flow tank model neglects conduction between segments of fluid and in the tank wall. It also does not account for any mixing due to inlet flows, or naturally occurring due to density gradients. More work should be done comparing the performance of the plug-flow storage tank model with experimental data to determine what degrees of thermal stratification are actually obtainable.

System performance predictions also depend heavily upon the

collector model. The model assumes a constant collector loss coefficient and neglects axial conduction in the collector fluid and absorber plate (i.e. one-dimensional conduction). These and other assumptions within the collector model that were valid at high flow rates may be less so at reduced flow rates. The performance predictions of the collector model at low flow rates should also be experimentally verified.

This study examined two-tank direct SDHW systems. Both single tank and indirect systems should also be investigated. In-tank heat exchanger systems tend to destroy stratification (2) and should therefore perform better at high collector flow rates, but a reduced collector flow rate optimum might exists in external heat exchanger systems.

APPENDIX A

COMPONENT MODEL PROGRAM LISTINGS AND DOCUMENTATION

This appendix contains subroutine listings and documentation for the following nonstandard TRNSYS components: collector, plug-flow storage tank, variable volume storage tank, RECIR, and IF-CALC.

COLLECTOR

This subroutine models flat plate collector performance with both fixed flow rate and variable flow rate to obtain a specified collector outlet temperature.

Parameters

1 MODE - 1 constant flow rate
2 not used
3 variable flow rate to obtain a specified collector outlet temperature

2 N_s - number of collectors in series

3 A_c - collector surface area

4 C_p - constant pressure specific heat of fluid

5 $F_R(\tau\alpha)_n|_{test}$ - intercept efficiency at test flow rate

6 $F_R U_L|_{test}$ - negative slope of efficiency curve at test flow rate

7 $\dot{m}_c|_{test}$ - flow rate per unit area at test conditions

8 b_o - incidence angle modifier constant

Inputs

1 T_i - inlet temperature

2 $\dot{m}_c$ - inlet flow rate

3 T_a - ambient temperature

4 G_T - instantaneous total radiation incident on collector

5 θ - incidence angle

6 G_{BT} - instantaneous beam radiation incident on collector

7 G_D - instantaneous horizontal diffuse radiation

8 β - collector slope

9 (MODE 3) T_o - specified outlet temperature

10 (MODE 3) $\dot{m}_{c,MAX}$ - maximum collector flow rate

Outputs

1 T_o - outlet temperature

2 $\dot{m}_c$ - outlet flow rate

3 Q_u - rate of useful energy collection

4 $K_{\tau\alpha}$ - incidence angle modifier

5 -

6 (MODE 1) $F_R U_L$ - negative slope of efficiency curve corrected for non-test flow rate

7 (MODE 1) $F_R(\tau\alpha)$ - intercept efficiency corrected for non-normal incidence angle and non-test flow rate

```
C  THIS SUBROUTINE MODELS FLAT-PLATE COLLECTOR
C  PERFORMANCE, WITH BOTH FIXED FLOW RATE AND
C  VARIABLE FLOW RATE TO ACHIEVE A SPECIFIED TO
      SUBROUTINE TYPE1(TIME,XIN,OUT,T,DTDT,PAR,INFO)
      DIMENSION PAR(15),XIN(10),OUT(20),INFO(10)
      DATA IUNIT/0/,RDCONV/0.017453/,PI/3.141593/
      DATA RATIO/1./,XKAT/1./,NSTK/7/
C
      TAUALF(THETA)=1.-B0*(1./AMAX1(0.5,COS(THETA*PI/180.))
-1.)
     .             - (1.-B0)*(AMAX1(60.,THETA)-60.)/30.
C
      IF(INFO(7).GT.-1) GO TO 5
C  FIRST CALL OF SIMULATION
      MODE=INT(PAR(1)+0.1)
      NI=8
      IF(MODE.EQ.3) NI=10
      NP=8
C
      CALL TYPECK(1,INFO,NI,NP,0)
C
5     IF(INFO(1) .EQ. IUNIT) GO TO 30
      IUNIT=INFO(1)
C
C  SET PARAMETERS
      MODE=INT(PAR(1)+0.1)
      NS=INT(PAR(2)+0.1)
      A=PAR(3)
      CP=PAR(4)
      FRTAN=PAR(5)
      FRUL=PAR(6)
      GTEST=PAR(7)
      FPUL=-GTEST*CP*ALOG(1.-FRUL/GTEST/CP)
      RTEST=GTEST*CP*(1.-EXP(-FPUL/GTEST/CP))
      B0=PAR(8)
C
      IF(MODE.EQ.1) INFO(6)=5
      IF(MODE.EQ.1) INFO(6)=1
      IF(MODE.EQ.1) INFO(6)=5
C
C  INPUTS
30    TI=XIN(1)
      FLW=XIN(2)
      TA=XIN(3)
      GT=XIN(4)
      THETA=XIN(5)
      GBT=XIN(6)
      GD=XIN(7)
      SLP=XIN(8)
```

```
      GDT=GT-GBT
      GDSKY=GD*(1.+COS(SLP*RDCONV))/2.
      GDGND=GDT-GDSKY
      IF(MODE.EQ.3) TOUT=XIN(9)
      IF(MODE.EQ.3) FLWMAX=XIN(10)
C
      IF(GT .GT. 0. .AND. THETA .LT. 90.) GO TO 40
C
C  NO RADIATION
      XKAT=0.
      GO TO 80
C
C**DETERMINE INCIDENCE ANGLE MODIFIER
C
C  FLAT PLATES
C
C  RELATIONS OF BRANDEMUEHL FOR EFFECTIVE INCIDENCE ANGLES
C    FOR DIFFUSE
40    EFFSKY=59.98-0.1388*SLP+0.001497*SLP*SLP
      EFFGND=90.-0.5788*SLP+0.002693*SLP*SLP
C
C    USE CONSTANT FROM ASHRAE TESTS
      XKATB=TAUALF(THETA)
      XKATDS=TAUALF(EFFSKY)
      XKATDG=TAUALF(EFFGND)
      XKAT=(XKATB*GBT+XKATDS*GDSKY+XKATDG*GDGND)/GT
C
C**THERMAL PERFORMANCE
80    GO TO (100,125,150) ,MODE
C  MODE 1, STANDARD ASHRAE PERFORMANCE
100   IF(INFO(7).EQ.NSTK) FLWS=FLW
      IF(INFO(7).GT.NSTK) FLW=FLWS
      IF(FLW .GT. 0.) GO TO 110
C    NO FLOW
      QU=0.
      TO=GT*FRTAN*XKAT/FRUL+TA
      GO TO 120
C    PUMP ON
110   R1=FLW*CP/A*(1.-EXP(-FPUL*A/FLW/CP))/RTEST
      XK=R1*A*FRUL/FLW/CP
      R2=(1.-(1.-XK)**NS)/FLOAT(NS)/XK
      RATIO=R1*R2
      QU=RATIO*A*(FRTAN*XKAT*GT-FRUL*(TI-TA))
      TO=QU/FLW/CP+TI
C
C  OUTPUTS
120   OUT(1)=TO
      OUT(2)=FLW
      OUT(3)=QU
      OUT(4)=XKAT
```

```
      OUT(5)=X
      OUT(6)=RATIO*FRUL
      OUT(7)=RATIO*XKAT*FRTAN
      RETURN
C
C  MODE 2, UTILIZABLE RADIATION
C
125   OUT(1)=0.
      IF(XKAT .LT. 1.E-03) RETURN
      FRTA=FRTAN*XKAT
      GC=FRUL*(TI-TA)/FRTA
      SUM=AMAX1(GT-GC,0.)
      OUT(1)=SUM
      RETURN
C
C  MODE 3, DETERMINE FLOW AND QU FOR FIXED OUTLET TEMP
C
  150 IF(INFO(7).GE.NSTK) GO TO 100
      OUT(1)=0.
      OUT(2)=0.
      OUT(3)=0.
      OUT(4)=0.
      OUT(5)=0.
      IF(XKAT .LT. 1.E-03) RETURN
      OUT(4)=XKAT
      FRTA=FRTAN*XKAT
      X=1.-(TOUT-TI)/(FRTA/FRUL*GT-(TI-TA))
      OUT(5)=X
      IF(X.LE.0. .OR. X.GE.1.) RETURN
      FLWC=-A*FPUL/CP/ALOG(X)
      FLWC=AMIN1(FLWC,FLWMAX)
  160 IF(FLWC.LT.FLWMAX) GO TO 170
      FLW=FLWMAX
      GO TO 100
  170 QU=FLWC*CP*(TOUT-TI)
      OUT(1)=TOUT
      OUT(2)=FLWC
      OUT(3)=QU
      RETURN
      END
```

PLUG-FLOW STORAGE TANK MODEL

This subroutine models the performance of a stratified liquid storage tank using an algebraic bookkeeping system which divides the tank into a variable number of variable size, uniform temperature segments of fluid.

Parameters

1	MODE	-	1 fixed inlet positions 2 variable inlet positions
2	V_T	-	tank volume
3	H_T	-	tank height
4	H_{IN}	-	height up from bottom of tank of inlet flow
5	C_p	-	constant pressure specific heat of fluid
6	ρ	-	fluid density
7	U_T	-	tank loss coefficient
8	T_I	-	initial temperature of fluid in tank

Optional Parameters

9	N	-	number of additional temperature outputs; divides tank into N+1 sections and gives the temperature at the bottom of each
10	$\dot{Q}_{AUX,MAX}$	-	maximum rate of auxiliary heat input
11	H_{AUX}	-	height of auxiliary heater above bottom of tank
12	H_t	-	height of thermostat above bottom of tank
13	T_{SET}	-	thermostat set temperature
14	T_{db}	-	temperature deadband for auxiliary heater
15	$(UA)_f$	-	conductance for heat loss to flue when auxiliary heater is off

Inputs

1	T_h	-	temperature of fluid from heat source

2 $\dot{m}_h$ - mass flow rate from heat source

3 T_L - temperature of replacement fluid form load

4 $\dot{m}_L$ - mass flow rate from load

5 T_{env} - temperature of tank environment

6 (optional) MIX - mixing parameter;MIX = 0, ordinary operation MIX = 1, complete mixing of tank

7 (optional) γ_{htr} - enable signal for auxiliary heater

Outputs

1 T_R - temperature of fluid returned to heat source

2 $\dot{m}_h$ - mass flow rate to heat source

3 T_D - temperature of fluid delivered to load

4 $\dot{m}_L$ - mass flow rate to load

5 $\dot{Q}_{env}$ - rate of energy loss from tank

6 $\dot{Q}_{sup}$ - rate of energy supply to load

7 ΔU - change in internal energy of tank

8 $\dot{Q}_{AUX}$ - rate of auxiliary input to tank

9 $\dot{Q}_{in}$ - rate of energy input to tank by fluid stream from heat source

10 $\overline{T}$ - average storage temperature

11 T_1 - temperature at bottom of 1st segment

12 T_2 - temperature at bottom of 2nd segment

13 T_3 - temperature at bottom of 3rd segment

. .

. .

. .

20 T_{10} - temperature at bottom of 10th segment

```
C  THIS SUBROUTINE MODELS THE PERFORMANCE OF A STRATIFIED
C  LIQUID STORAGE TANK  USING AN ALGEBRAIC BOOKKEEPING
C  SYSTEM WHICH DIVIDES THE TANK INTO A VARIABLE NUMBER OF
C  VARIABLE SIZE, UNIFORM TEMPERATURE SEGMENTS OF FLUID
      SUBROUTINE TYPE38(TIME,XIN,OUT,TDUM,DTDT,PAR,INFO)
      LOGICAL AUX,AUXLST
      REAL MSCP,MC,ML
      DIMENSION XIN(7),OUT(20),PAR(13),INFO(10)
      DIMENSION T(50),TLAST(50),X(50),XLAST(50)
      DIMENSION NORDER(50),NEXT(50),NLAST(50),THIGH(10)
      DIMENSION ACON(2),BCON(2),GRAV(2),TEM(10)
      COMMON /SIM/ TIME0,TIMEF,DELT
      DATA PI/3.1415927/,NMAX/46/,NTMAX/50/,ICALL/0/
      DATA NSTK/5/,ACON/1.,1.8/,BCON/0.,32./,GRAV/9.8,32.2/
C
      TCONV(T)=(T-BCON(IU))/ACON(IU)
      SG(T)=1.00026-4.05E-06*TCONV(T)**2-3.906E-05*TCONV(T)
C
      IF(INFO(7).GT.-1) GO TO 20
C
C--   ONLY ONE TYPE 38 ALLOWED
      ICALL=ICALL+1
      IF(ICALL.EQ.1) IUNIT=INFO(1)
      IF(IUNIT.NE.INFO(1)) CALL TYPECK(-6,INFO,0,0,0)
C--   SKIP TYPECK CALL, IF THERMOSYPHON SUBSYSTEM
      IPAR=20
      IF(INFO(2).EQ.37) GO TO 5
C
C--   CHECK NO. OF PARAMETERS AND INPUTS
      IPAR=0
      INFO(6)=10
      NP=8
      NI=5
      IF(INFO(4).EQ.9) NP=9
      IF(INFO(4).EQ.15) NP=15
      IF(INFO(3).EQ.6) NI=6
      IF(INFO(3).EQ.7) NI=7
      CALL TYPECK(1,INFO,NI,NP,0)
C
C--   PARAMETERS
5     IF(INFO(2).EQ.37) IU=INT(PAR(1)+0.1)
      MODE=INT(PAR(IPAR+1)+0.1)
      VOL=PAR(IPAR+2)
      HIGH=PAR(IPAR+3)
      HIN=PAR(IPAR+4)
      CPF=PAR(IPAR+5)
      RHO=PAR(IPAR+6)
      ULOSS=PAR(IPAR+7)
      TI=PAR(IPAR+8)
```

```
      IAUX=0
      IF(INFO(2).EQ.38.AND.INFO(4).EQ.8 .OR.
     .   INFO(2).EQ.37.AND.INFO(4).EQ.28) GO TO 10
      NTEMP=PAR(IPAR+9)
      INFO(6)=10+NTEMP
      IF(INFO(2).EQ.38.AND.INFO(4).EQ.9) GO TO 10
      IAUX=1
      QMAX=PAR(IPAR+10)
      HAUX=PAR(IPAR+11)
      HTH=PAR(IPAR+12)
      TSET=PAR(IPAR+13)
      TDB=PAR(IPAR+14)
      UAF=PAR(IPAR+15)
C
C--   PRELIMINARIES
10    DIA=(4.*VOL/PI/HIGH)**0.5
      USIDE=PI*DIA*ULOSS
      UAE=0.25*PI*DIA**2.*ULOSS
      MSCP=VOL*RHO*CPF
      ACROSS=VOL/HIGH
      NSEG=NTEMP+1
      XSEG=1.0/NSEG
      DO 12 I=1,NTEMP
      THIGH(I)=XSEG*I
12    CONTINUE
C
C--   PROFILE INITIALIZATIONS
      AUX=.FALSE.
      XCOL=1.-HIN/HIGH
      INEXT=0
      IF(IAUX.EQ.0) GO TO 15
      NTOT=2
      NORDER(1)=1
      NORDER(2)=2
      NEXT(1)=3
      NAUX=1
      NTH=1
      XAUX=1.-HAUX/HIGH
      XTH=1.-HTH/HIGH
      T(1)=TSET
      T(2)=TI
      X(1)=XAUX
      X(2)=1.-XAUX
      T0=T(1)*X(1)+T(2)*X(2)
      GO TO 17
C
15    NTOT=1
      NORDER(1)=1
      NEXT(1)=2
      NAUX=0
```

```
      X(1)=1.
      T(1)=TI
      T0=TI
C
17    TDEL=T(1)
      TRET=T(NTOT)
      QBTOT=0.
C
20    IF(TIME.EQ.TIME0) GO TO 21
      IF(INF0(7).GT.0) GO TO 21
C** CORRECT FOR TEMPERATURE INVERSIONS
      K=NTOT-1
      DO 86 N=1,K
      IF(N.GE.NTOT) GO TO 21
      IP1=NORDER(N-1)
      IP=NORDER(N)
      IP2=NORDER(N+1)
C  CHECK DOWN PROFILE
87    IF(T(IP2).LT.T(IP)) GO TO 86
      T(IP)=(T(IP)*X(IP)+T(IP2)*X(IP2))/(X(IP)+X(IP2))
      X(IP)=X(IP)+X(IP2)
      IX=NTOT-2
      DO 91 I=N,IX
      NORDER(I+1)=NORDER(I+2)
91    CONTINUE
      NTOT=NTOT-1
      IP2=NORDER(N+1)
      IF(N.GE.NTOT) GO TO 21
      IF(T(IP).LT.T(IP2)) GO TO 87
      IF(N.EQ.1) GO TO 86
C  CHECK UP PROFILE
88    IF(T(IP).LT.T(IP1)) GO TO 86
      T(IP)=(T(IP)*X(IP)+T(IP1)*X(IP1))/(X(IP)+X(IP1))
      X(IP)=X(IP)+X(IP1)
      DO 92 I=N,NTOT
      NORDER(I-1)=NORDER(I)
92    CONTINUE
      NTOT=NTOT-1
      IP1=NORDER(N-1)
      IP=NORDER(N)
      IF(T(IP).GT.T(IP1)) GO TO 88
86    CONTINUE
C--   INPUTS
21    TC=XIN(1)
      MC=XIN(2)
      TL=XIN(3)
      ML=XIN(4)
      TENV=XIN(5)
      MIX=INT(XIN(6)+.1)
      IGAM=1
```

```
      IF((INFO(2).EQ.38.AND.INFO(3).EQ.6) .OR.
     .   (INFO(2).EQ.37.AND.INFO(3).EQ.10)) IGAM=INT(XIN(7)
+0.1)
      IF(TIME.LT.TIME0+DELT/2.) GO TO 300
C
C--  VOLUMETRIC FLOWS RELATIVE TO TANK VOLUME
23    VCOL=MC/RHO*DELT/VOL
      VLD=ML/RHO*DELT/VOL
      IF(INFO(7).GT.0) GO TO 40
C
C--  FIRST CALL OF CURRENT INTERVAL
      IF(NTOT.LT.NMAX) GO TO 30
C
C--  TOO MANY NODES, COMBINE PAIRS
      N2=0
      IC=0
22    N1=N2+1
      IF(N1.GT.NTOT) GO TO 25
      N2=N1+1
      IF(N1.EQ.NAUX .OR. N1.EQ.NTOT .OR.
     .   (MODE.EQ.1 .AND. N2.EQ.NCOL)) N2=N1
      IC=IC+1
      IF(N2.EQ.NAUX) NAUX=IC
      IF(MODE.EQ.1 .AND. N1.EQ.NCOL) NCOL=IC
      IP1=NORDER(N1)
      IP2=NORDER(N2)
      NORDER(IC)=IP1
      T(IP1)=(T(IP1)*X(IP1)+T(IP2)*X(IP2))/(X(IP1)+X(IP2))
      IF(N1.NE.N2) X(IP1)=X(IP1)+X(IP2)
      GO TO 22
25    NTOT=IC
C
C--  INITIALIZE ARRAY OF NEXT AVAILABLE LOCATIONS
30    DO 32 N=1,NTMAX
32    NEXT(N)=N
C
C-- SAVE PROFILE FROM LAST INTERVAL, ELIMINATE UN-AVAILABLE
C-- LOCATIONS FROM NEXT ARRAY
      DO 35 N=1,NTOT
      NLAST(N)=NORDER(N)
      IP=NORDER(N)
      TLAST(IP)=T(IP)
      XLAST(IP)=X(IP)
35    NEXT(IP)=0
      NXLAST=NAUX
      NTLAST=NTOT
      AUXLST=AUX
      NCLST=NCOL
C
C--  FIND 1ST, 2ND, 3RD, AND 4TH AVAILABLE LOCATIONS
```

```
      L=0
      DO 37 N=1,NTMAX
      IF(NEXT(N).EQ.0) GO TO 37
      L=L+1
      NEXT(L)=NEXT(N)
      IF(L.EQ.4) GO TO 50
37    CONTINUE
      GO TO 50
C
C--   INITIALIZE PROFILE FROM LAST INTERVAL
40    NTOT=NTLAST
      NAUX=NXLAST
      AUX=AUXLST
      NCOL=NCLST
      DO 45 N=1,NTOT
      NORDER(N)=NLAST(N)
      IP=NORDER(N)
      X(IP)=XLAST(IP)
45    T(IP)=TLAST(IP)
C
50    INEXT=0
      IF(VLD.LT.1.E-06 .AND. VCOL.LT.1.E-06) GO TO 140
      IF(VCOL.LT.1.E-06) GO TO 70
      IF(MODE.EQ.1) GO TO 60
C
C
C--   FIND POSITION CLOSEST IN TEMP TO COLL INLET, MODE 2
      NCOL=1
      XC=0
      VNET=VCOL
      IF(TL.LE.TC) VNET=VCOL-VLD
      DO 55 N=1,NTOT
      IPC=NORDER(N)
      IF((1.-XC).LT.VNET) GO TO 58
      IF(TC.GT.T(IPC)) GO TO 60
      XC=XC+X(IPC)
      NCOL=N+1
55    CONTINUE
58    IF(NCOL.EQ.1) GO TO 60
C--   AVOID RECIRCULATING COLLECTOR INLET STREAM
      NCOL=NCOL-1
C
C--   ADJUST PROFILE DUE TO COLLECTOR FLOW
60    ICC=0
      IF(INFO(7).GT.NSTK) GO TO 64
      IF(NCOL.EQ.1) GO TO 61
      IPN=NORDER(NCOL-1)
      IF(ABS(TC-T(IPN)).GT.0.5) GO TO 61
      GO TO 63
61    IF(NCOL.EQ.(NTOT+1)) GO TO 64
```

```
      IPN=NORDER(NCOL)
      IF(ABS(TC-T(IPN)).GT.0.5) GO TO 64
C     COMBINE WITH NODE THAT IS WITHIN 1/2 DEGREE
63    T(IPN)=(TC*VCOL+T(IPN)*X(IPN))/(X(IPN)+VCOL)
      X(IPN)=X(IPN)+VCOL
      ICC=1
      GO TO 70
64    INEXT=1
      DO 65 N=NCOL,NTOT
      L=NTOT-N+NCOL+1
65    NORDER(L)=NORDER(L-1)
      NTOT=NTOT+1
      NC=NEXT(INEXT)
      X(NC)=VCOL
      T(NC)=TC
      NORDER(NCOL)=NC
C
70    IF(VLD.LT.1.E-06) GO TO 80
      NLD=NTOT+1
      IF(MODE.EQ.1) GO TO 75
C
C--   FIND POSITION CLOSEST IN TEMP TO LOAD FLOW, MODE 2
      XL=0.
      VNET=VLD
      IF(TL.LE.TC) VNET=VLD-VCOL
      DO 72 N=1,NTOT
      L=NTOT-N+1
      IPL=NORDER(L)
      IF((1.+VCOL-XL).LT.VNET) GO TO 73
      IF(TL.LT.T(IPL)) GO TO 75
      XL=XL+X(IPL)
      NLD=L
72    CONTINUE
73    IF(NLD.GT.NTOT) GO TO 75
C   AVOID RECIRCULATING LOAD INLET STREAM
      NLD=NLD+1
C
C--   ADJUST PROFILE DUE TO LOAD FLOW
75    ICL=0
      IF(INFO(7).GT.NSTK) GO TO 77
      IF(NLD.EQ.NTOT+1) GO TO 76
      IPN=NORDER(NLD)
      IF(ABS(TL-T(IPN)).GT.0.5) GO TO 76
      GO TO 74
76    IF(NLD.EQ.1) GO TO 77
      IPN=NORDER(NLD-1)
      IF(ABS(TL-T(IPN)).GT.0.5) GO TO 77
C     COMBINE WITH NODE THAT IS WITHIN 1/2 DEGREE
74    T(IPN)=(TL*VLD+T(IPN)*X(IPN))/(X(IPN)+VLD)
      X(IPN)=X(IPN)+VLD
```

```
      ICL=1
      GO TO 80
77    INEXT=INEXT+1
      NL=NEXT(INEXT)
      X(NL)=VLD
      T(NL)=TL
      IF(NLD.GT.NTOT) GO TO 79
      DO 78 N=NLD,NTOT
      L=NTOT-N+NLD
78    NORDER(L+1)=NORDER(L)
79    NORDER(NLD)=NL
      NTOT=NTOT+1
C
C FULLY MIX TANK PROFILE WHEN MIX=1
80    IF(MIX.EQ.0) GO TO 81
      TMIX=0.
      DO 24 I=1,NTOT
      IP=NORDER(I)
      TMIX=TMIX+T(IP)*X(IP)
24    CONTINUE
      IP1=NORDER(1)
      T(IP1)=TMIX
      X(IP1)=1.
      NTOT=1
C
C** CORRECT FOR TEMPERATURE INVERSIONS
C
81    IF(MODE.EQ.2) GO TO 140
C
C** CORRECT FOR TEMPERATURE INVERSIONS
      IF(VCOL.LT.1.E-06 .OR. ICC.EQ.1) GO TO 120
C--  DUE TO COLLECTOR FLOW
      IF(NCOL.EQ.NTOT) GO TO 90
      IPN=NORDER(NCOL+1)
      IF(TC.GE.T(IPN)) GO TO 90
C--  CORRECT DOWNWARD
      XS=0.
      TS=0.
      DO 85 N=NCOL,NTOT
      IP=NORDER(N)
      IF(N.LT.NTOT) IPN=NORDER(N+1)
      TS=TS+T(IP)*X(IP)
      XS=XS+X(IP)
      NLOC=N+1
      IF(TS/XS.GE.T(IPN)) GO TO 100
85    CONTINUE
      GO TO 100
C
90    IF(NCOL.EQ.1) GO TO 120
      IPN=NORDER(NCOL-1)
```

```
      IF(T(NC).LE.T(IPN)) GO TO 120
C
C--   CORRECT UPWARD
      NLOC=NCOL+1
      TS=T(NC)*X(NC)
      XS=X(NC)
95    NCOL=NCOL-1
      IP=NORDER(NCOL)
      IF(NCOL.GT.1) IPN=NORDER(NCOL-1)
      TS=TS+T(IP)*X(IP)
      XS=XS+X(IP)
      IF(TS/XS.GT.T(IPN) .AND. NCOL.GT.1) GO TO 95
C
C--   REORDER
100   T(IP)=TS/XS
      X(IP)=XS
      L=NCOL
      IF(NLOC.GT.NTOT) GO TO 110
      DO 105 N=NLOC,NTOT
      L=L+1
105   NORDER(L)=NORDER(N)
110   NTOT=L
      NORDER(NCOL)=IP
C
120   IF(VLD.LT.1.E-06 .OR. ICL.EQ.1) GO TO 140
C
C--   DUE TO LOAD FLOW
      IPN=NORDER(NTOT-1)
      IF(TL.LT.T(IPN)) GO TO 140
      XS=0.
      TS=0.
      DO 125 N=1,NTOT
      NL=NTOT-N+1
      IP=NORDER(NL)
      IF(NL.GT.1) IPN=NORDER(NL-1)
      TS=TS+T(IP)*X(IP)
      XS=XS+X(IP)
      IF(TS/XS.LE.T(IPN)) GO TO 130
125   CONTINUE
130   T(IP)=TS/XS
      X(IP)=XS
      NTOT=NL
C
C-- COMPUTE AVERAGE COLLECTOR RETURN TEMPERATURE
C
140   IBOT=NORDER(NTOT)
      TRET=T(IBOT)
      IF(VCOL.LT.1.E-06) GO TO 160
      TS=0.
      XS=0.
```

```
      DO 150 N=1,NTOT
      L=NTOT-N+1
      IP=NORDER(L)
      XS=XS+X(IP)
      TS=TS+X(IP)*T(IP)
      IF(XS.GT.VCOL) GO TO 155
150   CONTINUE
155   NTOT=L
      X(IP)=XS-VCOL
      TS=TS-X(IP)*T(IP)
      TRET=TS/VCOL
      IF(X(IP).GT.1.E-06*VCOL) GO TO 160
      NTOT=NTOT-1
C
C--   COMPUTE AVERAGE DELIVERY TEMPERATURE, BEFORE AUXILIARY
C
160   ITOP=NORDER(1)
      TDEL=T(ITOP)
      IF(VLD.LT.1.E-06) GO TO 180
      TS=0.
      XS=0.
      DO 170 N=1,NTOT
      L=N
      IP=NORDER(L)
      XS=XS+X(IP)
      TS=TS+X(IP)*T(IP)
      IF(XS.GT.VLD) GO TO 175
170   CONTINUE
175   X(IP)=XS-VLD
      TS=TS-X(IP)*T(IP)
      TDEL=TS/VLD
      IF(X(IP).GT.1.E-06*VLD) GO TO 176
      L=L+1
176   NTOT=NTOT-L+1
      DO 177 N=1,NTOT
177   NORDER(N)=NORDER(L+N-1)
C
180   IF(IAUX.EQ.0) GO TO 300
C
C--   DIVIDE NODE AT AUXILIARY AND FIND THERMOSTAT NODE
      NTH=1
      XLOC=0.
      DO 190 N=1,NTOT
      NAUX=N
      IP=NORDER(N)
      XLOC=XLOC+X(IP)
      IF(XLOC.GE.XTH) GO TO 185
      NTH=N+1
185   IF((XLOC-XAUX).GT.-1.E-06) GO TO 195
190   CONTINUE
```

```
195    IF(ABS(XLOC-XAUX).LT.1.E-06) GO TO 220
       DO 200 N=NAUX,NTOT
       L=NTOT-N+NAUX
200    NORDER(L+1)=NORDER(L)
       NTOT=NTOT+1
       X2=XLOC-XAUX
       INEXT=INEXT+1
       IP1=NEXT(INEXT)
       NORDER(NAUX)=IP1
       IP2=NORDER(NAUX+1)
       T(IP1)=T(IP2)
       X(IP1)=X(IP2)-X2
       X(IP2)=X2
C
C--  AUXILIARY HEATER
C
220    QBTOT=0.
       ITH=NORDER(NTH)
       AUX = IGAM.EQ.1 .AND. ((.NOT.(AUX) .AND. T(ITH).LT.(T
SET-TDB))
     .    .OR. (AUX .AND. T(ITH).LT.TSET))
       IF(.NOT.(AUX)) GO TO 300
C
C--  HEAT UNTIL TEMPERATURE OF TOP NODE IS REACHED
C
       XMCP=0.
       IP2=NORDER(1)
       IF(NAUX.EQ.1) GO TO 262
       DO 250 J=2,NAUX
       N=NAUX-J+2
       IP1=NORDER(N)
       IP2=NORDER(N-1)
       XMCP=XMCP+X(IP1)*MSCP
       IF(T(IP2).GT.TSET) GO TO 270
       QB=XMCP*(T(IP2)-T(IP1))/DELT
       IF(QBTOT+QB.GT.QMAX) GO TO 270
       QBTOT=QBTOT+QB
250    CONTINUE
C
C-- ENOUGH AUXILIARY TO REACH TEMP OF TOP NODE, CONTINUE
C-- HEATING, OUTLET SEGMENT HAS LINEAR TEMPERATURE PROFILE
       X(IP2)=XMCP/MSCP+X(IP2)
       L=1
       N2=NAUX+1
       DO 260 N=N2,NTOT
       L=L+1
260    NORDER(L)=NORDER(N)
       NTOT=L
       NAUX=1
262    QBADD=(X(IP2)*MSCP*(TSET-T(IP2))
```

```
     .    + VLD*MSCP*(TSET-TDEL)/2.)/DELT
      IF(QBADD.GT.(QMAX-QBTOT)) GO TO 265
C--   SET TEMPERATURE OBTAINED
      QBTOT=QBTOT+QBADD
      T(IP2)=TSET
      TDEL=(TSET+TDEL)/2.
      AUX=.FALSE.
      GO TO 300
C
C--   NOT ENOUGH AUXILIARY TO REACH TSET
265   QBADD=QMAX-QBTOT
      QBTOT=QMAX
      T(IP2)=(QBADD*DELT+MSCP*(X(IP2)*T(IP2)+VLD*TDEL/2.))/
     .    (MSCP*(X(IP2)+VLD/2.))
      IF(T(IP2).GT.TDEL) TDEL=(T(IP2)+TDEL)/2.
      GO TO 300
C
C--   DIDN'T HEAT UP TO TEMPERATURE OF TOP NODE
C--   COMBINE NODES WHERE NECESSARY
270   X(IP1)=XMCP/MSCP
      QBADD=QMAX-QBTOT
      IF(T(IP2).GT.TSET) QBADD=AMIN1(QBADD,XMCP*(TSET-T(IP1
))/DELT)
      QBTOT=QBTOT+QBADD
      T(IP1)=T(IP1)+QBADD*DELT/XMCP
      N2=NAUX+1
      NAUX=N
      L=NAUX
      DO 280 N=N2,NTOT
      L=L+1
280   NORDER(L)=NORDER(N)
      NTOT=L
C
300   IF(MODE.EQ.2 .AND. INFO(2).EQ.38) GO TO 350
      IF(TIME.LT.TIME0+DELT/2..AND.INFO(7).GT.-1) GO TO 350
C
C--   FIND COLL INLET POSITION IF MODE 1 OR THERMOSYPHON
C
      NCOL=1
      IF(XCOL.LT.1E-06) GO TO 350
      IF(IAUX.EQ.1 .AND. XCOL.GT.(XAUX-1.E-06)) NCOL=NAUX+1
      IF(IAUX.EQ.1 .AND. ABS(XCOL-XAUX).LT.1.E-06) GO TO 35
0
      XLOC=0.
C
      DO 310 N=1,NTOT
      NCOL=N+1
      IP=NORDER(N)
      XLOC=XLOC+X(IP)
```

```
      IF((XLOC-XCOL).GT.-1.E-06) GO TO 320
310   CONTINUE
C
320   IF(ABS(XLOC-XCOL).LT.1.E-06) GO TO 350
      DO 330 N=NCOL,NTOT
      L=NTOT-N+NCOL
330   NORDER(L+1)=NORDER(L)
      NTOT=NTOT+1
      IF(XCOL.LT.XAUX) NAUX=NAUX+1
      X2=XLOC-XCOL
      INEXT=INEXT+1
      IP2=NEXT(INEXT)
      NORDER(NCOL)=IP2
      IP1=NORDER(NCOL-1)
      T(IP2)=T(IP1)
      X(IP2)=X2
      X(IP1)=X(IP1)-X2
C
C--   STORAGE LOSSES AND AVERAGE TANK TEMPERATURE
C
350   TAVG=0.
      QLOSS=0.
      DO 360 N=1,NTOT
      IP=NORDER(N)
      UA=USIDE*X(IP)*HIGH
      IF(N.EQ.1 .OR. N.EQ.NTOT) UA=UA+UAE
      IF(NTOT.EQ.1) UA=UA+UAE
      IF(.NOT.(AUX) .AND. N.LE.NAUX) UA=UA+UAF*X(IP)/XAUX
      A=-UA/MSCP/X(IP)
      B=-A*TENV
      CALL DIFFEQ(TIME,A,B,T(IP),TF,TBAR)
      T(IP)=TF
      TAVG=TAVG+T(IP)*X(IP)
360   QLOSS=QLOSS+UA*(TBAR-TENV)
C
C
C--   OTHER ENERGY QUANTITIES
315   DELU=MSCP*(TAVG-T0)
      QIN=MC*CPF*(TC-TRET)
      QS=ML*CPF*(TDEL-TL)
C
C--  CALCULATE TEMPERATURE PROFILE
      DO 500 I=1,NTEMP
      XHIGH=0.
      DO 460 N=1,NTOT
      IP1=NORDER(1)
      IP=NORDER(N)
      IP2=NORDER(N+1)
      XHIGH=XHIGH+X(IP)
      IF(THIGH(I).GT.X(IP1)) GO TO 450
```

```
      TEM(I)=T(IP1)
      GO TO 500
450   XHIGH2=XHIGH+X(IP2)
      IF(THIGH(I).GT.XHIGH2) GO TO 460
      TEM(I)=T(IP2)
      GO TO 500
460   CONTINUE
500   CONTINUE
C
C--   OUTPUTS
      OUT(1)=TRET
      OUT(2)=MC
      OUT(3)=TDEL
      OUT(4)=ML
      OUT(5)=QLOSS
      OUT(6)=QS
      OUT(7)=DELU
      OUT(8)=QBTOT
      OUT(9)=QIN
      OUT(10)=TAVG
      OUT(11)=TEM(1)
      OUT(12)=TEM(2)
      OUT(13)=TEM(3)
      OUT(14)=TEM(4)
      OUT(15)=TEM(5)
      OUT(16)=TEM(6)
      OUT(17)=TEM(7)
      OUT(18)=TEM(8)
      OUT(19)=TEM(9)
      OUT(20)=TEM(10)
C
C
      IF(INFO(2).EQ.38) RETURN
C--   CALCULATE THERMOSYPHON HEAD
      HT=0.
      DO 400 N=NCOL,NTOT
      IP=NORDER(N)
      TN=T(IP)
400   HT=HT+SG(TN)*GRAV(IU)*RHO*X(IP)*HIGH
      OUT(11)=HT
      IPIN=NORDER(NCOL)
      OUT(12)=T(IPIN)
      RETURN
      END
```

VARIABLE VOLUME STORAGE TANK

This subroutine models a variable volume tank which has upper and lower volume limits

Parameters

1	V_T	- total tank volume
2	V_{MIN}	- minimum volume of fluid
3	V_{MAX}	- maximum volume of fluid
4	C_x	- circumference of tank
5	A_x	- cross-sectional area of tank
6	U_w	- loss coefficient for wetted area of tank
7	U_d	- loss coefficient for dry area of tank
8	C_p	- constant pressure specific heat of fluid
9	ρ	- density of fluid
10	T_I	- initial temperature of fluid in tank
11	V_I	- initial volume of fluid in tank

Inputs

1	T_h	- temperature of fluid from heat source
2	$\dot{m}_h$	- mass flow rate from heat source
3	$\dot{m}_L$	- mass flow rate to load
4	T_a	- ambient temperature

Outputs

1	T	- fluid temperature in tank (average over time step)
2	$\dot{m}_L$	- mass flow rate to load
3	$\dot{m}_r$	- mass flow rate of fluid returning to heat source (zero unless tank is full)
4	V_f	- volume of fluid (average over time step)

5	H_i	-	enthalpy of incoming stream
6	H_o	-	enthalpy of outgoing stream
7	$\dot{Q}_{env}$	-	rate of energy loss from tank
8	ΔU	-	change in internal energy of tank
9	LEVEL	-	indicator of fluid level in tank -1 - fluid at minimum level 0 - fluid between minimum and maximum levels +1 - fluid at maximum level
10	T_F	-	temperature of fluid at end of time step
11	$V_{f,F}$	-	volume of fluid in tank at end of time step

```
      SUBROUTINE TYPE37(TIME,XIN,OUT,T,DTDT,PAR,INFO)
C THIS SUBROUTINE MODELS A VARIABLE VOLUME TANK WHICH
C HAS UPPER AND LOWER VOLUME LIMITS
      DIMENSION PAR(11),XIN(4),OUT(17),INFO(10)
      REAL MIN,MOUT,LHTAV,MFIN,MAV,MFST,MZERO,MRET
      COMMON/SIM/TIME0,TFINAL,DELT
      DATA IUNIT/0/
      DELTA = DELT
      DATA TUNE/10000.0/
      IF(INFO(7).GT.-1) GO TO 5
      INFO(6)=11
      NI = 4
      NP = 11
      ND = 0
      CALL TYPECK(1,INFO,NI,NP,ND)
C SET T-ZERO AND M-ZERO FOR DELTA-E CALCULATION
      TZERO = PAR(10)
      MZERO = PAR(11)*PAR(9)
C SET PARAMETERS
5     IF(INFO(1).EQ.IUNIT) GO TO 10
      IUNIT=INFO(1)
      VOL = PAR(1)
      VMIN = AMAX1(PAR(2),0.001*VOL)
      VMAX = AMIN1(PAR(3),0.999*VOL)
      CIRC=PAR(4)
      AEND=PAR(5)
      HEIGHT=VOL/AEND
      UW = PAR(6)
      UD = PAR(7)
      CP = PAR(8)
      DEN = PAR(9)
      TFST = PAR(10)
      VFST = PAR(11)
      MFST=VFST*DEN
10    IF(INFO(7) .NE. 0 ) GO TO 15
C SET T INITIAL AND M INITIAL
      TFST = OUT(10)
      VFST = OUT(11)
      MFST=VFST*DEN
   15 CONTINUE
C READ INPUTS
      TIN = XIN(1)
      MIN = XIN(2)
      MOUT = XIN(3)
      TAMB = XIN(4)
      MRET=0.
      LEVEL=0
      IF(TIME.GT.TIME0) GO TO 16
C  USE INITIAL CONDITIONS AT START OF SIMULATION
```

```
      TAV=TFST
      VOLAV=VFST
      TFIN=TFST
      VOLFIN=VFST
      MFIN=VOLFIN*DEN
      GO TO 150
C CHECK FOR MAXIMUM OR MINIMUM LIQUID VOLUME
16    VFTEST=VFST+DELTA*(MIN-MOUT)/DEN
      IF(VFTEST .LT. VMAX) GO TO 17
      MRET=MIN-MOUT-AMAX1((VMAX*DEN-MFST)/DELTA,0.)
      MOUT=MOUT+MRET
      LEVEL = 1
      GO TO 20
   17 IF(VFTEST .GT. VMIN) GO TO 20
      MOUT=AMAX1((MFST-VMIN*DEN)/DELTA,0.)+MIN
      LEVEL = -1
   20 CONTINUE
C CALC FINAL AND AVERAGE FOR TANK FLUID MASS AND VOLUME
      MFIN = MFST +DELTA*(MIN-MOUT)
      MAV = (MFST+MFIN)/2.0
      VOLFIN = MFIN/DEN
      VOLAV = MAV/DEN
      LHTAV = VOLAV/AEND
C CALC  AVERAGE TANK UA BASED ON DRY AREA AND WETTED AREA
      UAW = UW * (AEND+CIRC * LHTAV)
      UAD = UD * (AEND + CIRC * (HEIGHT - LHTAV))
      UA = UAW + UAD
C CHECK FOR MIN = MOUT
      CHECK = ABS(MIN-MOUT)
      XXTEST = (MIN + UA/CP)/TUNE
      IF(CHECK .LT. XXTEST) GO TO 75
C CHECK FOR NO FLOW
      IF(MIN .LT. 0.001 .AND. MOUT .LT. 0.001) GO TO 75
C EQUATIONS FOR FLOW CONDITION
   50 CONTINUE
      B = MIN + UA/CP
      C = MIN - MOUT
      D = MIN * TIN + (UA/CP) * TAMB
      CC = TFST-D/B
      DD = (1+(C*DELTA)/MFST)**(-B/C)
      TFIN = CC*DD+D/B
      AA = (TFST-D/B)/(C-B)
      BB = (1+(C*DELTA)/MFST)**(1-B/C)
      TAV = AA*(MFST/DELTA)*(BB-1.0) + D/B
      GO TO 150
   75 CONTINUE
C EQUATIONS FOR MIN = MOUT CONDITION
      B = MIN + UA/CP
      D = MIN *TIN + (UA/CP) * TAMB
      G = -B/MFST
```

```
      H = 1.0/(DELTA*(-B))
      A1 = D - B*TFST
      E = A1 * EXP(DELTA*G)
      TFIN = (E-D)/(-B)
      TAV =H*((E-A1)/G)+D/B
  150 CONTINUE
      DE = CP*(MFIN*TFIN-MZERO*TZERO)
      HIN=CP*MIN*TIN
      HOUT=CP*MOUT*TAV
      QLOSS = UA*(TAV - TAMB)
C SET OUTPUTS
      OUT(1) = TAV
      OUT(2) = MOUT-MRET
      OUT(3) = MRET
      OUT(4) = VOLAV
      OUT(5) = HIN
      OUT(6) = HOUT
      OUT(7) = QLOSS
      OUT(8) = DE
      OUT(9)  = LEVEL
      OUT(10) = TFIN
      OUT(11) = VOLFIN
      RETURN
      END
```

RECIR

This subroutine calculates the instantaneous recirculation flow rate and the minimum volume of cold water in the tank over a user specified period of time for the plug-flow storage tank.

Parameters

1	ρ	- density of fluid in tank
2	V_T	- volume of tank
3	RESET	- resets the minimum amount of cold water in the tank to the tank volume every RESET number of hours

Inputs

1	$\dot{m}_c$	- mass flow rate from heat source
1	$\dot{m}_L$	- mass flow rate from load

Outputs

1	$\dot{m}_r$	- mass flow rate of heated fluid returning to heat source
2	M_{cold}	- mass of cold fluid in tank
3	-	
4	M_{MIN}	- minimum mass of could fluid in tank since last reset

```
C  THIS SUBROUTINE CALCULATES THE INSTANEOUS RECIRCULATION
C  FLOW RATE FOR A LIQUID STORAGE TANK
      SUBROUTINE TYPE37(TIME,XIN,OUT,T,DTDT,PAR,INFO)
      COMMON/SIM/TIME0,TIMEF,DELT
      DIMENSION XIN(2),OUT(4),PAR(3),INFO(10)
C PARMETERS
      RHO=PAR(1)
      VT1=RHO*PAR(2)
      RST=PAR(3)
C  INPUTS
      FC=XIN(1)
      FL=XIN(2)
C  PERFORM CALCULATIONS
      IF(INFO(7).NE.0) GO TO 15
      IF(TIME.EQ.TIME0) COUNT=-DELT
      IF(COUNT.EQ.RST) COUNT=0.
      IF(TIME.EQ.TIME0.OR.COUNT.EQ.0.) VMIN=VT1
      COUNT=COUNT+DELT
      IF(TIME.NE.TIME0) GO TO 2
      VCLD=VT1
      V=0.
      GO TO 4
   2  V=(FC-FL)*DELT
   4  VCLD1=VCLD-V
      IF(VCLD1.GE.VT1) VCLD=VT1
      IF(VCLD1.LT.VT1.AND.VCLD1.GT.0.) VCLD=VCLD1
      IF(VCLD1.LE.0.) VCLD=0.
      IF(VCLD1.LT.0.) GO TO 5
      VREC=0.
      GO TO 10
   5  VREC=-1*VCLD1/DELT
  10  IF(VCLD.LT.VMIN) VMIN=VCLD
C  OUTPUTS
      OUT(1)=VREC
      OUT(2)=VCLD
      OUT(3)=V
      OUT(4)=VMIN
  15  RETURN
      END
```

IF-CALC

This subroutine performs algebraic operations with logical if statements for critical radiation calculations.

Parameters

1	KTA	-	minimum acceptable value of $K_{\tau\alpha}$

Inputs

1	T_i	-	collector inlet temperature
2	T_a	-	ambient temperature
3	$K_{\tau\alpha}$	-	incidence angle modifier

Outputs

1	$(T_i - T_a)/K_{\tau\alpha}$	-	if $K_{\tau\alpha}$ is greater than KTA
	0		if $K_{\tau\alpha}$ is less than or equal to KTA

```
C  THIS SUBROUTINE PERFORMS ALGEBRAIC OPERATIONS
C  WITH LOGICAL IF STATEMENTS FOR ICRIT CALCULATIONS
      SUBROUTINE TYPE39(TIME,XIN,OUT,T,DTDT,PAR,INFO)
      COMMON/SIM/TIME0,TIMEF,DELT
      DIMENSION XIN(3),OUT(1),PAR(1),INFO(10)
C  PARMETERS
      AKMIN=PAR(1)
C  INPUTS
      TI=XIN(1)
      TA=XIN(2)
      AKTA=XIN(3)
C  PERFORM CALCULATIONS
      OUT(1)=0.
      IF(AKTA.LE.AKMIN) RETURN
      XX=(TI-TA)/AKTA
      OUT(1)=XX
C  OUTPUTS
      RETURN
      END
```

APPENDIX B

SAMPLE TRNSYS SIMULATION DECKS

This appendix contains listing of three of the TRNSYS simulation decks used in this research.

PLUG2R-H1 — This models the base case (constant storage volume, constant reduced collector flow rate, on-off control, stratified preheat storage) system. A typical constants deck used with PLUG2R-H1 is also included

CALC-C2&C3 — This calculates the daily proportionality constant C_2, (outlined in section 3.3.3) for use with variable collector flow rate proportional to the utilizable radiation.

VV-H1PROP — This models the variable storage volume system with variable collector flow proportional to the utilizable radiation.

```
CONSTANTS 24
START = 1417.,STOP = 2160.,DT = .5,NDAY = 60.,LAT = 43.,MCP
A = 10.,
SLP = 43.,AC = 4.2,FRTAN = .805,FRUL = 17.028,MTEST = 72.,B
0 = .0989,
TI = 60.,TAI = 20.,TI1 = 10.4,TI2 = 60.,TSET = 60.,MC = MCP
A * AC,
VT1 = .303,VT2 = .151,LOAD = 300.,
STPSM = START + 24,TMI = 10.4,VT = VT1 + VT2
```

```
* * * * * * * * * * * * * * * * * * * * * * * * * * * * * * * * * * *
*                                                                     *
*        SOLAR WATER HEATING, 2 TANK, FIXED FLOW                      *
*                          PLUG2R-H1                                  *
*                                                                     *
* * * * * * * * * * * * * * * * * * * * * * * * * * * * * * * * * * *
NOLIST
SIMULATION START STOP DT
TOL -.01 -.01
LIMITS 50 5 45
WIDTH 132
UNIT 9 TYPE 9 DATA READER
PAR 10
3 1 -1 1 0 -2 1 0 -1 1
(T20,F4.0,T25,F4.0,T30,F4.1)
UNIT 19 TYPE 16 SOLAR RADIATION PROCESSOR
PARAMETERS 7
5 1 NDAY LAT 4871. 0 -1
INPUTS 7
9,2 9,1 9,19 9,20 0,0 0,0 0,0
0.0 0.0 0.0 1.0 0.2 SLP 0.0
UNIT 1 TYPE 1 COLLECTOR (FIXED FLOW)
PARAMETERS 8
1 1 AC 4.19 FRTAN FRUL MTEST BO
INPUTS 8
3,1  3,2  9,3  19,6 19,9 19,7 19,5 0,0
TI1 0.0 TAI  0.0 0.0 0.0 0.0 SLP
UNIT 13 TYPE 13 PRESSURE RELIEF VALVE
PAR 2
```

```
100. 4.19
INPUTS 3
1,1 1,2 1,1
15. 0.0 15.
UNIT 2 TYPE 2 PUMP CONTROLLER
PARAMETERS 3
3  8.9 1.7
INPUTS 3
1,1  4,1  2,1
TI1 TI1  0.0
UNIT 3 TYPE 3 PUMP
PARAMETERS 1
MC
INPUTS 3
4,1  4,2  2,1
TI1  0.0  0.0
UNIT 14 TYPE 14 LOAD
PARAMETERS 82
0,0 5,0 5,.125 6,.125 6,.391 7,.391 7,.625 8,.625
8,.703 9,.703 9,.549 10,.549 10,.391 11,.391
11,.297 12,.297 12,.422 13,.422 13,.242 14,.242
14,.203 15,.203 15,.156 16,.156 16,.297 17,.297
17,.549 18,.549 18,1.0 19,1.0 19,.786 20,.786
20,.549 21,.549 21,.422 22,.422 22,.391 23,.391
23,.156 24,.156 24,0
UNIT 18 TYPE 14 MAINS TEMPERATURE
PAR 48
0,8.2 744,8.2 744,9.6 1416,9.6 1416,10.4
2160,10.4 2160,12.5 2880,12.5 2880,17.7
3624,17.7 3624,19.1 4344,19.1 4344,19.5
5088,19.5 5088,24.9 5832,24.9 5832,26.1
6552,26.1 6552,20.8 7296,20.8 7296,13.1
8016,13.1 8016,10.4 8760,10.4
UNIT 4 TYPE 38 PLUG FLOW PREHEAT
PARAMETERS 9
2 VT1  2. 0.   4.19  1000  3.89  TI1 3
INPUTS 5
13,1  13,2  10,1 10,2  0,0
15.0  0.0  TMI  0.0  21
UNIT 6 TYPE 37 RECIR
PAR 3
1000 VT1 24.
INPUTS 2
13,2 10,2
0 0
UNIT 16 TYPE 15 CALC. LOAD MASS FLOW, AND TO GREATER THAN 0
PAR 11
0 0 2 0 1 -4 0 -1 0. 12 -4
INPUTS 4
0,0 0,0 14,1 1,1
```

```
LOAD 8.254 0.0 0
UNIT 5 TYPE 4 AUX TANK
PAR 9
VT2 1.6 4.19 1000. 3.77 32400. 3. 1. TSET
INPUTS 5
0,0 0,0 4,3 4,4 0,0
0.0 0.0 TI1 0.0 21.
DERIVATIVES 1
TI2
UNIT 10 TYPE 11 FLOW DIVERTER
PAR 2
4. 4.
INPUTS 4
0,0 16,1 5,3 0,0
TMI 0. TI1 TSET
UNIT 11 TYPE 11 TEE PIECE
PAR 1
1
INPUTS 4
5,3 5,4 10,3 10,4
TI2 0. TMI 0.
UNIT 39 TYPE 39 IF-CALC
PAR 1
.001
INP 3
3,1 9,3 1,4
TMI TAI 0
UNIT 17 TYPE 15 CALC. QLOAD & ICRIT
PAR 17
0 0 4 -1 4.19 1 0 1 -4
0 -1 FRUL 1 -1 FRTA 2 -4
INPUTS 4
11,1 18,1 16,1 39,1
0 0 0 0
UNIT 20 TYPE 15 CALC. MCOL, MLOAD, MLOADC, ATTKOB, ATTKIT,M
LDTC
PAR 46
0 0 1 -4 -11 -13 1 -4 -13 -14 1 -4
-14 -15 1 -4 -14 -16 1 -4
-12 -1 31 2 -17 -1 31 2 -3 -14 1 4 -4 -17 -14 1 -3 -1 31 2
-4
-12 -1 31 2 -4
INPUTS 7
0,0 13,2 10,2 2,1 4,1 13,1 16,1
DT  0.0 0.0 0 0 0 0
UNIT 25 TYPE 28 SIM SUM DAILY
PAR 34
24 START STOP 0 1 0 0 -4 -4 0 -4 0 -4
0 -4 -17 -16 2 -4 -18 -16 2 -4
-19 -3 -20 -19 3 2 -4 -13 -14 2 -4
```

```
INPUTS 10
6,2 19,6 13,2 10,2 6,1 2,1 20,5 20,4 4,6 5,8
LABLES 10
HT DELMCD MC ML  MREC ATTKIT ATTKOB QTANK1 FSOL MC/ML
UNIT 22 TYPE 28 SIM SUM DAILY 2
PAR 25
24 START STOP 0 2 0 -4 0 -4 0 -4 0 -4 0 -4 0 -4
0 -4 0 -4 0 0 2 -4
INPUTS 10
4,7 5,7 4,5 5,5 13,3 5,6 5,8 17,1 17,2 2,1
LABLES 9
DELT1 DELT2 QENV1 QENV2 QRELF QTANK2 QAUX QLOAD ICRIT
UNIT 24 TYPE 25 PRINTER
PAR 4
DT 1441 1465 0
INPUTS 9
19,6 1,3 1,2 4,4 4,6 4,5 6,2 4,7 5,8
HT QU COLLFL LOADFL QTANK1 QENV MCLDTK DELT1 QAUX
UNIT 21 TYPE 25 PRINTER
PAR 4
DT 1441 1465 0
INPUTS 9
16,2 4,3 4,11 4,12 4,13 4,1 5,5 5,7 17,1
TOCOLL TTOP T1 T2 T3 TBOT QENV2 DELT2 QLOAD
UNIT 26 TYPE 25 PRINTER
PAR 4
24 START STOP 0
INPUTS 6
6,2 13,1 4,1 6,4 10,1 4,3
MCLDTK TTKIT TTKOB MCLMIN TTKIB TTKOT
UNIT 28 TYPE 28 SIM SUM
PAR 40
-1 0 10000 0 1 0 0 -1 AC 1 -4 0 -4  -4  0  -4 0 -4 0 -4  0
-2 -1 24. 2 2 -4
-1 MCPA -4 -15 -18 -15  3 2 -4 -20 -19 2 -4
INPUTS 10
4,7 19,6 1,3 4,5 4,6 13,3 16,1 5,8 2,1 20,4
LABLES 10
HT*AC TOTQU DELT1 QENV1 QTANK1 QRELF USAGE  MC/AC FSOL ATTK
OB
CHECK .05 2,-3,-4,-5,-6
UNIT 29 TYPE 28 SIM SUM
PAR 52
-1 0 10000 0 1 0 0 -4 -4 0 -4 0 -4 0 -4 0
-2 -1 24. 2 2 -3 0 -2 -1 24 2 2 2 -4
0  -2 -1 24. 2 2 -4
-16 -2 -1 24 2 2 -19 -2 -1 24 2 2 -4 -20 -4
INPUTS 10
5,7 5,6 5,5 5,8 17,1 13,2 16,1 20,3 20,8 6,1
LABLES 10
```

```
QTANK2 DELT2 QENV2 QAUX  QLOAD  ADMCOL MC/USG ADMLDC ADMLTC
 MREC
CHECK .05 4,-1,-2,-3
UNIT 23 TYPE 27 HISTO PLOT
PAR 8
2 24 24 1441 1465 0 24 24
INPUTS 4
19,6 1,3 13,2 10,2
HT QU MC ML
UNIT 30 TYPE 26 PLOTTER
PAR 4
.5 1441 1465 1
INP 8
16,2 4,3 4,11 4,12 4,13 4,1 4,4 2,1
TOCOLL TTOP T1 T2 T3 TBOT LDFLO TIMEON
END:
```

```
* * * * * * * * * * * * * * * * * * * * * * * * * * * * * * * * * * * *
*                                                                       *
*     SOLAR WATER HEATING, 2 TANK, VARIABLE FLOW                        *
*        PROPORTIONAL TO UTILIZABLE RADIATION                           *
*                          CALC-C2&C3                                   *
* * * * * * * * * * * * * * * * * * * * * * * * * * * * * * * * * * * *
SIMULATION START STOP DT
TOL -.01 -.01
LIMITS 50 5 45
WIDTH 132
UNIT 9 TYPE 9 DATA READER
PAR 10
3 1 -1 1 0 -2 1 0 -1 1
(T20,F4.0,T25,F4.0,T30,F4.1)
UNIT 19 TYPE 16 SOLAR RADIATION PROCESSOR
PARAMETERS 7
5 1 NDAY LAT 4871. 0 -1
INPUTS 7
9,2 9,1 9,19 9,20 0,0 0,0 0,0
0.0 0.0 0.0 1.0 0.2 SLP 0.0
UNIT 1 TYPE 1 COLLECTOR (JIMS MODEL)
PARAMETERS 8
3 1 AC 4.19 FRTAN FRUL MTEST BO
INPUTS 10
0,0 0,0  9,3  19,6 19,9 19,7 19,5 0,0 0,0 0,0
TI1 0.0 TAI  0.0 0.0 0.0 0.0 SLP TO 630
UNIT 15 TYPE 39
PAR 1
.001
INPUTS 3
0,0 9,3 1,4
TMI TAI 0
UNIT 14 TYPE 14 LOAD
PARAMETERS 82
0,0 5,0 5,.125 6,.125 6,.391 7,.391 7,.625 8,.625
8,.703 9,.703 9,.549 10,.549 10,.391 11,.391
11,.297 12,.297 12,.422 13,.422 13,.242 14,.242
14,.203 15,.203 15,.156 16,.156 16,.297 17,.297
17,.549 18,.549 18,1.0 19,1.0 19,.786 20,.786
20,.549 21,.549 21,.422 22,.422 22,.391 23,.391
23,.156 24,.156 24,0
UNIT 18 TYPE 14 MAINS TEMPERATURE
PAR 48
0,8.2 744,8.2 744,9.6 1416,9.6 1416,10.4
2160,10.4 2160,12.5 2880,12.5 2880,17.7
3624,17.7 3624,19.1 4344,19.1 4344,19.5
5088,19.5 5088,24.9 5832,24.9 5832,26.1
6552,26.1 6552,20.8 7296,20.8 7296,13.1
8016,13.1 8016,10.4 8760,10.4
```

```
UNIT 16 TYPE 15 CALC. LOAD MASS FLOW & PART OF C3
PAR 17
0 0 2 0 1 -4
0 0 -1 FRUL 1 -1 FRTA 2 4 8 -4
INPUTS 5
0,0 0,0 14,1 19,6 15,1
LOAD 8.254 0.0 0 0
UNIT 26 TYPE 28 SIM SUM DAILY
PAR 23
24 0 10000 10 0 -3 0 -3 0 -1 FRUL 1 -1 FRTA 2 -3
4  2 -4 -11 -14 2 -4
INPUTS 4
16,1 19,6 15,1 16,2
LABLES 5
ML HT HTCRIT  C2 C3
END
```

```
* * * * * * * * * * * * * * * * * * * * * * * * * * * * * * * * * * * *
*                                                                       *
*   SOLAR WATER HEATING, 2 TANK, VARIABLE VOLUME,                       *
*  VARIABLE FLOW, PROPORTIONAL TO UTILIZABLE RADIATION                  *
*                      VV-H1PROP                                        *
*                                                                       *
* * * * * * * * * * * * * * * * * * * * * * * * * * * * * * * * * * * *
SIMULATION START STOP DT
TOL -.01 -.01
LIMITS 50 5 45
WIDTH 132
UNIT 8 TYPE 9 C3 DATA READER
PAR 7
1 24 -1 1 0 10 1
(T55,1PE11.3)
UNIT 9 TYPE 9 DATA READER
PAR 10
3 1 -1 1 0 -2 1 0 -1 1
(T20,F4.0,T25,F4.0,T30,F4.1)
UNIT 19 TYPE 16 SOLAR RADIATION PROCESSOR
PARAMETERS 7
5 1 NDAY LAT 4871. 0 -1
INPUTS 7
9,2 9,1 9,19 9,20 0,0 0,0 0,0
0.0 0.0 0.0 1.0 0.2 SLP 0.0
UNIT 1 TYPE 1 COLLECTOR (FIXED FLOW)
PARAMETERS 8
1 1 AC 4.19 FRTAN FRUL MTEST BO
INPUTS 8
6,1 17,3  9,3  19,6 19,9 19,7 19,5 0,0
TI1 0.0 TAI  0.0 0.0 0.0 0.0 SLP
UNIT 13 TYPE 13 PRESSURE RELIEF VALVE
PAR 2
100. 4.19
INPUTS 3
1,1 1,2 1,1
15. 0.0 15.
UNIT 2 TYPE 15 FLOW CHECK, CF/AC
PAR 10
0 -1 .000001 9 -4 -11 -1 AC 2 -4
INPUTS 1
1,2
0
UNIT 14 TYPE 14 LOAD
PARAMETERS 82
0,0 5,0 5,.125 6,.125 6,.391 7,.391 7,.625 8,.625
8,.703 9,.703 9,.549 10,.549 10,.391 11,.391
11,.297 12,.297 12,.422 13,.422 13,.242 14,.242
14,.203 15,.203 15,.156 16,.156 16,.297 17,.297
```

```
17,.549 18,.549 18,1.0 19,1.0 19,.786 20,.786
20,.549 21,.549 21,.422 22,.422 22,.391 23,.391
23,.156 24,.156 24,0
UNIT 18 TYPE 14 MAINS TEMPERATURE
PAR 48
0,8.2 744,8.2 744,9.6 1416,9.6 1416,10.4
2160,10.4 2160,12.5 2880,12.5 2880,17.7
3624,17.7 3624,19.1 4344,19.1 4344,19.5
5088,19.5 5088,24.9 5832,24.9 5832,26.1
6552,26.1 6552,20.8 7296,20.8 7296,13.1
8016,13.1 8016,10.4 8760,10.4
UNIT 4 TYPE 37 VARIABLE VOLUME TANK-FM
PAR 11
VT1 0 VT1 1.3798 .1515 3.89 3.89 4.19 1000 TI1 VT1
INP 4
13,1 13,2 16,4 0,0
15.0 0.0 0.0 21.0
UNIT 6 TYPE 11 TEE PIECE BEFORE PUMP
PAR 1
1
INPUTS 4
18,1 16,3 4,1 4,3
TMI 0 TI1 0
UNIT 7 TYPE 11 TEE PIECE AFTER PREHEAT
PAR 1
1
INPUTS 4
4,1 4,2 0,0 16,6
TI1 0 TMI 0
UNIT 16 TYPE 15 CALC. LOAD MASS FLOW & COLL FLOW & AUX MAKE
 UP FLOW
PAR 33
0 0 2 0 1  -21 -31 -3 0 4 0 3 0 4 -4 -15 -16 4 -4
-31 -17 4 -4 -18 -19 1 -4
-31 -14 4 -17 4 -4
INPUTS 9
0,0 0,0 14,1 4,2 1,2 4,3 10,4 13,1 2,1
LOAD 8.254 0.0 0 0 0 0 0 0
UNIT 5 TYPE 4 AUX TANK
PAR 9
VT2 1.6 4.19 1000. 3.77 32400. 3. 1. TSET
INPUTS 5
0,0 0,0 7,1 7,2 0,0
0.0 0.0 TI1 0.0 21.
DERIVATIVES 1
TI2
UNIT 10 TYPE 11 FLOW DIVERTER
PAR 2
4 6
INPUTS 4
```

```
0,0 16,2 5,3 0,0
TMI 0. TI1 TSET
UNIT 11 TYPE 11 TEE PIECE AFTER AUX TANK
PAR 1
1
INPUTS 4
5,3 5,4 10,3 10,4
TI2 0. TMI 0.
UNIT 15 TYPE 15 QSOLAR OR QTANK1
PAR 11
0 0 1 0 0 1 4  -1 4.19 1 -4
INP 4
7,1 7,2 10,1 10,2
TI1 0 TMI 0
UNIT 39 TYPE 39 IF-CALC
PAR 1
.001
INP 3
6,1 9,3 1,4
TMI TAI 0
UNIT 17 TYPE 15 CALC. QLOAD & ICRIT & COLL FLOW
PAR 32
0 0 1 0 0 1 4 -1 4.19 1 -4
0 -1 FRUL 1 -1 FRTA 2 -4
0 -15 -1 FRUL 1 -1 FRTA 2 4 8 -17 1 -4
INPUTS 7
11,1 16,1 18,1 16,2 39,1 19,6 8,1
0 0 0 0 0 0 0
UNIT 20 TYPE 15 CALC. MCOL, MLOAD, MLOADC, ATTKOB, ATTKIT,M
LDTC
PAR 20
0 0 1 -4 -11 -13 1 -4 -13 -14 1 -4
-14 -15 1 -4 -14 -16 1 -4
INPUTS 7
0,0 13,2 4,2 2,1 6,1 13,1 16,1
DT  0.0 0.0 0 0 0 0
UNIT 25 TYPE 28 SIM SUM DAILY
PAR 35
24 START STOP 0  0  -4 0 -4 0 -4
0 -4 -16 -15 2 -4 -17 -15 2 -4
-18 -3 -19 -18 3 2 -4 -12 -13 2 -4
-12 -20 2 -4
INPUTS 10
19,6 13,2 4,2 4,3 2,1 20,5 20,4 15,1 5,8 7,2
LABLES 10
HT  MC MLT  MREC ATTKIT  ATTKOB QTANK1 FSOL MC/MLT MC/ML
UNIT 22 TYPE 28 SIM SUM DAILY 2
PAR 25
24 START STOP 0 2 0 -4 0 -4 0 -4 0 -4 0 -4 0 -4
0 -4 0 -4 0 0 2 -4
```

```
INPUTS 10
4,8 5,7 4,7 5,5 13,3 5,6 5,8 17,1 17,2 2,1
LABLES 9
DELT1 DELT2 QENV1 QENV2 QRELF QTANK2 QAUX QLOAD ICRIT
UNIT 24 TYPE 25 PRINTER
PAR 4
DT 1441 1465 0
INPUTS 9
19,6 1,3 1,2 4,3 15,1 4,7 4,11 4,8 5,8
HT QU COLLFL RECFL QTANK1 QENV1 PTVOL DELT1 QAUX
UNIT 21 TYPE 25 PRINTER
PAR 4
DT 1441 1465 0
INPUTS 9
16,5 4,1 4,2 7,2 16,1 7,1 5,5 5,7 17,1
TOCOLL PTT PTFL AXINFL LDFL AXINT QENV2 DELT2 QLOAD
UNIT 26 TYPE 25 PRINTER
PAR 4
24 START STOP 0
INPUTS 2
4,11 4,1
PTVOL PTT
UNIT 28 TYPE 28 SIM SUM
PAR 40
-1 0 10000 0 1 0 0 -1 AC 1 -4 0 -4  -4  0  -4 0 -4 0 -4  0
 -2 -1 24. 2 2 -4
 -1 MCPA -4 -15 -18 -15  3 2 -4 -20 -19 2 -4
INPUTS 10
4,8 19,6 1,3 4,7 15,1 13,3 16,1 5,8 2,1 20,4
LABLES 10
HT*AC TOTQU DELT1 QENV1 QTANK1 QRELF USAGE  MC/AC FSOL ATTK
OB
CHECK .05 2,-3,-4,-5,-6
UNIT 29 TYPE 28 SIM SUM
PAR 43
-1 0 10000 0 1 0 0 -4 -4 0 -4 0 -4 0 -4 0
-2 -1 24. 2 2 -3 0 -2 -1 24 2 2 2 -4
0  -2 -1 24. 2 2 -4
-16 -19 2 -4 -20 -4
INPUTS 10
5,7 5,6 5,5 5,8 17,1 13,2 16,1 20,3 7,2 4,3
LABLES 10
QTANK2 DELT2 QENV2 QAUX  QLOAD  ADMCOL MC/MLT ADMLDC MC/ML
MREC
CHECK .05 4,-1,-2,-3
UNIT 23 TYPE 27 HISTO PLOT
PAR 8
2 24 24 1441 1513 0 24 24
INPUTS 5
19,6 1,3 13,2 4,2 7,2
```

```
HT QU MC MLT ML
UNIT 30 TYPE 26 PLOTTER
PAR 4
DT 1441 1465 1
INP 6
16,5 4,1 4,2 7,2 1,2 6,1
TOCOLL TTKOB TKLDFL LDFL COLFL TINCOL
END:
```

REFERENCES

1. Cole, R.L., and Bellinger, J.O., "Natural Thermal Stratification in Tanks", Argone National Lab, 82-7 (February 1982).

2. Fanney, A.H., and Klein, S.A., "Performance of Solar Domestic Hot Water Systems at NBS-Measurements and Predictions", in review ASME.

3. Jesch, L.F., "Solar Energy Storage in Variable Level Tanks.", Proceedings UKISES Midlands Branch Meeting, M3, Birmingham, solar energy benefits evaluated, pp. 99-104 (1982).

4. Jesch, L.F., and Braun, J.E., "Variable Volume Storage and Stratified Storage for Improved Water Heater Performance", submitted to Solar Energy Journal (1982).

5. van Koppen, C.W.F, et al., "The Actual Benefits of Thermally Stratified Storage in a Small and a Medium Size Solar", Proceedings ISES, Atlanta (1979).

6. Veltkamp, W.B., "Thermal Stratification in Heat Storage", In C. den Ouden, Thermal Storage of Solar Energy, Martinus Nijhoff, The Hague, 2, p.47 (1980).

7. Rademaker, O., "On the Dynamics of (Thermal Solar) Systems Using Stratified Storage", In C. den Ouden, Thermal Storage of Solar Energy, Martinus Nijhoff, The Hague, 2, p.6 (1980).

8. Veltkamp, W.B., and van Koppen, C.W.J., "Optimisation of the Flows in a Solar Heating System", Report WPS3-82.09.R335, (September 1982).

9. Veltkamp, W.B., and van Koppen, C.W.J., "Third Interim Report", Report WPS3-83.01.R345 (January 1983).

10. University of Wisconsin-Madison Solar Energy Laboratory, TRNSYS 11.1, EES Report 38-11 (1981).

11. Hottel, H.C., and Whillier, A., "Evaluation of Flat-Plate Collector Performance", Transactions of Conference on Use of Solar Energy, Part 1, p.74, University of Arizona Press (1958).

12. van der Oogen AAJ, Referentiejaar voor Nederland (A reference meteorological year for the Netherlands), Verwarming en.

13. University of Wisconsin-Madison Solar Energy Laboratory, TRNSYS 12.1, to be released (December 1983).

14. Duffie, J.A., and Beckman, W.A., Solar Engineering of Thermal Processes, Whiley Interscience, New York (1980).

15. Brandemuehl, M.J., and Beckman, W.A., "Transmission of Diffuse Radiation Through CPC and Flat-Plate Collector Glazings", Solar Energy, 25, p.511, (1980).

16. Kays, W.M., and Crawford, M.E., Convective Heat and Mass Transfer, 2nd edition, McGraw-Hill (1980).

17. Phillips, W.F., "The Effects of Axial Conduction on Collector Heat Removal Factor", Solar Energy, 23, p.187 (1979).

18. Mutch, J.J., "Residential Water Heating, Fuel Consumption Economics and Public Policy, RAND, Department R1498, NSF (1974).

19. Hall, I.J., et al., "Generation of a Typical Meteorological Year", Sandia National Laboratory, Report SAND78-1601 (1979).

20. Buckles, W.E., and Klein, S.A., "Analysis of Solar Domestic Hot Water Heaters", Solar Energy, 25, pp.417-424, (May 1980).

21. Fisher, R.A., and Fanney, A.H., "Thermal Performance Comparisons for a Solar Hot Water System Subjected to Various Hot Water Load Profiles", in review ASME

22. Klein, S.A., and Theilacker, J.C., "An Alogrithm for Calculating Monthly-Average Radiation of Inclined Surfaces", ASME Journal of Solar Energy Engineering, 103, pp.29-33, (February 1981).

23. Klein, S.A., "Calculation of Flat-Plate Collector Utilizability", Solar Energy, 21, p.393 (1978).

24. Collares-Pereira, M., and Rabl, A.,"Simple Procedure for Predicting Long-Term Average Performance of Nonconcentrating and Concentrating Solar Collectors", Solar Energy, 23, p.235 (1979).

25. Huget, R.G., "A Method for Estimating the Daily Utilizability of Flat-Plate Solar Collectors", M.S. Thesis in Mechanical Engineering, University of Waterloo, Ontario (1981).

26. Theilacker, J.C., and Klein, S.A., "Improvements in the Utilizability Relationships", Proceedings AS/ISES, Phoenix (1980).

27. Evans, D.L., Rule, T.T., and Wood, B.D., "A New Look at Long Term Collector Performance and Utilizability", Solar Energy, 28, p.13 (1982).